

**MODIFIED FUZZY GAIN SCHEDULING  
SPEED CONTROLLER FOR BLDC WITH  
SEAMLESS SPEED REVERSAL USING  
DIRECT COMMUTATION SWITCHING  
SCHEME**

**SATISHRAO POTHORAJOO**

**UMP**

**MASTER OF SCIENCE**

**UNIVERSITI MALAYSIA PAHANG**

## UNIVERSITI MALAYSIA PAHANG

### DECLARATION OF THESIS AND COPYRIGHT

Author's Full Name : SATISHRAO POTHORAJOO

Date of Birth : 28 OCT 1991

Title : Modified Fuzzy Gain Scheduling Speed Controller  
for BLDC with Seamless Speed Reversal using  
Direct Commutation Switching Scheme

Academic Session : SEM 1 2017/2018

I declare that this thesis is classified as:

- CONFIDENTIAL (Contains confidential information under the Official Secret Act 1997)\*
- RESTRICTED (Contains restricted information as specified by the organization where research was done)\*
- OPEN ACCESS I agree that my thesis to be published as online open access (Full Text)

I acknowledge that Universiti Malaysia Pahang reserves the following rights:

1. The Thesis is the Property of Universiti Malaysia Pahang
2. The Library of Universiti Malaysia Pahang has the right to make copies of the thesis for the purpose of research only.
3. The Library has the right to make copies of the thesis for academic exchange.

Certified by:

\_\_\_\_\_  
(Student's Signature)

911028105347  
New IC/Passport Number  
Date: 29 MARCH 2018

\_\_\_\_\_  
(Supervisor's Signature)

Dr.Hamdani Bin Daniyal  
Name of Supervisor  
Date: 29 MARCH 2018

NOTE : \* If the thesis is CONFIDENTIAL or RESTRICTED, please attach a thesis declaration letter.

## SUPERVISOR'S DECLARATION

I hereby declare that I have checked this thesis and, in my opinion, this thesis is adequate in terms of scope and quality for the award of the degree of Master of Science in Electrical Engineering

---

(Supervisor's Signature)

Full Name : Dr. Hamdan Bin Daniyal

Position : Associate Professor

Date : 29 MARCH 2018



UMP

### STUDENT'S DECLARATION

I hereby declare that the work in this thesis is based on my original work except for quotations and citations which have been duly acknowledged. I also declare that it has not been previously or concurrently submitted for any other degree at Universiti Malaysia Pahang or any other institutions.

---

(Student's Signature)

Full Name : SATISHRAO POTHORAJOO

ID Number : MEE16008

Date : 29 MARCH 2018



UMP

MODIFIED FUZZY GAIN SCHEDULING SPEED CONTROLLER FOR BLDC  
WITH SEAMLESS SPEED REVERSAL USING DIRECT COMMUTATION  
SWITCHING SCHEME

The logo of the University of Malaysia Pahang (UMP) is a shield-shaped emblem. It features a central white vertical band. The left side of the shield is light blue, and the right side is light purple. At the top, there is a yellow diamond shape with a light blue ring around it. The letters 'UMP' are prominently displayed in white at the bottom of the shield.

SATISHRAO POTHORAJOO

Thesis submitted in fulfilment of the requirements  
for the award of the degree of  
Master of Science

UMP

Faculty of Electrical & Electronics Engineering

UNIVERSITI MALAYSIA PAHANG

MARCH 2018

## ACKNOWLEDGEMENTS

I am very grateful and would like to express my sincere gratitude to my one and only supervisor, Dr. Hamdan Daniyal, for his germinal ideas, invaluable guidance, continuous encouragement and constant support in making this research possible. He has always impressed me with his outstanding professional conduct and his strong conviction for science. I am truly grateful for his progressive vision about my final year project, his tolerance of my naive mistakes, and his commitment to my future career. I am also wanted to thank you for the time spent proofreading and correcting my many mistakes.

Next, I would like to thank Universiti Malaysia Pahang for granting me research funding to complete my study. I also wish to express my gratitude towards the staff of Institute of Postgraduate Studies for providing help directly or indirectly to complete my studies. My special gratitude also goes to the Institute of Postgraduate Studies and Research and Innovation Department for financial support, without their funding, this work would not have happened

A sincere thanks to all my lecturers, lab instructors and staffs of the Electrical & Electronics Engineering Department in UMP, whose had helped me in many ways and made my stay at UMP pleasant and unforgettable especially Mdm. Salmiah. Besides that, special thanks go to my members of course mates and friends in UMP for their excellent cooperation, inspirations and supports during this study.

Finally, I would like to thank to my beloved parents, lovely sister and brothers and to my relatives for their loves, dreams and sacrifices throughout my life. I cannot find the appropriate words that could properly describe my appreciation for their devotion, support and faith in my ability to attain my goals.



UMP

## ABSTRAK

Sejak beberapa dekad ini Motor Arus Terus Tanpa Berus (BLDC) telah mendapat populariti dalam pelbagai sektor seperti pengangkutan, robotik, dan automasi. Populariti ini disebabkan oleh kecekapan yang tinggi, kos penyelenggaraan yang rendah dan ketumpatan kuasa yang tinggi oleh motor BLDC. Aplikasi motor BLDC dalam automasi, aeroangkasa dan automasi industri memerlukan motor untuk dikendalikan dwi-arah. Walaupun pelbagai pengawal kelajuan BLDC telah dibangunkan, namun kebanyakan penyelesaian hanya memfokuskan pada pemanduan ke hadapan sahaja dan bukan dwi-arah. Pengawal kelajuan BLDC 4-kuadran yang pertama telah dibangunkan oleh S.Joice untuk menangani isu ini, walaubagaimanapun tidak jelas sama ada pengawal dapat mencapai operasi dwi-arah kerana kekurangan bukti dalam penerbitan. Untuk menilai keupayaan pengawal dwi-arah ini, kajian ini menguji pengawal ini dalam simulasi *MATLAB Simulink*. Didapati bahawa pengawal ini, tidak mampu mencapai kelajuan rujukan ketika operasi kuadran ketiga dan mempunyai 67.5 % perbezaan kelajuan semasa operasi perubahan kuadran. Untuk mengatasi kekurangan ini, kajian ini mencadangkan satu skim komutasi BLDC yang baharu, yang dipanggil skim komutasi secara menerus (DCS). Pengawal kelajuan PID digabungkan dengan skim DCS diuji melalui dua kes ujian. Dari kes ujian, dapat disimpulkan bahawa skim DCS dapat memandu motor BLDC secara dwi-arah. Analisis lanjut mendapati bahawa PID menunjukkan prestasi yang tidak memuaskan ketika keadaan beban tidak tetap. Ini adalah masalah klasik yang menyebabkan banyak teknik telah dibangunkan untuk mengatasinya, termasuklah Logik Kabur dan Rangkaian Neural Buatan. Teknik pengoptimuman menggunakan Logik Kabur adalah begitu popular kerana mudah berbanding pengawal kelajuan pintar yang lain. Kajian ini cuba untuk membangunkan pengawal BLDC baru dengan Logik Kabur, maka pengawal kelajuan Pengjadualan Logik Kabur yang diubahsuai (*M.F.G.S*) menggunakan skim DCS telah dicadangkan. Pengawal yang dicadangkan dibandingkan dengan pengawal PID dan Swa-penelaan Logik Kabur (*S.T.Fuzzy*) di bawah enam kes ujian. Pengawal yang dicadangkan telah terbukti mempunyai masa pemulihan yang paling pendek ketika perubahan daripada tanpa beban hingga 5 Nm. Pengawal ini dapat dapat pengikut perubahan kelajuan ketika perubahan kelajuan mendadak dengan mencapai steady state error terendah. Keupayaan pengawal motor BLDC untuk beroperasi dalam empat kuadran adalah satu keperluan namun kekurangan pembangunan dalam bahagian ini. Supaya motor BLDC dapat transit antara kuadran dengan lancar, keperluan untuk menentukan kedudukan motor yang ideal untuk pembalikan motor untuk mengelakkan tersekat adalah penting. Untuk menilai kebolehan pengawal yang dicadangkan, *M.F.G.S* menggunakan skim DCS telah dinilai bersama *PID* dan *S.T.Fuzzy* dibawah empat kes perubahan kuadran. Pengawal yang bangunkan mempunyai *overshoot* terkurang dan *steady state error* terkecil pada 0.015 % ketika perubahan daripada kuadran pertama ke kuadran kedua dalam keadaan berbeban. Secara keseluruhannya, *M.F.G.S* menggunakan skim DCS telah mengatasi prestasi dua pengawal kelajuan lain dalam kajian ini. Pengawal laju ini mempunyai potensi untuk digunakan sebagai pemacu dwi-arah ketika beban yang bersifat dinamik.

## ABSTRACT

Over the past decade the Brushless Direct Current (BLDC) motors have gained popularity in multiple sectors such as transportation, robotics, and automation. This is due to its high efficiency, low maintenance and high-power density. BLDC motor applications in automation, aerospace and industrial automation requires the motor to be operated bidirectionally. Although many BLDC drive controllers have been developed, most solutions are focusing only on forward motoring instead of bidirectional. A 4-quadrant BLDC controller was developed by S.Joice was the first to address this issue, although it is unclear whether the controller able to achieve bidirectional operations due to lack of evidence in the literature. To assess this bidirectional capability of S.Joice controller, a test platform was developed in MATLAB Simulink simulation. It is found that the controller is incapable of achieving reference speed in third quadrant and has 67.5 % of speed error during quadrant transient operations. To overcome this limitation, this study proposes a new BLDC commutation scheme, called direct commutation switching (DCS) scheme. A PID speed controller coupled with DCS scheme is tested for two test cases. From the test cases, it can be concluded that DCS scheme is able to drive the BLDC motor bidirectionally. Further analysis points out that the PID exhibits the typical unsatisfying performance under nonlinear load conditions. This is a classic problem that have lead many different types techniques to be developed, including Fuzzy Logic and Artificial Neural Network (ANN). Among others, fuzzy logic optimization technique is preferable due to simplicity compared other intelligent speed controller. This study attempts to develop a new BLDC controller by modifying fuzzy gain, hence proposes M.F.G.S speed controller. This proposed controller's step responses are compared to PID and S.T.Fuzzy speed controllers under six test cases. The proposed controller has the shortest recovery time during load changes from no load to 5 Nm load. It is also able to adapt with sudden speed changes by achieving lowest steady state error. As for quick reversal operation, BLDC motor requires transient capabilities between quadrants. It is necessary to determine the instance when the rotor is ideally positioned for reversal to prevent standstill position. In order to examine the quadrant transient capabilities, M.F.G.S speed controller together with PID and S.T.Fuzzy speed controllers were evaluated under four cases of quadrant transient. From the study, the M.F.G.S controller had the lowest overshoot and steady state error of 0.015 % while transiting from first quadrant to second quadrant under loaded conditions. Overall, M.F.G.S Speed Controller for BLDC outperforms the other two controllers in this study. Hence, the M.F.G.S controller has potential to be used as bidirectional drive in highly dynamic load conditions.



## TABLE OF CONTENT

<b>DECLARATION</b>	
<b>TITLE PAGE</b>	
<b>ACKNOWLEDGEMENTS</b>	<b>ii</b>
<b>ABSTRAK</b>	<b>iii</b>
<b>ABSTRACT</b>	<b>iv</b>
<b>TABLE OF CONTENT</b>	<b>v</b>
<b>LIST OF TABLES</b>	<b>viii</b>
<b>LIST OF FIGURES</b>	<b>ix</b>
<b>LIST OF SYMBOLS</b>	<b>xi</b>
<b>LIST OF ABBREVIATIONS</b>	<b>xii</b>
<b>CHAPTER 1 INTRODUCTION</b>	<b>1</b>
1.1 Overview	1
1.2 Problem Statement	2
1.3 Objectives	4
1.4 Scope and Limitations	4
1.5 Overview of the Thesis	5
<b>CHAPTER 2 LITERATURE REVIEW</b>	<b>6</b>
2.1 Introduction	6
2.2 Brushless Direct Current Motor (BLDC)	6
2.3 Speed Controllers for BLDC Motor Drives	8
2.3.1 PI Controller	9

2.3.2	PID Controller	10
2.3.3	Intelligent Speed Controller	11
2.4	Four Quadrant Operations	13
2.4.1	Four quadrant BLDC Controller	14
2.5	Summary	15
<b>CHAPTER 3 METHODOLOGY</b>		<b>18</b>
3.1	Introduction	18
3.2	Four Quadrant BLDC Speed Controller by S.Joice	20
3.3	Development of Test platform	24
3.4	Development of Direct Commutation Switching (DCS)	28
3.5	BLDC speed control techniques	35
3.5.1	PID	36
3.5.2	Self-Tuning Fuzzy PID (S.T.Fuzzy)	37
3.5.3	Modified Fuzzy Gain Scheduling (M.F.G.S)	40
3.6	Summary	44
<b>CHAPTER 4 RESULTS AND DISCUSSION</b>		<b>45</b>
4.1	Introduction	45
4.2	Verification Development of Test Platform	45
4.3	Simulation of PID controller using Direct Commutation Switching (DCS) Scheme and conventional method	48
4.3.1	Step Response of the motor for clockwise direction for No Load conditions	48
4.3.2	Step Response of the motor for counter-clockwise direction for No Load conditions	49
4.3.3	DCS Scheme overall discussion	50

4.4	Simulation of transient capabilities using DCS	51
4.4.1	Step Response of the motor for clockwise and counter-clockwise direction for No Load conditions	51
4.4.2	Step Response of the motor for step change for constant load condition of 10 Nm	53
4.4.3	Step Response of the motor for constant speed dynamic load conditions	56
4.4.4	Step Response of the motor during quadrant change for No Load conditions	60
4.4.5	Step Response of the motor during quadrant change for load condition of 10 Nm	63
4.5	Summary	66
<b>CHAPTER 5 CONCLUSION</b>		<b>67</b>
5.1	Introduction	67
5.2	Statement of Contribution	68
5.3	Recommendation for future research	68
<b>REFERENCES</b>		<b>69</b>
<b>APPENDIX A BLDC SPEED CONTROLLER</b>		<b>75</b>
<b>APPENDIX B LIST OF PUBLICATION</b>		<b>76</b>

## LIST OF TABLES

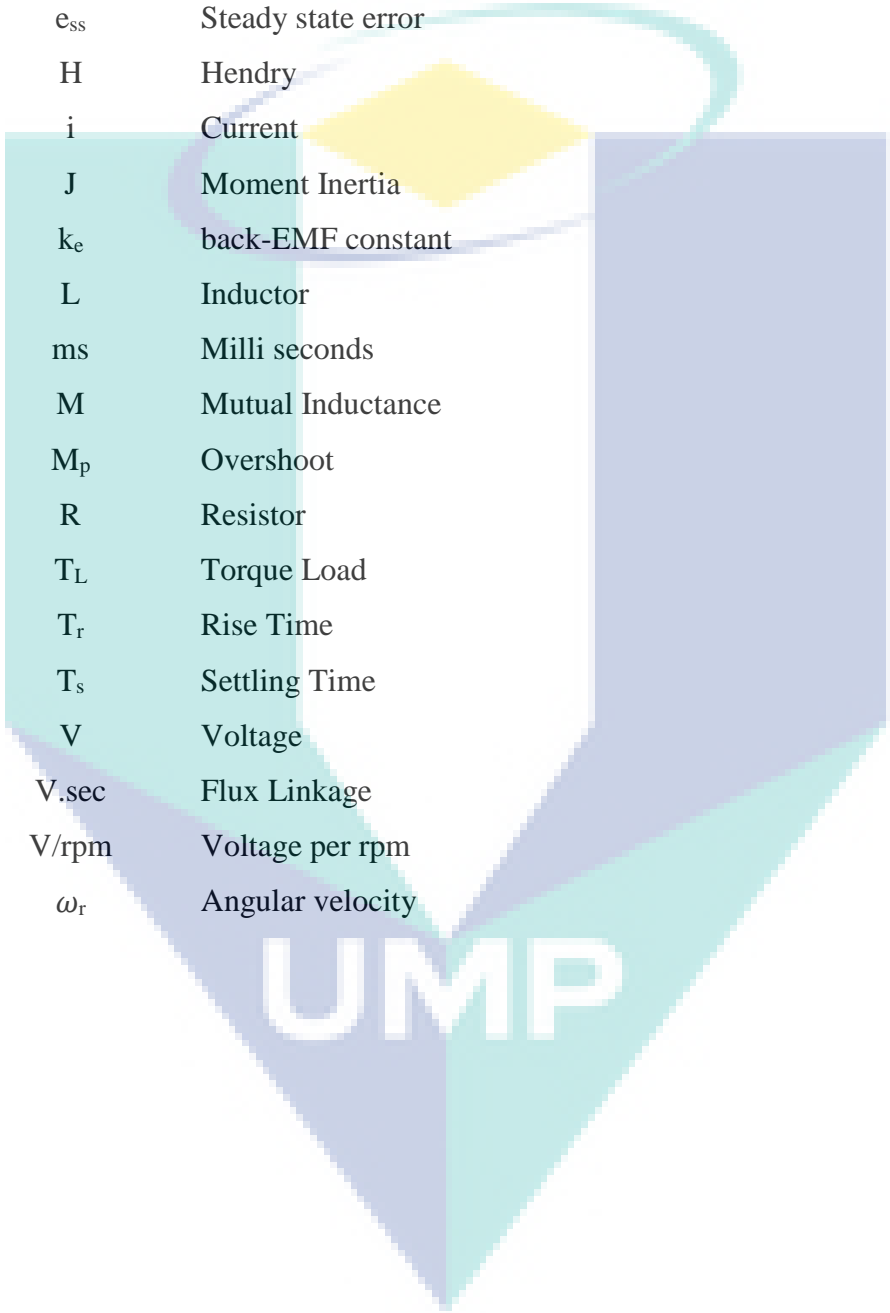
Table 2.1	Summary of literature review	16
Table 3.1	Specification of BLDC Motor	21
Table 3.2	Commutation sequence for clockwise direction	34
Table 3.3	Commutation sequence for counter-clockwise direction	34
Table 3.4	Fuzzy controller's $K_p$ , $K_i$ and $K_d$ rule table	39
Table 3.5	Fuzzy Rules for $K_p$	43
Table 3.6	Fuzzy Rules for $K_d$	43
Table 3.7	Fuzzy Rules for Alpha	43
Table 4.1	Motor response during clockwise for No Load	49
Table 4.2	Motor response during counter-clockwise for No Load	50
Table 4.3	Motor response during clockwise for No Load	53
Table 4.4	Motor response during counter-clockwise for No Load	53
Table 4.5	Motor response for the step-changing speed (a)	54
Table 4.6	Motor response for the step-changing speed (b)	54
Table 4.7	Motor response for the step-changing speed (a)	55
Table 4.8	Motor response for the step-changing speed (b)	55
Table 4.9	Motor response during 0 Nm to 5 Nm Load	56
Table 4.10	Motor response during 10 Nm to 15 Nm Load	57
Table 4.11	Motor response during 10 Nm to 5 Nm Load	58
Table 4.12	Motor response during 10 Nm to 0 Nm Load	59
Table 4.13	Motor response for the clockwise direction	60
Table 4.14	Motor response for the counter-clockwise direction	61
Table 4.15	Motor response for the counter-clockwise direction	62
Table 4.16	Motor response for the clockwise direction	62
Table 4.17	Motor response for the clockwise direction	64
Table 4.18	Motor response for the counter-clockwise direction	64
Table 4.19	Motor response for the counter-clockwise direction	65
Table 4.20	Motor response for the clockwise direction	65

## LIST OF FIGURES

Figure 2.1	Cross section of BLDC Motor	7
Figure 2.2	BLDC Torque/Speed Characteristic	8
Figure 2.3	Speed Controller of BLDC Motor	9
Figure 2.4	PI controller system used for velocity control	10
Figure 2.5	PID controller system used for velocity control	11
Figure 2.6	Four Quadrants of operations of a motor	13
Figure 3.1	Flow of research work	19
Figure 3.2	Block diagram representation of the four quadrant BLDC digital speed	20
Figure 3.3	Four quadrant BLDC speed controller in Matlab Simulink model	21
Figure 3.4	Four quadrant BLDC speed controller hardware setup	22
Figure 3.5	Matlab Simulink results	23
Figure 3.6	Hardware results	23
Figure 3.7	BLDC motor electrical circuit representation showing the interconnection of the phase resistance and inductance	24
Figure 3.8	Testing platform MATLAB simulation model	27
Figure 3.9	Hall sensor output and EMF waveform of BLDC motor drive	29
Figure 3.10	Back-EMF during clockwise direction from MATLAB	31
Figure 3.11	Back-EMF during counter-clockwise direction from MATLAB	31
Figure 3.12	Hall effect sensor output during CW directions using MATLAB	32
Figure 3.13	Hall effect sensor output during CCW directions using MATLAB	32
Figure 3.14	Hardware setup for Halls sensors data collection	33
Figure 3.15	Hall effect sensor output during clockwise directions using actual BLDC motor	33
Figure 3.16	Direct commutation switching scheme controller	34
Figure 3.17	BLDC speed controller techniques used in this study	35
Figure 3.18	PID Speed control system	36
Figure 3.19	Self-Tuning Fuzzy PID Speed control system	37
Figure 3.20	Membership function for $e(k)$ and $\Delta e(k)$	38
Figure 3.21	Membership function for $\Delta K_p$ , $\Delta K_i$ and $\Delta K_d$	39
Figure 3.22	Modified Fuzzy Gain Scheduling Speed control system	40
Figure 3.23	Degree of membership of $e(k)$ and $\Delta e(k)$	41
Figure 3.24	Degree of membership for $K_p$ and $K_d$	42


Figure 3.25	Degree of membership for alpha	42
Figure 4.1	The Matlab results obtained by the original developer	46
Figure 4.2	The Matlab results obtained using the test platform	46
Figure 4.3	The hardware results obtained by the original developer	47
Figure 4.4	The hardware results obtained using the test platform	47
Figure 4.5	Motor respond during clockwise directions for NL conditions	48
Figure 4.6	Motor respond during counter-clockwise directions for NL conditions	50
Figure 4.7	Motor speed response during No Load for clockwise direction	52
Figure 4.8	Motor speed response during no load for counter-clockwise direction	52
Figure 4.9	Motor speed response during clockwise direction for 10 Nm	53
Figure 4.10	Motor speed response during counter-clockwise direction for 10 Nm	55
Figure 4.11	Motor speed response during 0 Nm to 5 Nm Load for clockwise direction	56
Figure 4.12	Motor speed response during 10 Nm to 15 Nm Load for clockwise direction	57
Figure 4.13	Motor speed response during 10 Nm to 5 Nm Load for clockwise direction	58
Figure 4.14	Motor speed response during 10 Nm to 0 Nm Load for counter-clockwise direction	59
Figure 4.15	Motor speed response during No Load for direction change from clockwise to counter-clockwise direction	60
Figure 4.16	Motor speed response during No Load for direction change from counter-clockwise to clockwise direction	62
Figure 4.17	Motor speed response during 10 Nm Load for direction change from clockwise to counter-clockwise direction	63
Figure 4.18	Motor speed response during 10 Nm Load for direction change from counter-clockwise to clockwise direction	65

## LIST OF SYMBOLS



$\Delta e(k)$	Rate of Error
B	Frictional Coefficient
D	Duty Cycle
$e_{ss}$	Steady state error
H	Hendry
i	Current
J	Moment Inertia
$k_e$	back-EMF constant
L	Inductor
ms	Milli seconds
M	Mutual Inductance
$M_p$	Overshoot
R	Resistor
$T_L$	Torque Load
$T_r$	Rise Time
$T_s$	Settling Time
V	Voltage
V.sec	Flux Linkage
V/rpm	Voltage per rpm
$\omega_r$	Angular velocity

## LIST OF ABBREVIATIONS



AC	Alternating Current
ANN	Artificial Neural networks
BA	Bat algorithm
BLDC	Brushless Direct Current Motor
CCW	Counter-clockwise
CW	Clockwise
DCS	Direct commutation switching
EMF	Electro Magnetic Force
F.G.S	Fuzzy Gain Scheduler
FL	Full Load
FLC	Fuzzy Logic Control
GA	Genetic Algorithm
Kd	Derivative gains
Ki	Integral gain
Kp	Proportional gain
M.F.G.S	Modified Fuzzy Gain Scheduler
NB	Negative Big
NL	No Load
NM	Negative Medium
NS	Negative Small
PB	Positive Big
PI	Proportional Integral
PID	Proportional Integral derivative
PM	Positive Medium
PS	Positive Small
PSO	Particle Swarm Optimization
RPM	Revolution per minute
SA	Simulated Annealing
ZN	Ziegler & Nichols
ZO	Zero (Z0)



## CHAPTER 1

### INTRODUCTION

#### 1.1 Overview

Brushless Direct Current (BLDC) motor is an electronically commutated machine. Instead of utilizing brush as commutator as in DC motor, it is using sequential phase energization to drive the motor. BLDC motors have several advantages over conventional brushed motors and induction motors. Some of these advantages are; high power density, better speed versus torque characteristics, high dynamic response, high efficiency, long operating life, noiseless operation and higher speed ranges (Nag, Chatterjee, Ganguli, Santra, & Chatterjee, 2016; Zhou, Chen, Zeng, & Tang, 2017).

Due to their favourable electrical and mechanical properties, BLDC motors are widely used in servo applications such as automotive, aerospace, medical, instrumentation, actuation, robotics, machine tools, and industrial automation equipment (Premkumar & Manikandan, 2013). From a study report in Global Brushless DC Market 2016-2020, it was forecasted the demand for BLDC motor globally is at a CAGR of 12.91% during the period 2016-2020 (TechNavio, 2016).

With the increment of demand for BLDC motor the electrical drive plays an important role to cater for the variety of applications. BLDC motor's applications in transportation, aerospace and industrial automation requires the motor to be operated bidirectionally (Larminie & Lowry, 2003). However, most developed controllers' emphasis on forward motoring only. Therefore, it is uncertain how the developed controllers will perform during speed reversal.

As for the speed controller, classical controllers such as Proportional Integral (PI) and Proportional Integral Derivative (PID) are commonly used in industries due to their simplicity and ease of implementation (Premkumar & Manikandan, 2015a). However, during dynamic load conditions or disturbance in the system occurs the performance of the classical controller declines. This performance issue directly affects the efficiency of the BLDC motor (Ramya, Imthiaz, & Balaji, 2016; Zhang & Wang, 2016).

To improve the performance of classical BLDC motor drive, intelligence controllers such as fuzzy logic, Genetic Algorithm (GA) and Artificial Neural Network (ANN) were developed (Hentunen, Suomela, Leivo, Liukkonen, & Sainio, 2011; Vikkaraga, 2014). Fuzzy Logic based controllers have many advantages compared to other intelligence controllers in terms of complexity and computational time. Furthermore, it does not require an exact mathematical model of the system and therefore, it is less sensitive to the system parameter changes. Design objectives that are difficult to express mathematically can be easily incorporated into a fuzzy controller by linguistic rules that makes it to be the preferred intelligent controller (Premkumar & Manikandan, 2013; Usman & Rajpurohit, 2016).

On the other hand, a high speed four quadrant application that utilizes BLDC motor requires the motor to transient between quadrants for fast reversal. However, without proper controller to allow the motor to transient between quadrant could force the motor to a standstill position (Joice, Paranjothi, & Kumar, 2013). This will greatly affect the motor's efficiency and life span.

Hence a controller that able to achieve bidirectional capabilities for dynamic load conditions are required to sustain the ever-growing demand of BLDC motor for various applications.

## **1.2 Problem Statement**

As the application demand for BLDC motors increase, the need for an efficient BLDC controller also increases. However, most developed controller emphasizes on forward motoring only and uncertainty on how the developed controller will perform during reversal has become an alarming issue especially for application that require bidirectional capabilities. Furthermore, there is limited amount of literature on motor

reversal to suggest that conventional BLDC controller will be able to operate for all four quadrant operations.

Conventional controllers such as PI and PID are commonly used in industries due to their simplicity and ease of implementation (Premkumar & Manikandan, 2015a). However, the parameter deviation and uncertainties that occur during the sudden speed change or dynamic load applied causes the conventional controller's performances to deteriorate is an emerging problem especially in load varying conditions. Fuzzy logic has been utilized into BLDC motor's controller to cater the varying load/dynamic load conditions and fuzzy logic outperforms the PID controller in regards to overshoot and settling time (Premkumar & Manikandan, 2013). Yet, it is unclear how this optimization technique will perform in improving the response time of BLDC in dynamic load in both first and third quadrant operations.

High speed four quadrant application that utilizes BLDC motor requires the motor to transient between quadrants for fast reversal however lack of development and testing in this area. To address this issue, a digital speed control using PI for four quadrant was proposed by (Joice et al., 2013). The developed controller was able to achieve quadrant 2 operations but with high rate of error between reference speed and actual speed. Furthermore, results shown in the study only shows 2 quadrant operations and not four quadrant operations.

The necessity to determine the instance when the rotor of the machine is ideally positioned for reversal as the motor is forced to a standstill position when reversal command due to control error was address by both authors (Joice et al., 2013; Suganya & Rameshkumar, 2014). Without a proper controller to allow the motor to transient between quadrant, it could affect the motor's efficiency (Park, Kim, Ahn, & Hyun, 2003; Sivarani, Jawhar, & Kumar, 2016).

Hence, this study to develop a controller that can achieve bidirectional capabilities for dynamic load conditions is required to sustain the ever-growing demand of BLDC motor for various applications has become the motivation of the study.

### 1.3 Objectives

The aim of this research is to develop optimized speed controller for BLDC motor to operate in four quadrant and tackle speed control problem in load varying conditions.

The specific objectives of this study are:

- i. To assess the 4-quadrant dynamic performance of currently available PI BLDC speed control for BLDC motor.
- ii. To develop direct commutation scheme (DCS) that allows BLDC motor to operate bidirectionally using classical PI speed controller.
- iii. To further improve the step-respond time and transient capabilities of the developed BLDC controller using Modified Fuzzy Gain Scheduling (M.F.G.S) speed controller and achieve seamless speed reversal.

### 1.4 Scope and Limitations

This study focuses at a specific scope and bound by limitations. This study covers the overall study of BLDC motor; from grid connected supply, BLDC Motor, and converters. The focus of the study is on the Controller Algorithm. The converters are not part of the study as well as the power generated during regeneration conditions of the motor. The model of BLDC used are Permanent Magnet Synchronous Machine and the settings follows the developed by (Joice et al., 2013).

For the study of the algorithm, conventional ZN-Tuned PID and Self-Tuning Fuzzy controller are included in the study. The improved algorithm will be evaluated with several test cases such as constant speed during no load condition, constant speed during full load condition, constant speed with speed during no load to full load condition, constant speed with speed during full load to half load condition, step-changing speed during full load conditions and varying direction during full load conditions to ensure smooth operation of BLDC in all four quadrants.

## 1.5 Overview of the Thesis

This study comprises of two parts. The first part is to develop the test platform in MATLAB based on the study done by (Joice et al., 2013) and assess the results from the test platform. While, the second part deals with different speed control technique developments. Chapter 1 briefly discusses the introduction of BLDC motor and conventional BLDC speed controller techniques This chapter also highlights the problem and objective that need to be carried out in this study. Chapter 2 discusses related literatures related to the study along with the review of various journals, articles, and books. The literature in this study focuses on the BLDC motor, the speed controller techniques and different types of algorithm that potentially could solve problems in this study. Methodology of this study is discussed in Chapter 3. This includes the development of test platform and algorithms to solve the problem and satisfy the objective of the study. In Chapter 4, the results obtained from the developed controller scheme for several test cases. The results were represented in graphs and tables, the results were discussed. In Chapter 5, the study was summarised and concluded based on the proposed methodology and results obtained during the study. Future recommendations for this study were also included in Chapter 5.

The logo of Universiti Wawasan Putrajaya (UWP) is a large, stylized 'V' shape composed of four overlapping triangles in shades of teal and light blue. The letters 'UWP' are printed in white, bold, sans-serif font across the center of the 'V' shape.

UWP

## CHAPTER 2

### LITERATURE REVIEW

#### 2.1 Introduction

Brushless Direct Current (BLDC) Motor made a breakthrough in 1960s due to the advancements in solid state technology and better permanent magnet materials (Wilson & Trickey, 1962). BLDC motors were preferred due to high power density, higher efficiency and lower susceptibility to mechanical wear compared to brushed DC motor (Concari & Troni, 2010; Davoudkhani & Akbari, 2016; Jang, Park, & Chang, 2002). However, more complex, and expensive controllers were required to drive this type of motor.

Despite the increase for the demand of BLDC motor in past decade, the challenge of good speed controller to drive the BLDC motor in variable conditions still exists. In this chapter, the characteristic of the BLDC motor, techniques of BLDC speed controller and four quadrant operations were discussed.

#### 2.2 Brushless Direct Current Motor (BLDC)

Brushless DC (BLDC) motors are used widely in the industrial sector such as in the automotive, aerospace, and industrial automation equipment and instrumentation due to high reliability, high efficiency, low maintenance and many advantages (Premkumar & Manikandan, 2015a). In addition, the ratio of torque delivered to the size of the motor is higher, making it useful in application where space and weight are critical factors. The cross section of BLDC is depicted in Figure 2.1.

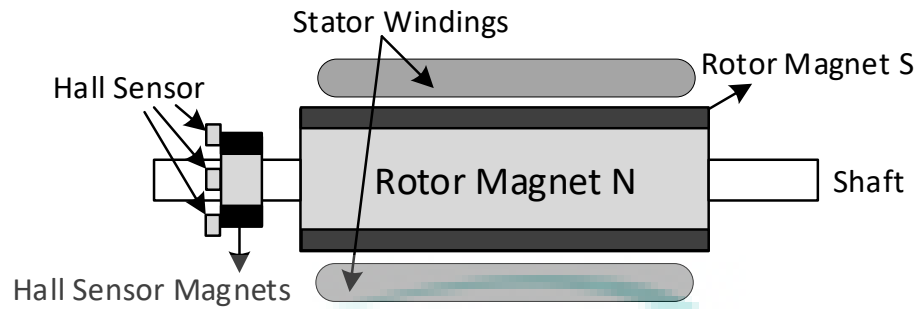


Figure 2.1 Cross section of BLDC Motor

Source: Shamseldin (2016)

BLDC motor was developed based on brushed DC motor design and did not receive positive response due to lack of proper commutation device (Brailsford Harrison D, 1955). However, with the development of hall sensor in 1962, it has paved the pathway for productization for BLDC motor using electronic commutations. For a BLDC motor, alternating current (AC) does not means a sinusoidal waveform but a bi-directional current with no restriction on waveform.

Electronic commutation of a BLDC motor is where; the stator winding is energized in a sequence to rotate it. Winding energization sequence is based on rotor position (Concari & Troni, 2010). Three or more hall sensors are used to obtain the rotor position and speed measurement for a sensor-ed BLDC motor.

The hall sensors coupled with trapezoidal or rectangular voltage drives the BLDC motor (Hanselman, 2003; Vikkaraga, 2014). A closed loop speed controller required to ensure the motor operates at a desired speed and direction. The design of BLDC motor is simpler as it eliminates the complication power transfer to the spinning motor from outside the motor.

In fact, the torque of the BLDC motor is mainly influenced by the waveform of back-EMF (the voltage induced into the stator winding due to rotor movement). Ideally, the BLDC motors have trapezoidal back-EMF waveform and are fed with rectangular stator currents, which give a theoretically constant torque. Figure 2.2 shows the BLDC Torque/Speed Characteristic. By referring to Figure 2.2, BLDC motor can be divided into Peak torque (TP) and Rated Torque (TR). The motor can sustain up to the rated torque during continuous operations.

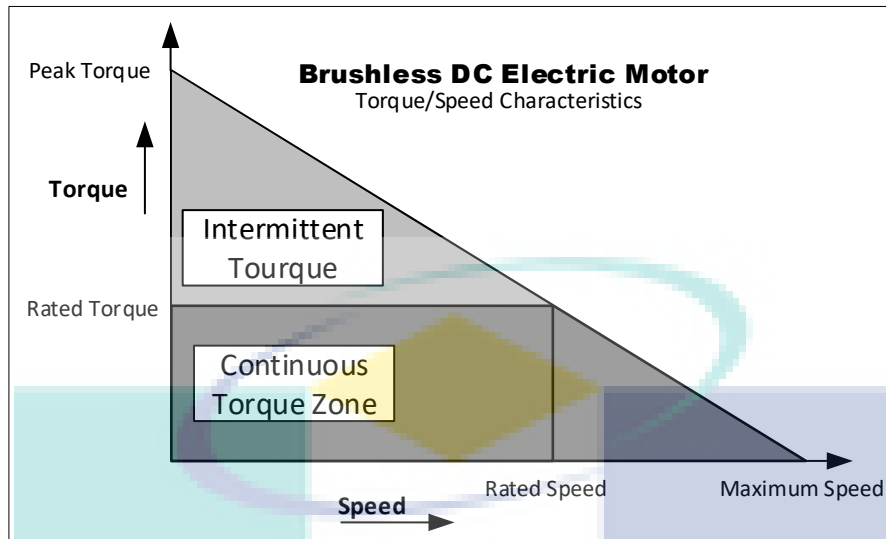


Figure 2.2 BLDC Torque/Speed Characteristic  
 Source: Aris & Adiimah (2011)

In a BLDC motor, the torque remains constant for speed range up to rated speed. It is capable to run up to the 150 % higher than rated speed but the torque drops to compensate it (Pillay & Krishnan, 1988). This shows that the controller must be able to cater this torque/speed characteristics of the BLDC motor to maintain the efficiency of the motor.

Regardless the efficiency of design of BLDC motor, improper BLDC motor control design reduces the overall performance of the motor. This has caused a momentum to develop a controller that could able to fully utilized the BLDC motor.

### 2.3 Speed Controllers for BLDC Motor Drives

In this section, various existing BLDC speed control techniques will be discussed as many speed controller techniques were developed to cater to the BLDC motor operations through the years such as PID, PI and intelligent controllers. Commonly used BLDC speed control system as shown in Figure 2.3 has many techniques to obtain optimal speed control.



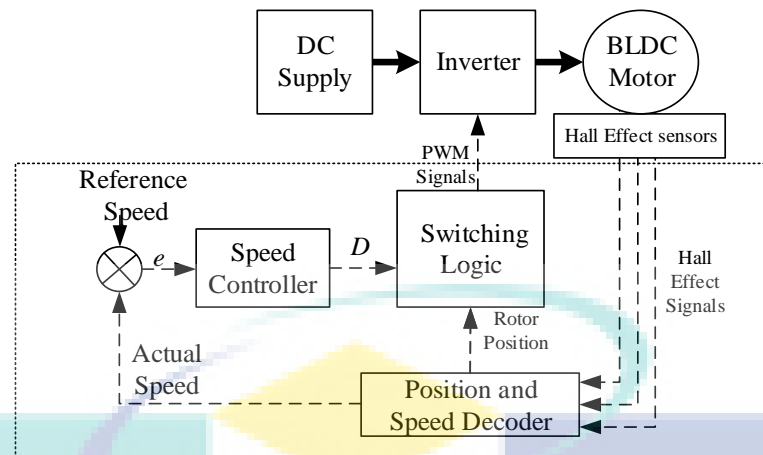


Figure 2.3 Speed Controller of BLDC Motor

### 2.3.1 PI Controller

Proportional ( $P$ ) controller was first developed by Foxboro Company for a pneumatic system in 1919. This controller had problems due to the high gain which required the system to be split into two different controls that increases the cost and increase the system wear as it was sensitive to fluctuations of air pressure (Bennett, 1996).

In order to overcome this issue, an automatic control system that combines two actions of control of proportional step and integral action that became PI controller was utilized (Morris E. Leeds, 1920). However, this proposed system has its limitations where the control limits need to be sacrificed to cater for the throttling action as the PI controller utilizes two parameters; the proportional gain ( $K_p$ ) and integral gain ( $K_i$ ) (Ho, Hang, & Cao, 1992).

The proportional gain ( $K_p$ ) produces the output which is proportional to the current error value. However, if the value of the  $K_p$  is very high the system becomes unstable. To keep the  $K_p$  value in check without compromising the system stability the integral gain ( $K_i$ ) is used to accumulate a steady state error and provide slow response (Hagglund, 1992). PI controllers are usually designed by ignoring the non-linearity in a linear region (Shin, 1998). The PI controller system used for velocity control is shown in Figure 2.4.

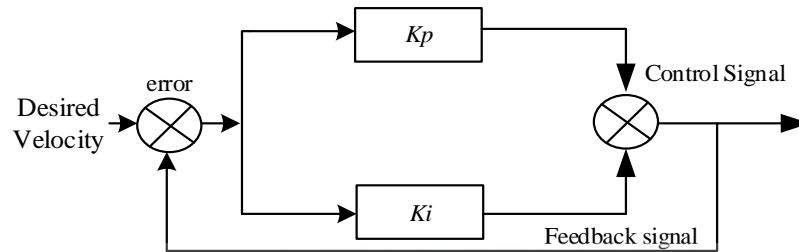


Figure 2.4 PI controller system used for velocity control

### 2.3.2 PID Controller

To overcome the limitations of the developed PI controllers for closed loop control systems, a PID controller was proposed by Minorsky (1922). Commonly used PID controller for velocity control is shown in Figure 2.5. The PID controller utilizes the proportional gain ( $K_p$ ) and integral gain ( $K_i$ ) similar to a PI controller. In contrast, it has derivative gains ( $K_d$ ) that control the rate of changes in measured variables. This development enabled for a faster response system as the tuning of the gain was using heuristic method.

Heuristic method used to tune the PID controller was optimal but it was time consuming and costly (Hazen, 1934; Hughes, 1971). In order to address this issue, Ziegler and Nichols (1942) developed two methods to obtain the optimized value for the PID controller. Ziegler-Nichols (ZN) Tuned PID controller was implemented in many controllers due to the simplicity and easy to tune. However, this types of controller required some manual tuning as the ZN optimization method neglected the process lag during development (Bennett, 2001; Hazen, 1934).

To improve the controller's response during the damped closed-loop system, Chien, Hrones and Reswick (CHR) tuning method was utilized and response time was improved during 0 % load but the response was similar to ZN-Tuned method during 20 % load. This allowed the ZN tuning method to be preferred due to the simplicity and less complex compared to other tuning method for a PID controller (Araki, 2009). PID controller's performances deteriorates during non-linear conditions outside tuned conditions. This is an emerging problem especially if precision control is required. The performance deterioration is due to the fixed values of gains for the PID controller (Xia, Guo, Shi, & Wang, 2004).

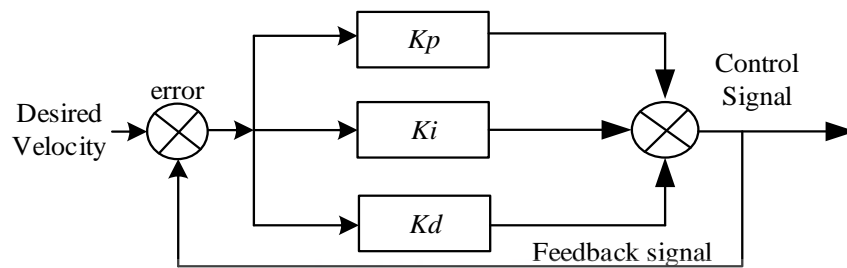


Figure 2.5 PID controller system used for velocity control

### 2.3.3 Intelligent Speed Controller

PI and PID controller are preferred and required manual tuning to achieve optimized control (Premkumar & Manikandan, 2013), however due to uncertainty performance during the non-linear condition has become an emerging problem especially for precision applications due to manual tuning (Krohling & Rey, 2001). Another setback for PID controllers, it requires an accurate mathematical model and system response for each design (Navaneethakkannan & Sudha, 2012). To overcome the PI and PID controller weakness, research focusing on intelligent control has increased in last era. In this section, various existing intelligent BLDC speed control technique's will be discussed.

Fuzzy controller utilizing self-tuning capabilities replaces the fixed values gains of the PID controller. Thus, with varying values of the gains based on the fuzzy rules had improved the settling time and overshoot. However, this system is suitable to be used for the positional controller and not for velocity controller as it uses peak values to modify the fuzzy rules (Woo, Chung, & Lin, 2000).

To improve the PID controller's limitations while sustaining a stable control during linear and non-linear conditions, an adaptive fuzzy control using state and output feedback was deployed Rigatos (2009). Two separate controllers were required to produce an accurate and stable feedback to the system which increase the cost and complexity of the system (Feng, Yu, & Han, 2013).

Genetic Algorithm (GA) optimized controller proposed by Ansari and Alam (2011) was much more efficient than PI controller in terms of rise time, settling time, and overshoots set point tracking. However, the GA optimized controller requires large computation time for optimal operations. This is a drawback as most preferable is fast acting controller.

Fuzzy logic controller for BLDC motor used to generate current reference was able to improve the step response for the BLDC compared to PI controller. However, there was no testing for loaded conditions as PI controller's limitation was during the non-linear conditions (Blessy & Murugan, 2014).

Neuro-fuzzy speed controllers for BLDC was proposed by Premkumar and Manikandan (2014) and Prabu, Poongodi, and Premkumar (2016) displayed better control compared to the previously developed controllers due to system's ability to learn. The setback of this system is it required heavy computation and the hardware is difficult to be implemented as many sensors are required for smooth operations.

ANN based speed controller gives better results than PI controllers in terms of the speed, torque, current and back-EMF in a very short span of time with accurate outputs. Conversely, ANN required some training before it can provide accurate and fast performance (Ch & Palakeerthi, 2015; Leena & Shanmugasundaram, 2014). Thus, the ANN system requires heavy computation and the hardware is difficult to implement due to the complexity (Prabu et al., 2016).

To further improve the abilities of BLDC's speed controllers, a nature inspired algorithm was introduced by Premkumar and Manikandan (2015) and a Hybrid Self Tuned Fuzzy PID BLDC speed controller was proposed by Ramya, Imthiaz, and Balaji (2016) has shown to improve the steady state error and more robust to dynamic load changes however high computation time is required which make it not desirable.

Although most of the developed controllers was able to surpass the limitations of the PID controllers however, the developed controllers were only for motor's forwarding mode despite growth of BLDC motor in industrial and transport (Ahmed, Topalov, Dimitrov, & Bonev, 2016). Furthermore, the lack of literature on BLDC bidirectional capabilities and it is unclear if the existing controllers can operate for bidirectionally has become the motivation for this study.

## 2.4 Four Quadrant Operations

There are four possible modes or quadrants of operation using a Brushless DC Motor which is depicted in Figure 2.6. When BLDC motor is operating in the first and third quadrant, the supplied voltage is greater than the back emf which is forward motoring and reverse motoring modes respectively, but the direction of current flow differs. When the motor operates in the second and fourth quadrant the value of the back emf generated by the motor should be greater than the supplied voltage which are the forward braking and reverse braking modes of operation respectively, here again the direction of current flow is reversed.

The BLDC motor is initially made to rotate in clockwise direction, but when the speed reversal command is obtained, the control goes into the clockwise regeneration mode, which brings the rotor to the standstill position. Instead of waiting for the absolute standstill position, continuous energization of the main phase is attempted.

This rapidly slows down the rotor to a standstill position therefore, there is the necessity for determining the instant when the rotor of the machine is ideally positioned for reversal (Joice et al., 2013; Sanita & Kuncheria, 2013).

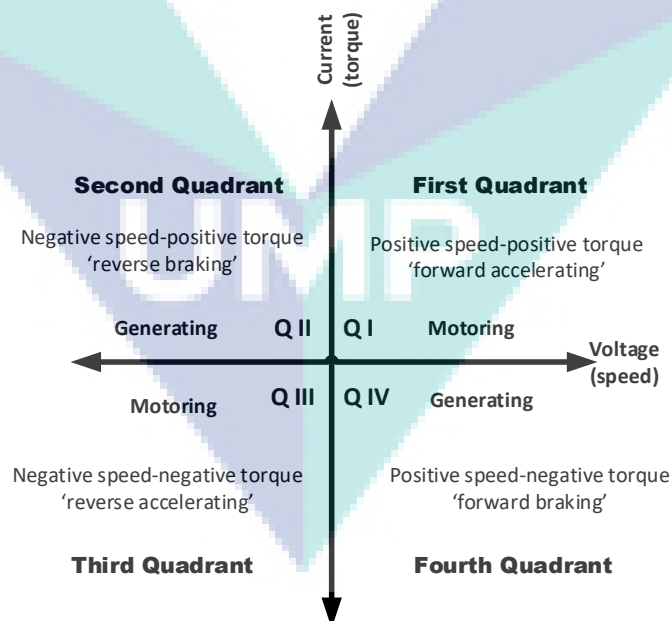


Figure 2.6 Four Quadrants of operations of a motor

### 2.4.1 Four quadrant BLDC Controller

As most developed controllers developed focuses on speed control and operation ranges, applications that require fast and accurate four-quadrant importance was first addressed by Schauder and Caddy (1982). The proposed method solely focuses on the inverter and not for a BLDC motor operation. Four-quadrant brushless dc motor drive for satellite stability. This controller claimed to achieve four quadrant operations with reversal capabilities despite lack of evidence was provided by US4644234 A (1987).

Four-quadrant BLDC motor drive using sensor less control algorithm was proposed by Matsui and Shigyo (1992). This controller was able to drive the motor for all four-quadrant operations with reversal capabilities but it required all the information such dead time, dc voltage and PWM pattern for the drive BLDC motor. Hence, for smooth operations using this controller a fast-complex mathematical computations and additional sensors are required.

Sensor-ed BLDC motor drive using Neural Network was able to achieve four quadrant operations. However, this method experiences large current oscillation and it needs to be trained for optimal performance (Senjyu, Urasaki, & Uezato, 1997). Low cost four-quadrant BLDC motor driver uses one switch to control motor's operation but it is only able to control a quadrant at a time and speed reversal was not achieved (Krishnan, Park, & Ha, 2005).

A four quadrant BLDC controller using dsPIC for applications that require quick reversal was developed Joice (2011). Although the developed scheme was for four quadrant operations but only bidirectional capabilities without any load variations was discussed. However, during this study an emerging problem where the motor slows down to a standstill position during counter-clockwise direction was attempted. This problem was also discovered by Suganya and Rameshkumar (2014).

To solve this emerging problem along with PID controllers dynamic load problem, (Joice et al., 2013) proposed a digital control strategy with load variation for four quadrant operations. The developed controller was able to achieve four quadrant operations with load variations. However, the system was not producing preferred results as 48 % of speed error was obtained during second quadrant operations.

Position control using Fuzzy Logic for four quadrant operations was developed by Manikandan and Arulmozhiyal (2016). The controller was able to achieve four quadrant operations individually but it is unclear how it operates during quadrant transient.

Many controllers were able to achieve four quadrant operations individually and not many have attempted quadrant transient. During quadrant transient, there is the necessity for determining the instant when the rotor of the machine is ideally positioned for reversal (Joice et al., 2013; Sanita & Kuncheria, 2013) as it will cause the motor to standstill due to control error. This is an emerging problem as it will greatly affect the motor's efficiency and life span (Kamal, Thyagarajan, Selvakumari, & Kalpana, 2017).

## **2.5 Summary**

This chapter explained the constructions of BLDC motor and control techniques that have been developed to drive the BLDC motor. For the BLDC speed controller, various control optimization techniques were discussed. The control techniques can be divided into two main categories which they were; conventional and intelligent controller.

For conventional BLDC motor controllers, PI and PID are commonly used due to the simple design and easy to be implemented but this type of controller requires manual tuning. Conventional controller requires an accurate mathematical model and system response for each design in order to operate in optimal conditions. Furthermore, a conventional controller's performances deteriorate during the non-linear conditions such as speed variations and dynamic load conditions outside tuned conditions. This is an emerging problem especially if precision control is required. The performance deterioration is due to fixed values of gains for the PI and PID controllers.

For intelligent controllers, Fuzzy Logic based controller was most commonly used for the optimization technique due to the simplicity and faster computation compared to the other optimization techniques such as Neuro based optimization and swarm intelligent. Although most of the developed controllers were able to surpass the limitations of the PID controllers, the developed controllers were only focusing on forwarding mode despite growth of BLDC motor in industrial and transport that require bidirectional applications. Furthermore, lack of literature on BLDC bidirectional

capabilities and it is unclear if the existing controllers can operate for bidirectionally has become the motivation for this study.

Most developed controllers developed focuses on speed control and operation ranges, applications that require fast and accurate four-quadrant importance such satellite stability and spindle machine was neglected. Most four quadrant BLDC controllers developed were able to achieve the four quadrant operations by utilizing individual quadrant control and not many had attempted quadrant transient. Admittedly, during quadrant transient there is the necessity to determine the instant when the rotor of the machine is ideally positioned for reversal as it will cause the motor to a standstill position if control error occurs. This is an emerging problem as this greatly affect the motor's efficiency while quadrant transient allows for faster speed reversal.

Table 2.1 Summary of literature review

Previous works	Achievements	What is need to improve
PI and PID controllers (Araki, 2009)	Simple and easy to implement	Require manual tuning and the performance declines during non-linear
Adaptive fuzzy control using state and output feedback (Davoudkhani & Akbari, 2016)		Focuses on forward motoring only despite the growth of BLDC motor dependency in industry and transport that require bidirectional operations.
Genetic Algorithm (GA) optimized controller (Ansari & Alam, 2011)	Better performance than PI and PID controllers during non-liner conditions	
Neuro-fuzzy speed controller (Premkumar & Manikandan, 2013)		Lack of literature on BLDC bidirectional capabilities and unclear if existing controller can operate bidirectionally
ANN based speed controller (Ch & Palakeerthi, 2015)		
Nature inspired algorithm (Premkumar & Manikandan, 2015a)		



Table 2.1 Continued

Previous works	Achievements	What is need to improve
<p>Four-quadrant BLDC motor drive using sensor less control (Matsui and Shigyo 1992)</p>	<p>Able to drive the motor for all four-quadrant operations utilizing individual quadrant control</p>	<p>Applications that require fast and accurate four-quadrant importance such satellite stability and spindle machine was neglected.</p>
<p>Sensor-ed BLDC motor drive using Neural Network (Senjyu et al., 1997).</p>	<p>Developed controller focuses on speed control and operation ranges</p>	<p>The four quadrant operations were achieved by utilizing individual quadrant control and not many had attempted quadrant transient</p>
<p>Four quadrant BLDC controller using dsPIC (Joice 2011)</p>	<p>Developed controller focuses on speed control and operation ranges</p>	<p>The necessity to determine the instant when the rotor of the machine is ideally positioned for reversal as it will cause the motor to a standstill position if control error occurs</p>
<p>Digital control strategy with load variation for four quadrant operations (Joice et al., 2013)</p>	<p>Developed controller focuses on speed control and operation ranges</p>	<p>The necessity to determine the instant when the rotor of the machine is ideally positioned for reversal as it will cause the motor to a standstill position if control error occurs</p>

## CHAPTER 3

### METHODOLOGY

#### 3.1 Introduction

In this chapter, the methodology used in the study to achieve the targeted objectives within the scopes of studies is discussed. The study was split into three segments. The first segment is to develop a BLDC motor speed controller test platform based on the design of (Joice et al., 2013) which includes the modelling of the BLDC motor in MATLAB Simulink and verified the results by comparing with author's results.

The second segment is to develop a controller that allows the BLDC motor to operate bidirectionally during nonlinear loads and transient capabilities using conventional speed control technique. Direct commutation switching (DCS) scheme was proposed to address this issue and the performance of the proposed scheme was assessed.

The final segment is to develop a speed control technique that has better step respond time and transient capabilities compared to existing BLDC speed control techniques such as PID and Self-Tuning Fuzzy using MATLAB Simulink. Fuzzy Gain Scheduling (FGS) technique by (Zhao, Tomizuka, & Isaka, 1993) was adopted and examined its performance as speed controller technique. In order improve the performance of the FGS speed controller, a Modified Fuzzy Gain Scheduling (MFGS) method was developed and the performance was examined. The Figure 3.1 shows the flow of research work used in this study.

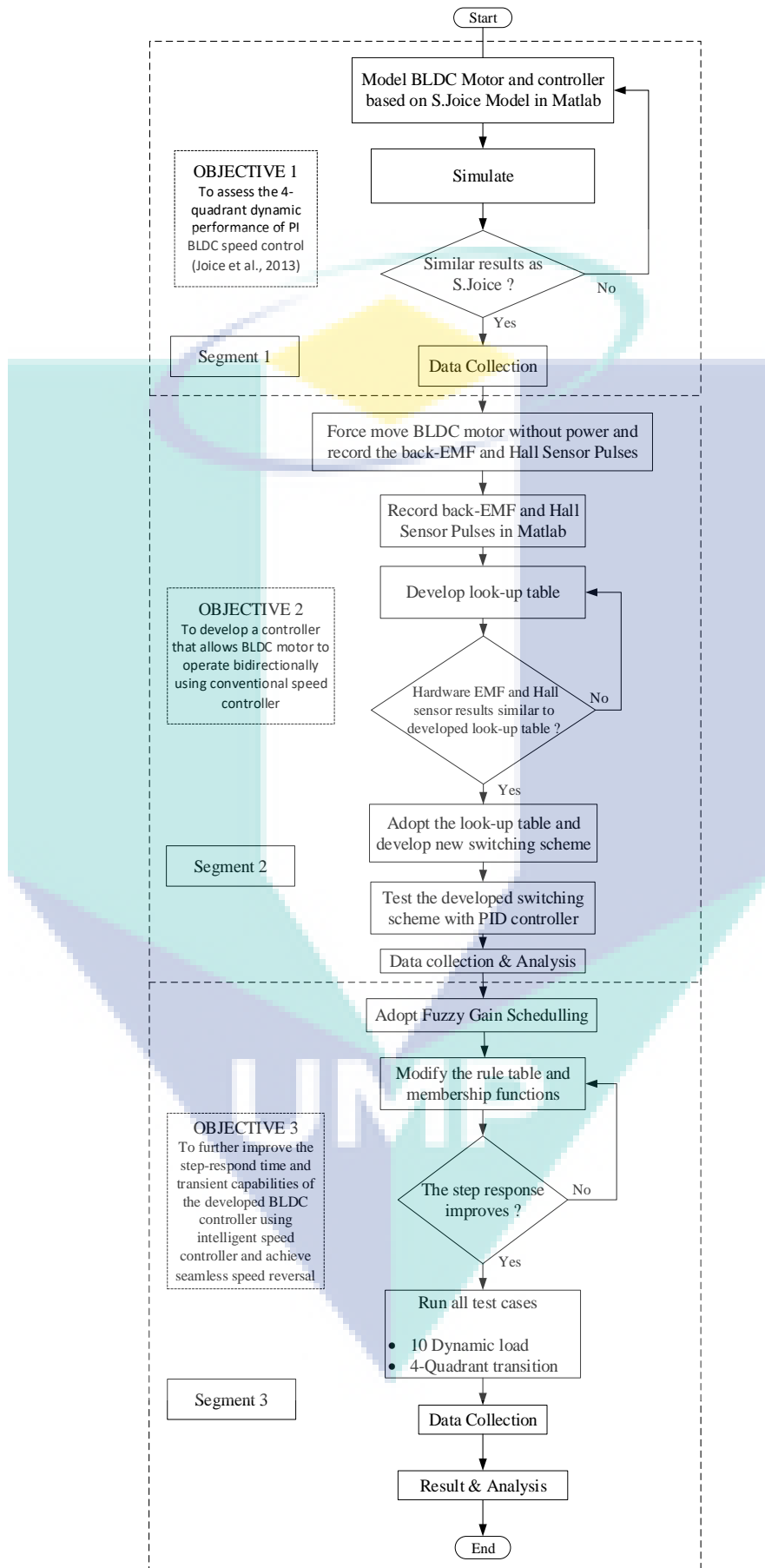


Figure 3.1 Flow of research work

### 3.2 Four Quadrant BLDC Speed Controller by S.Joice

The block diagram representation of the four quadrant BLDC digital speed controller by (Joice et al., 2013) shown in Figure 3.2. The Matlab simulated part of developed four quadrant BLDC digital speed controller consists models of a BLDC motor, PI controller, Pulse Width Modulated (PWM) module, 3-phase inverter (3-level IGBT Bridge), rectifier circuit and a battery. The four quadrant BLDC speed controller in Matlab Simulink model is as shown in Figure 3.2. While hardware implementation consists of a BLDC motor, 3-phase inverter circuits, dsPIC, relay circuit and a battery. The four quadrant BLDC speed controller hardware setup is as shown in Figure 3.4. The BLDC motor's specifications are as shown in Table 3.1.

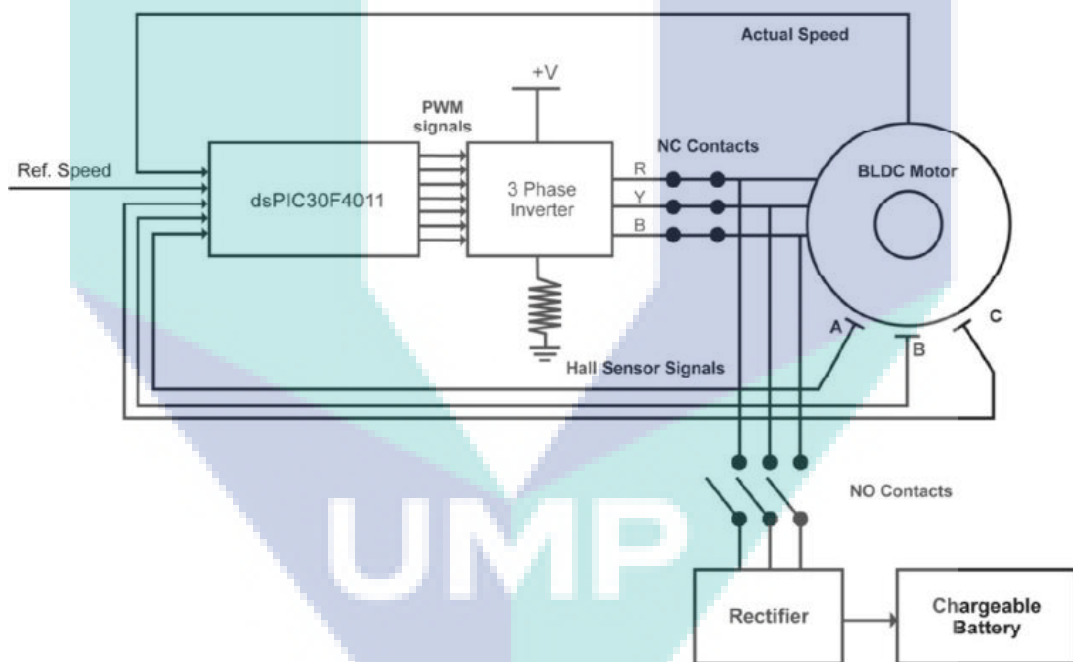


Figure 3.2 Block diagram representation of the four quadrant BLDC digital speed

Table 3.1 Specification of BLDC Motor

Specification	Value
Stator phase resistance R (ohm)	2.875
Stator phase induction L (mH)	1.0
Flux linkage established by magnets (V.sec)	0.175
Voltage Constant (V/rpm)	0.1466
Torque Constant (N.m/A)	1.4
Moment of Inertia (kg.m <sup>2</sup> /rad)	0.0008
Friction Factor (N.m/(rad/sec))	0.001
Pole pairs	4

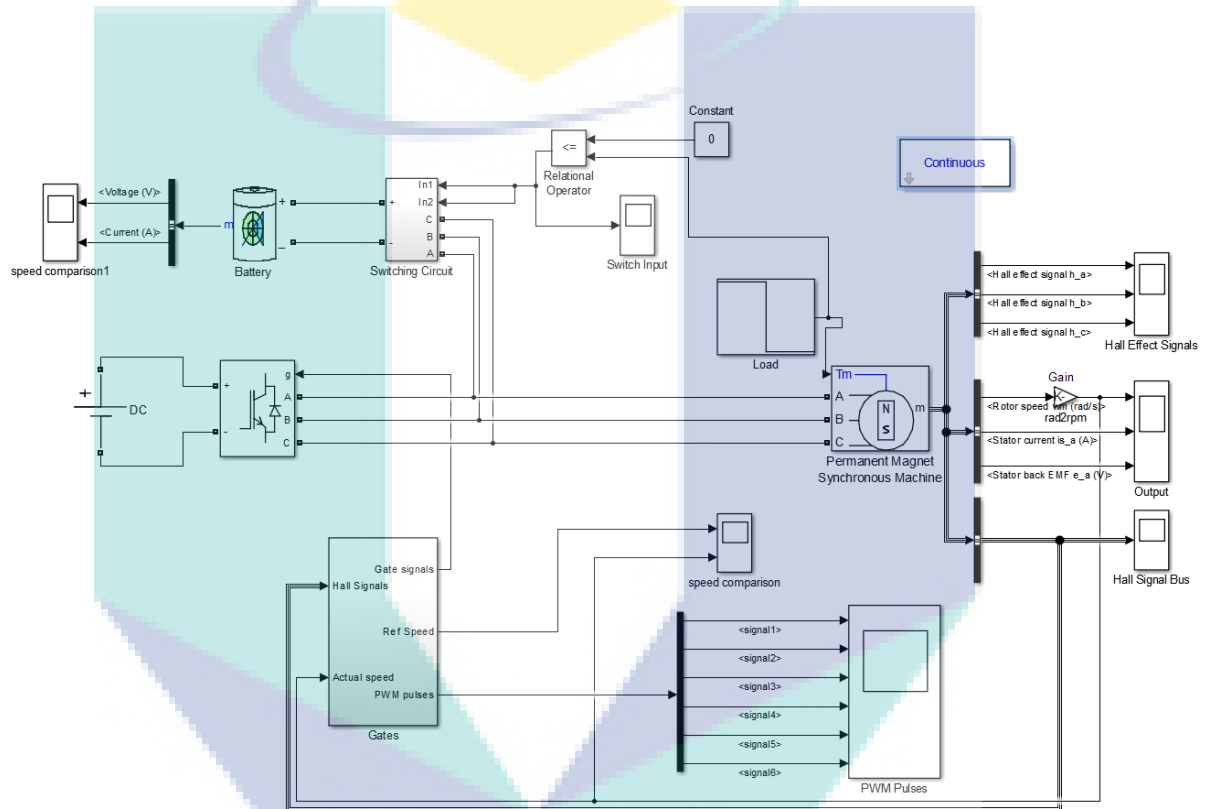


Figure 3.3 Four quadrant BLDC speed controller in Matlab Simulink model

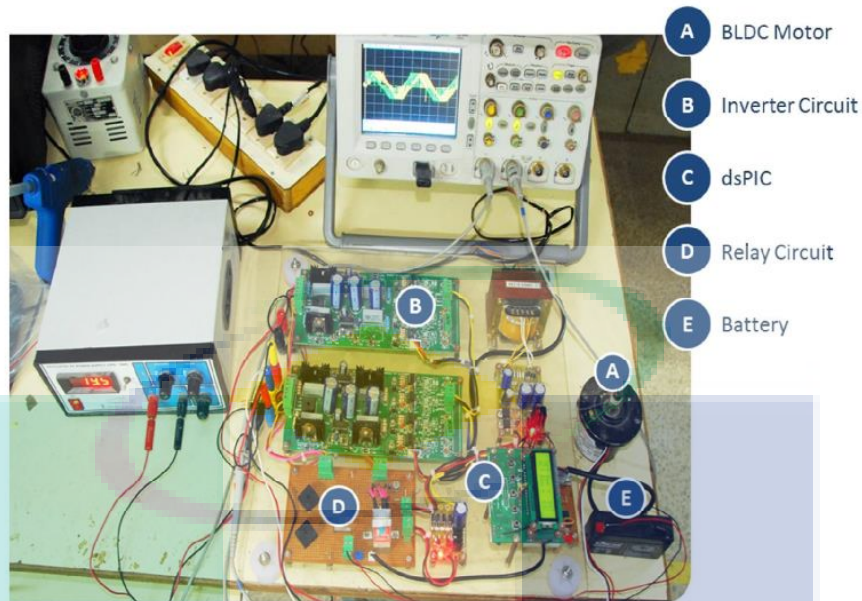


Figure 3.4 Four quadrant BLDC speed controller hardware setup

Based on Figure 3.3, the controller powers the 3-level IGBT bridge via a DC power supply. The rotor positions of the BLDC motor were feed to directly to the decoder in the system. The decoder determines excitation sequence of the BLDC motor and produce excitation sequence signal. Based on the error from the actual speed and reference speed, the PI controller determines duty cycle for the PWM generator. The PWM signal coupled with excitation sequence signal produces self-commutated IGBT gate signal which is feed to the inverter gate signal. With the self-commutated IGBT gate signals, the inverter is actuated in a sequence and drive the BLDC motor to required speed and directions in first and third quadrant operations. For the second and forth quadrant operations, BLDC motor is manually driven using external signal. As the BLDC motor is manually driven the motor becomes a generator and the generated voltage is used to charge the battery with a rectifier.

The simulation result in Figure 3.5 shows that the system was able to achieve first quadrant where speed reference was set at 400 rpm and the controller was able to obtain the reference speed. However, as the reference speed is set to 400 rpm for third quadrant operations the controller has 67.5 % of speed error when the reference speed and actual speed compared and it could not go more than 130 rpm. As for the second quadrant and forth quadrant operations no results were presented.

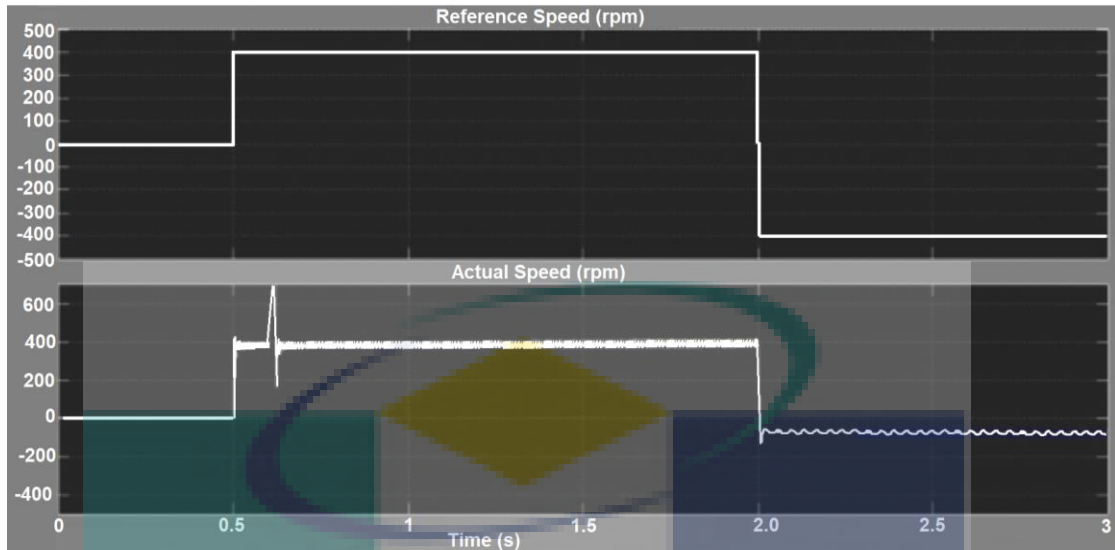


Figure 3.5 Matlab Simulink results

For the hardware results only the first quadrant operations were presented as shown in Figure 3.6, the reference speed was set to 500 rpm initially and the speed was increased to 3000 rpm and reduced to 1000 rpm. No results respect to third quadrant was presented and discussed.

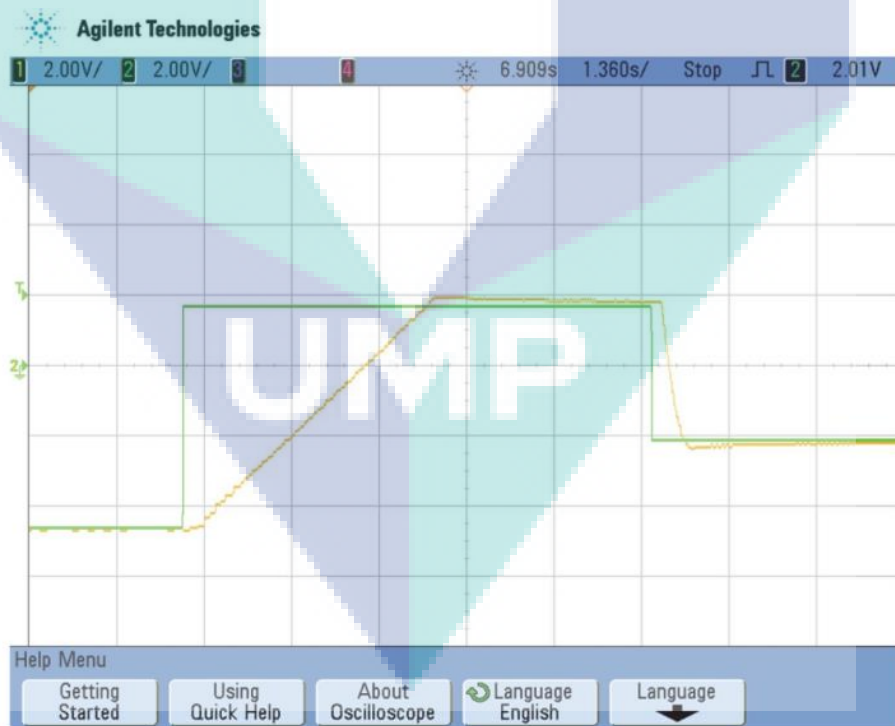


Figure 3.6 Hardware results

### 3.3 Development of Test platform

The test platform was developed to test the developed controller by (Joice et al., 2013). It was chosen because it was the first 4-quadrant BLDC controller that address the quadrant transient problem. Firstly, the mathematical model of the BLDC motor was developed. BLDC motors are synchronous motors, where the rotor rotational speed and the stator's magnetic field are the same frequency. The stator magnetic circuit usually made from magnetic steel sheets with windings placed in the slots that are cut along the inner periphery or can be wound as a single coil in the magnetic pole. The permanent magnets are placed on the rotor in such way that the back-EMF shape is trapezoidal. This allows the three-phase voltage system to be used to create a rotational field with low torque ripple. The BLDC electrical circuit representation can be seen in Figure 3.7.

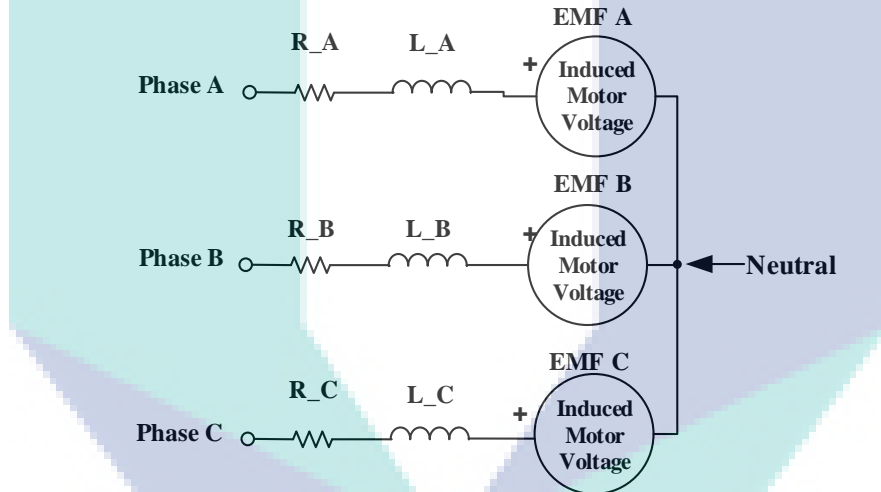


Figure 3.7 BLDC motor electrical circuit representation showing the interconnection of the phase resistance and inductance

In order to simulate BLDC Motor, the mathematical equation was derived based on the BLDC motor electrical circuit representation. For a symmetrical winding of motor is expressed as:

$$V_a = R_a i_a + L_a \frac{di_a}{dt} + M_{ab} \frac{di_b}{dt} + M_{ac} \frac{di_c}{dt} + e_a \quad 3.1$$

$$V_b = R_b i_b + L_b \frac{di_b}{dt} + M_{ba} \frac{di_a}{dt} + M_{bc} \frac{di_c}{dt} + e_b \quad 3.2$$

$$V_c = R_c i_c + L_c \frac{di_c}{dt} + M_{ca} \frac{di_a}{dt} + M_{cb} \frac{di_b}{dt} + e_c \quad 3.3$$



where

$V_a$ ,  $V_b$  and  $V_c$  denotes phase voltage of the motor,

$R_a$ ,  $R_b$  and  $R_c$  represents stator winding resistances,

$i_a$ ,  $i_b$  and  $i_c$  are the phase current of the motor,

$L_a$ ,  $L_b$  and  $L_c$  denoted self-inductance of the motor winding,

$M_{ab}$ ,  $M_{ac}$ ,  $M_{ba}$ ,  $M_{bc}$ ,  $M_{ca}$  and  $M_{cb}$  denotes mutual inductances between stator windings, and

$e_a$ ,  $e_b$  and  $e_c$  represents back-EMF waveforms functions of angular velocity of the rotor shaft.

Based on the back-EMF, the following equation can be derived:

$$e = k_e * \omega_m \quad 3.4$$

where  $k_e$  is the back-emf constant.

Considering the equation 3.4, the BLDC Motor mathematical model can be represented by the following equations:

$$\begin{bmatrix} L_a & M_{ab} & M_{ac} \\ M_{ba} & L_b & M_{bc} \\ M_{ca} & M_{cb} & L_c \end{bmatrix} \frac{d}{dt} \begin{bmatrix} i_a \\ i_b \\ i_c \end{bmatrix} = \begin{bmatrix} V_a \\ V_b \\ V_c \end{bmatrix} - \begin{bmatrix} R_a & 0 & 0 \\ 0 & R_b & 0 \\ 0 & 0 & R_c \end{bmatrix} \begin{bmatrix} i_a \\ i_b \\ i_c \end{bmatrix} - \begin{bmatrix} e_a \\ e_b \\ e_c \end{bmatrix} \quad 3.5$$

by assuming all three symmetric phases, inductances and mutual inductance are assumed to be symmetric for all phase yield the following equations:

$$\begin{bmatrix} L & M & M \\ M & L & M \\ M & M & L \end{bmatrix} \frac{d}{dt} \begin{bmatrix} i \\ i \\ i \end{bmatrix} = \begin{bmatrix} V_a \\ V_b \\ V_c \end{bmatrix} - \begin{bmatrix} R & 0 & 0 \\ 0 & R & 0 \\ 0 & 0 & R \end{bmatrix} \begin{bmatrix} i_a \\ i_b \\ i_c \end{bmatrix} - \begin{bmatrix} e_a \\ e_b \\ e_c \end{bmatrix} \quad 3.6$$

The electromechanical torque is expressed as:

$$T_{em} = J \frac{d\omega_r}{dt} + B\omega_r + T_L \quad 3.7$$

where

$J$  is the moment of inertia,

$B$  is the frictional coefficient,

$\omega_r$  is the angular velocity of the motor, and

$T_L$  is the load torque.

Electrical rotor speed and position are related by:

$$\frac{d\theta}{dt} = \left(\frac{P}{2}\right) * \omega \quad 3.8$$

where  $P$  is the number of poles in the motor.

By using the derived equation 3.1-3.8 of the BLDC motor, MATLAB BLDC motor was developed. The BLDC motor uses the parameters in Table 3.1, to benchmark the BLDC motor's performance and eliminate any modelling errors.

The next part is to reconstruct the test platform's power circuit and speed controller to mirror the simulation model and hardware model in Chapter 3.2. The Figure 3.8 show the testing platform MATLAB simulation model. To assess the performance of the test platform, the test platform was tested under the same parameters in the study done in Chapter 3.2. The test platform results were compared with the results of obtained from the study. The results will be further discussed in the next chapter.

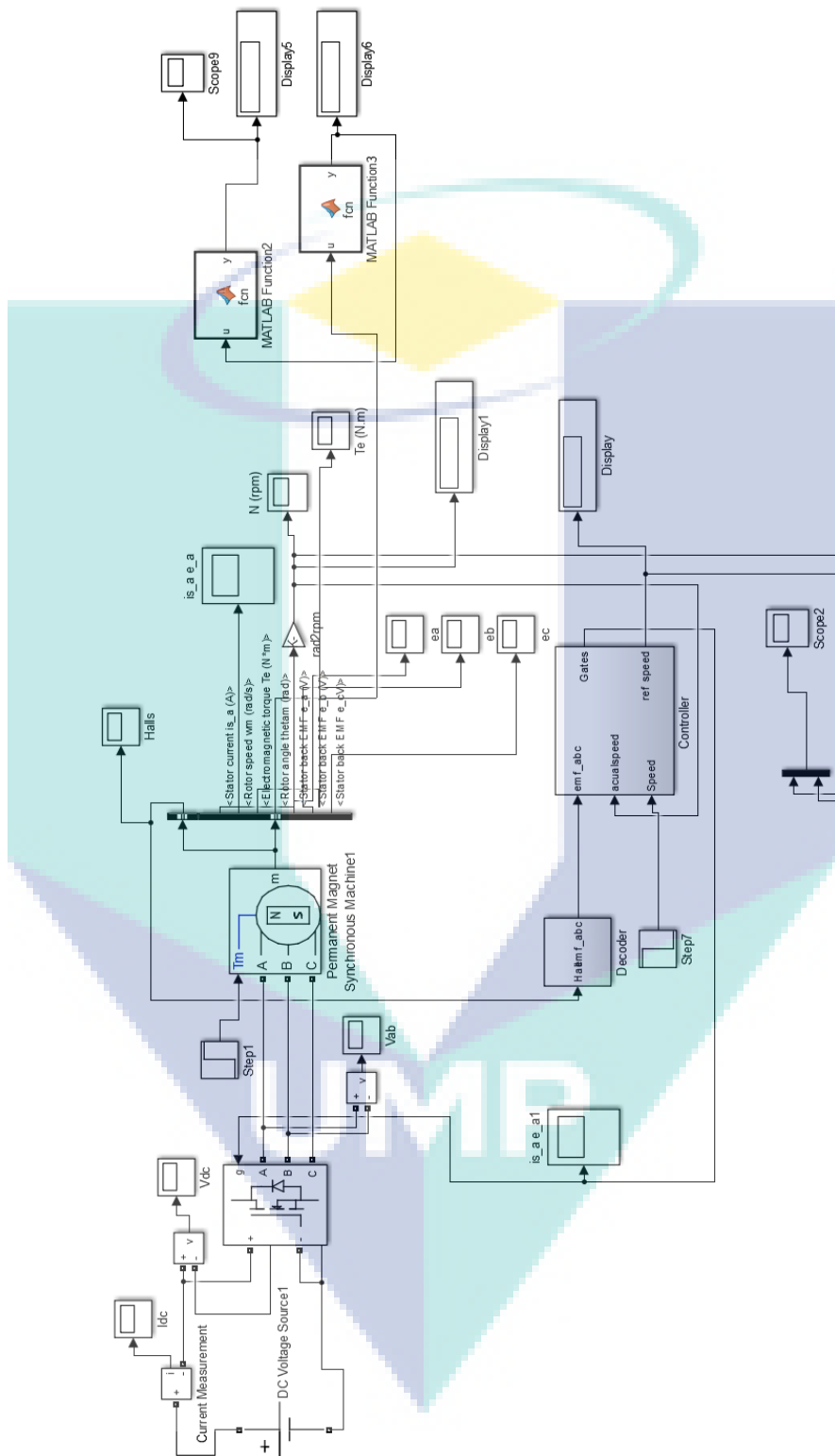


Figure 3.8 Testing platform MATLAB simulation model

### 3.4 Development of Direct Commutation Switching (DCS)

A BLDC motor requires the stator winding to be energized in a specific sequence to drive it. Hall sensor is a transducer that varies its output voltage in response to a magnetic field. The hall sensor usually positioned  $120^\circ$  apart for BLDC motor with three hall sensor design. For this design every  $60^\circ$  of electrical degree of rotation, the Hall sensors changes its state from low (0) to high (1) or high (1) to low (0) depending on the rotors position respect to the magnetic field. As the rotor of the motor rotates each hall sensor produces its own signals that corresponds to back-EMF and it takes six steps to complete an electrical cycle.

With every  $60^\circ$  of electrical degree of rotation the phase current would update. However, one electrical cycle, does not correspond to a complete mechanical revolution of the rotor. The number of the electrical cycles to be completed for a complete mechanical revolution depends on rotor pole pairs. For each rotor pole pairs, one electrical cycle is completed. The number of electrical cycles/rotations equals to the rotor pole pairs. The Figure 3.9 shows Hall sensor output and EMF waveform of a BLDC motor drive.



UMP

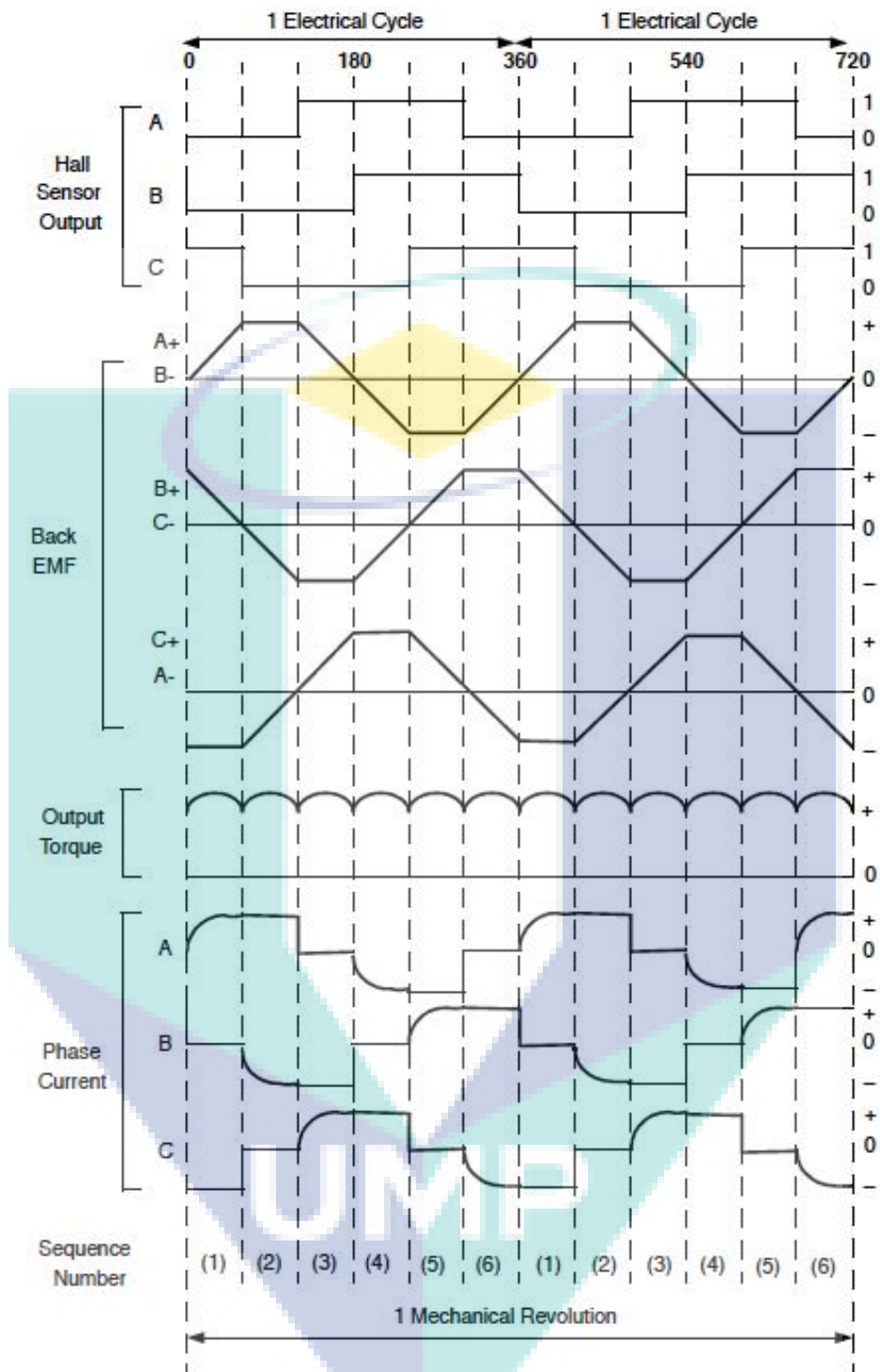


Figure 3.9 Hall sensor output and EMF waveform of BLDC motor drive  
 Source: Krause, Wasynczuk, & Sudhoff (2002)

Direct Commutation Switching (DCS) was developed to allow the BLDC motor to operate bidirectionally. To develop the switching sequence for BLDC motor, the back-EMF of the Matlab BLDC motor was recorded for a complete electrical cycle for both clockwise (CW) and counter clockwise (CCW) directions as depicted by Figure 3.10 and Figure 3.11. The back-EMF was labelled EMF A, EMF B and EMF C based on the phase the corresponds to the BLDC motor. The back-EMF signals obtained using MATLAB was verified by comparing to the study conducted by Pillay and Krishnan (1989). This was to ensure the modelling of the BLDC motor is accurate and does not have modelling error.

The BLDC motor in Matlab has three hall sensors and the sensors are labelled Hall A, Hall B and Hall C. As explained previously hall sensor is a transducer that varies its output voltage in response to a magnetic field. In this study, the hall sensor changes its output from 0 V to 1 V when the magnetic field is near the sensor and vice versa. The pulses from the hall effect sensor form BLDC motor using MATLAB as depicted by Figure 3.12 and Figure 3.13 was also recorded for a complete electrical cycle for both CW and CCW directions.

To verify the data obtained using Matlab the hall effect sensor pulses from an actual BLDC motor was recorded and compared. The Figure 3.14 shows the hardware setup and Figure 3.15 shows the Hall effect sensor output during clockwise directions using actual BLDC motor. The signals in Figure 3.12, Figure 3.13 and Figure 3.15 was labelled 0 during 0 V output signal and 1 during 1 V signal output. The signals in Figure 3.12, Figure 3.13 and Figure 3.15 were decoded and a sequence was derived for every 60° of electrical degree of rotation and labelled as a-b-c-d-e-f.

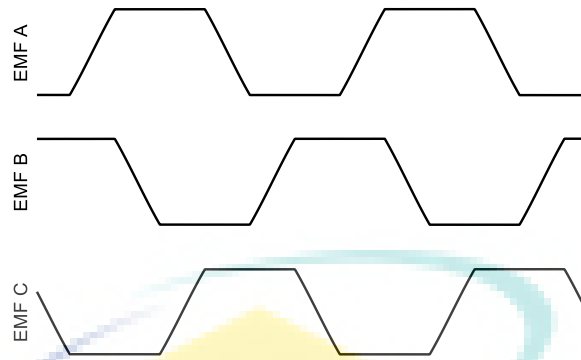


Figure 3.10 Back-EMF during clockwise direction from MATLAB

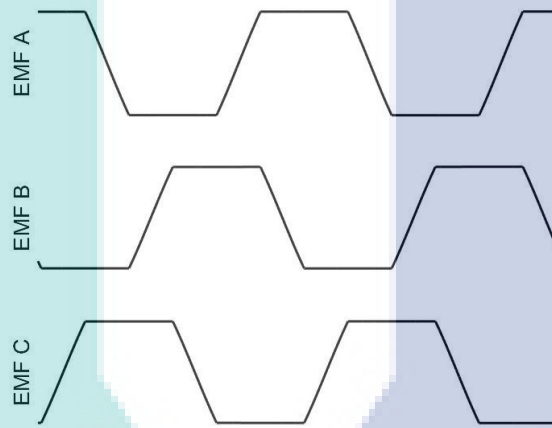


Figure 3.11 Back-EMF during counter-clockwise direction from MATLAB

UMP

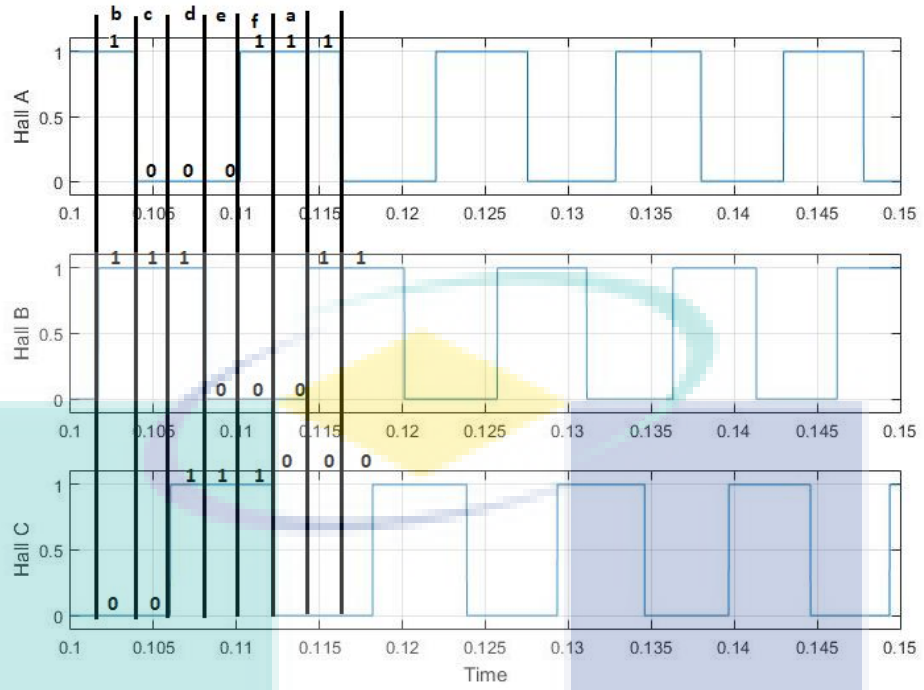


Figure 3.12 Hall effect sensor output during CW directions using MATLAB

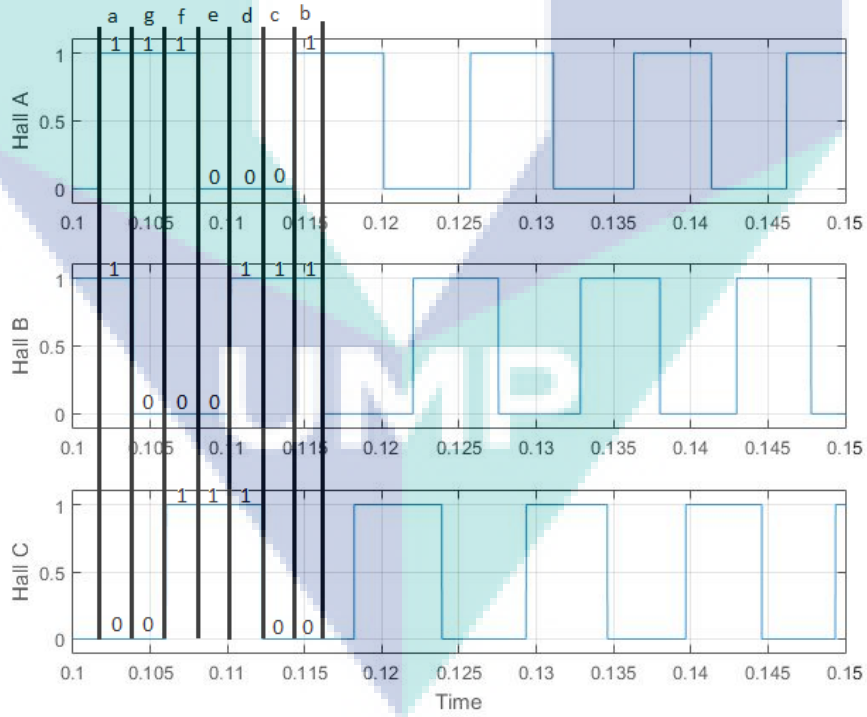


Figure 3.13 Hall effect sensor output during CCW directions using MATLAB



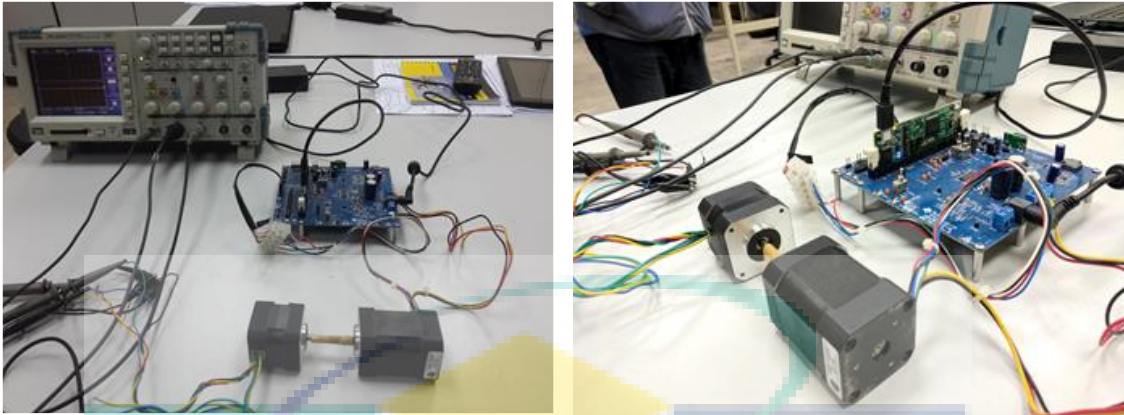


Figure 3.14 Hardware setup for Halls sensors data collection

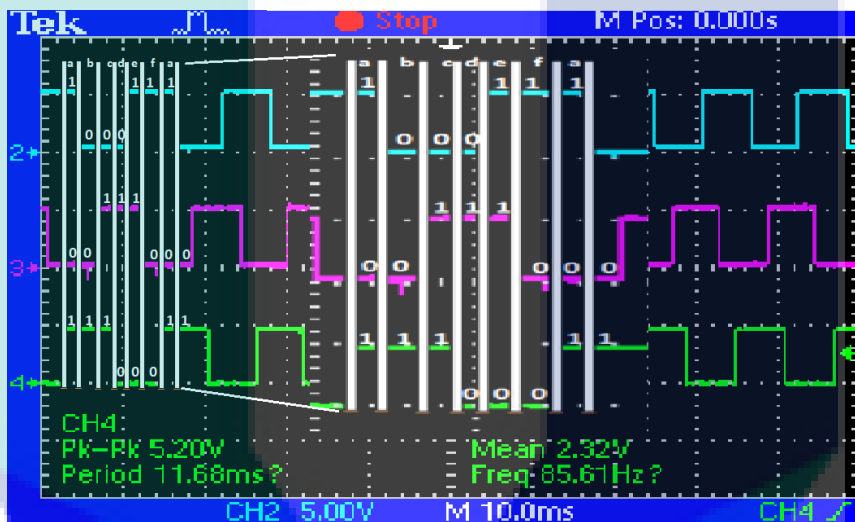


Figure 3.15 Hall effect sensor output during clockwise directions using actual BLDC motor

For the clockwise direction the sequence obtained was a-b-c-d-e-f and for counter-clockwise was f-e-d-c-b-a for Hall sensor signals using MATLAB. The exactly similar sequence was obtained using actual BLDC motor for both directions. By using this sequence, back-emf from the MATLAB and Figure 3.9, a look-up table was developed as shown in Tables 3.2 and 3.3 for both directions.

Table 3.2 Commutation sequence for clockwise direction

Sequence	Hall Sensor Input			Back EMF Phase Current		
	A	B	C	a	b	c
1	0	1	1	I+	I-	0
2	0	0	1	I+	0	I-
3	1	0	1	0	I+	I-
4	1	0	0	I-	I+	0
5	1	1	0	I-	0	I+
6	0	1	0	0	I-	I+

Table 3.3 Commutation sequence for counter-clockwise direction

Sequence	Hall Sensor Input			Back EMF Phase Current		
	A	B	C	a	b	c
1	0	1	1	0	I-	I+
2	0	0	1	I-	0	I+
3	1	0	1	I-	I+	0
4	1	0	0	0	I+	I-
5	1	1	0	I+	0	I-
6	0	1	0	I+	I-	0

The Figure 3.16 shows DCS controller's block diagram. A complex mathematical switching scheme and look-up Table 3.2 and 3.3 was used to develop the direction-based commutation tables. The rotor's position, rotational direction and commutation tables is used to determines the sequence and timing for commutation in form of six PWM signals that fed into the inverter. Hence, driving the motor at desired speed and direction.

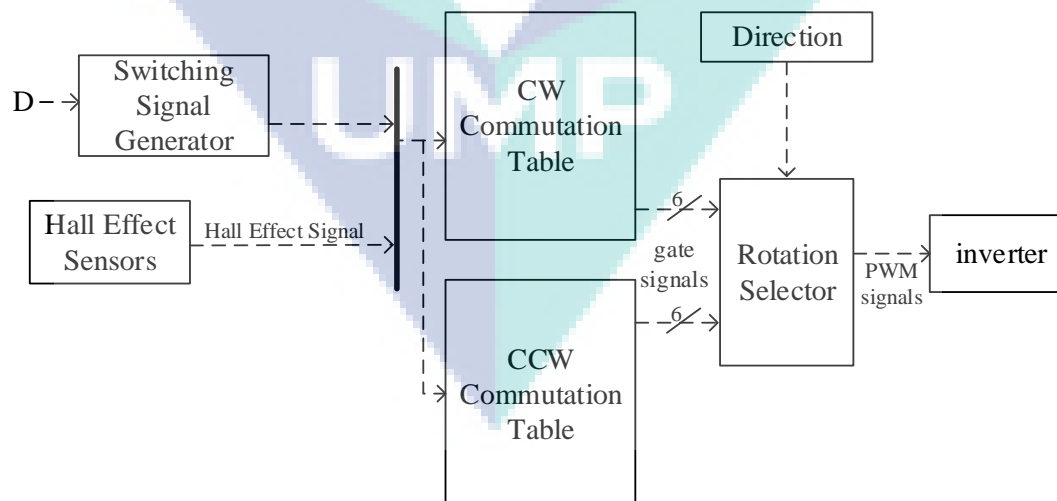


Figure 3.16 Direct commutation switching scheme controller

### 3.5 BLDC speed control techniques

Several speed control techniques were developed as BLDC Speed Controller. The first speed control techniques developed was a PI controller as developed by (Joice et al., 2013). This modelled controller acts as a testing platform for the different type of speed control techniques that were developed. Each technique was tested under the same test cases. PI controller was not included into rest of the of the study and replaced with PID controller due to better stability control (Premkumar & Manikandan, 2015a). The Figure 3.17 shows the BLDC speed controller techniques used in this study.

The Hall sensor's signals is decoded by a position and speed decoder to obtain the actual speed and rotor position. The rotor position is used by DCS controller located in the switching logic block. The speed error from the actual speed and reference speed is feed to different techniques such as PID, Self-Tuning Fuzzy PID and Modified Fuzzy Gain Scheduling. The techniques will determine the duty cycle that needed by the DCS to reduce the speed error. The DCS which later produces PWM signals to the inverter to drive the BLDC motor at desired speed by utilizing the rotor position, duty cycle and direction. The techniques used was explained in detail in the following sub-chapters. The entire speed controller in MATLAB is attached in Appendix A.

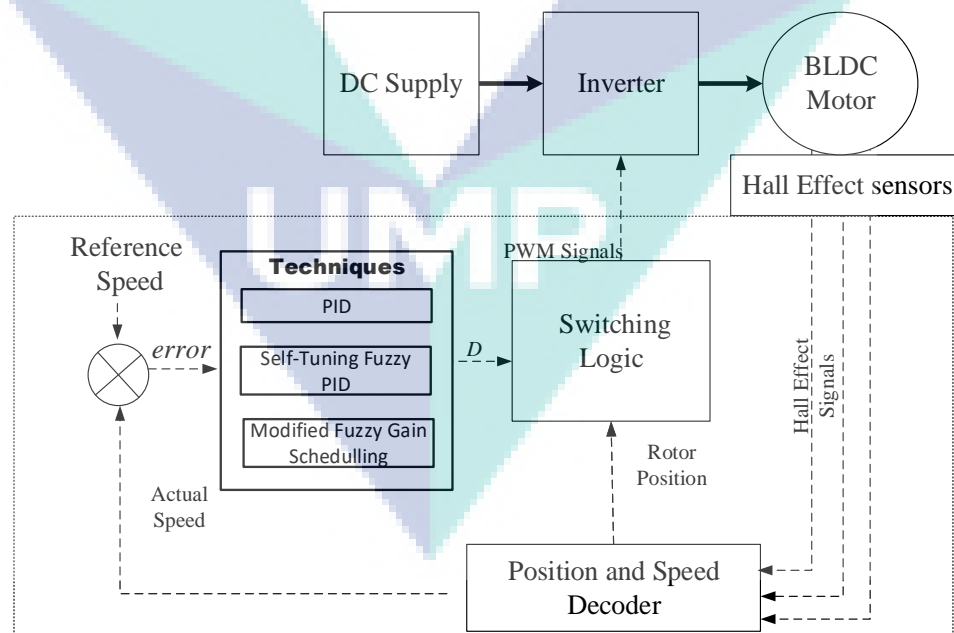


Figure 3.17 BLDC speed controller techniques used in this study

### 3.5.1 PID

If the speed of the motor is varied, the PID will calculate the error value  $e(t)$  by comparing the actual speed and the desired speed and reduce the error based on the proportional, integral and derivative as shown in Figure 3.18. The equation of PID controller is:

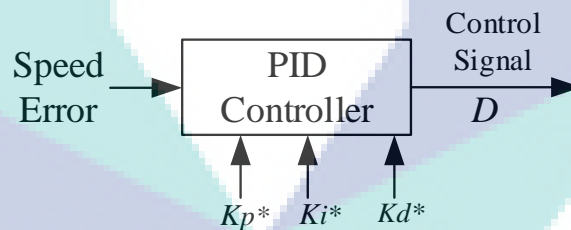
$$u(t) = K_p e(t) + K_i \int_0^t e(\tau) d\tau + K_d \frac{\partial e(t)}{\partial t} \quad 3.9$$

where:  $K_p$  depicts proportional gain coefficient

$K_i$  depicts integration time coefficient

$K_d$  depicts derivative time coefficient.

For this study, the values of  $K_p$ ,  $K_i$ , and  $K_d$  was calculated using Ziegler-Nichols (ZN)'s step response method (Ziegler & Nichols, 1942).



\* All PID coefficient based on Ziegler-Nichols (ZN) method

Figure 3.18 PID Speed control system

Source : Ibrahim, Hassan, & Shomer (2014)

### 3.5.2 Self-Tuning Fuzzy PID (S.T.Fuzzy)

Self-Tuning Fuzzy PID (S.T.Fuzzy) controller designed for this study is depicted by Figure 3.19. This controller was developed based on study by Premkumar and Manikandan (2015b) to overcome the problem faced by PID controllers with consideration for forward motoring mode only.

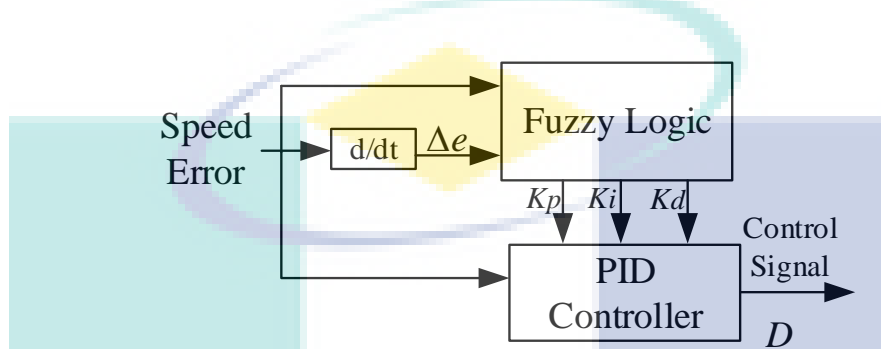


Figure 3.19 Self-Tuning Fuzzy PID Speed control system

Source : Premkumar & Manikandan (2015)

This controller uses the same equation as PID controller to produce the control signal. However, the controller the values of  $K_p$ ,  $K_i$  and  $K_d$  varies based on rate of error and error as shown by the following equations.

$$u(t) = K_p e(t) + K_i \int_0^t e(\tau) d\tau + K_d \frac{\partial e(t)}{\partial t} \quad 3.10$$

$$K_p = \Delta K_p + K_p' \quad 3.11$$

$$K_i = \Delta K_i + K_i' \quad 3.12$$

$$K_d = \Delta K_d + K_d' \quad 3.13$$

where  $K_p$  proportional gain coefficient,  $K_i$  integration time coefficient and  $K_d$  derivative time coefficient.  $K_p'$ ,  $K_i'$  and  $K_d'$  are the pervious sampling time's coefficient parameters.  $\Delta K_p$ ,  $\Delta K_i$  and  $\Delta K_d$  are the fuzzy output.

Internal structure of the fuzzy controller made of two inputs and three outputs. This controller uses Sugano fuzzy inference method. The rate of error  $\Delta e(k)$  and current error  $e(k)$  acts as the inputs and  $\Delta Kp$ ,  $\Delta Ki$  and  $\Delta Kd$  were the outputs of the fuzzy.

Figure 3.20 represents current error  $e(k)$  and rate of error  $\Delta e(k)$ 's membership functions, where Positive Big (PB), Negative Small (NS), Positive Small (PS), Negative Big (NB), Positive Medium (PM), Zero (ZO), and Negative Medium (NM). The membership functions for  $\Delta Kp$ ,  $\Delta Ki$  and  $\Delta Kd$  is represented by Figure 3.21.

Table 3.4 shows rule table for Fuzzy's  $\Delta Kp$ ,  $\Delta Ki$  and  $\Delta Kd$ . This rule table was used to obtain the 49 set of membership function rules that used in the controller. The fuzzy controller uses the Equation 3.10-3.12 and membership functions rules to decide the best value of  $Kp$ ,  $Ki$  and  $Kd$  to suite the demand. The MATLAB simulation model for this controller is attached in Appendix A.

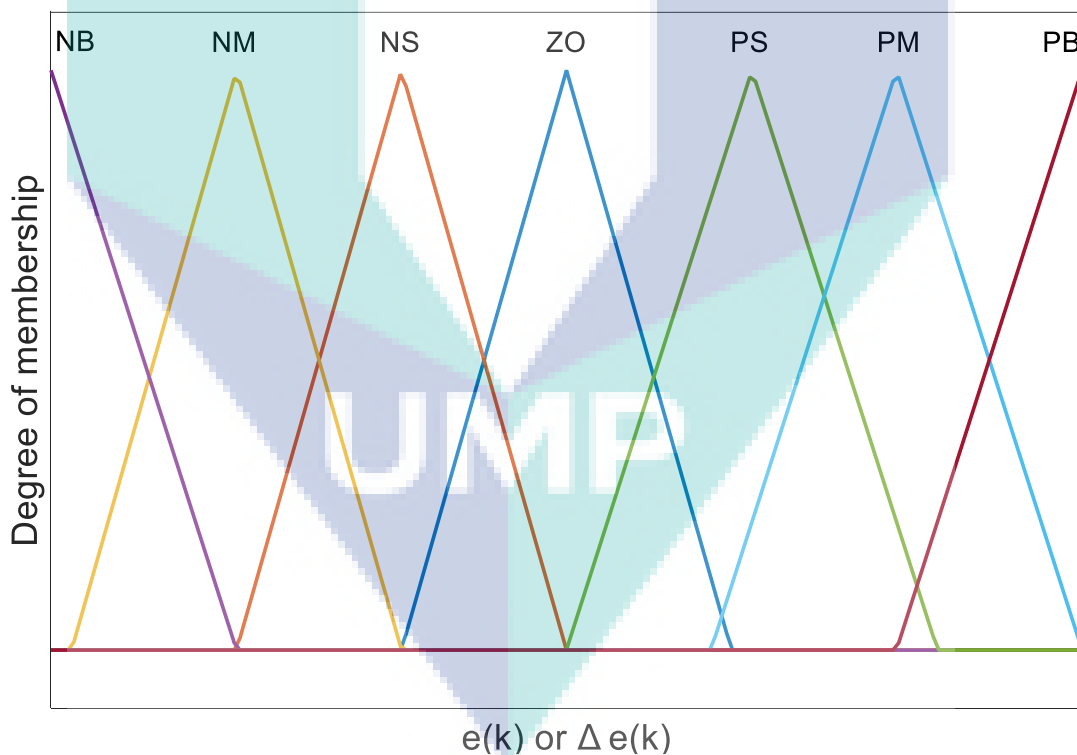


Figure 3.20 Membership function for  $e(k)$  and  $\Delta e(k)$

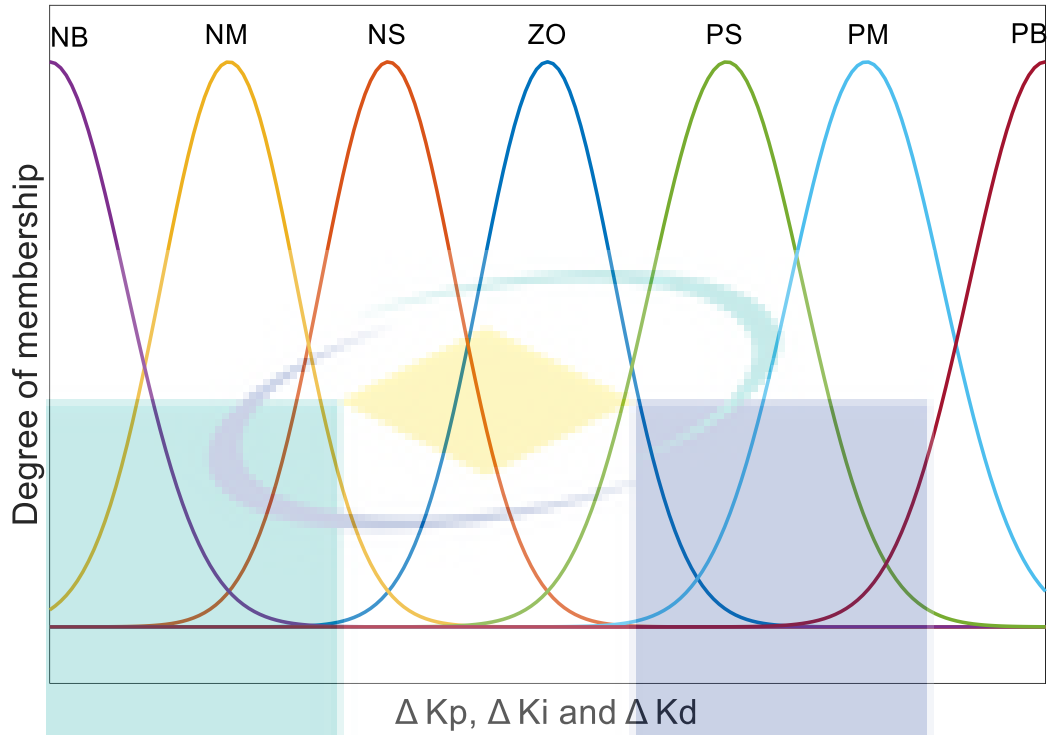


Figure 3.21 Membership function for  $\Delta Kp$ ,  $\Delta Ki$  and  $\Delta Kd$

Table 3.4 Fuzzy controller's  $Kp$ ,  $Ki$  and  $Kd$  rule table

		Error $e(k)$						
		NB	NM	NS	ZO	PS	PM	PB
Change of error $\Delta e(k)$	NB	NB	NM	NS	ZO	PS	PM	PB
	NB	NB	NM	NB	PB	PB	PM	PB
	PS	PM	PB	NB	NB	NB	NM	ZO
	ZE	PS	PS	NS	ZO	ZO	NS	ZO
	PB	NM	NM	PS	PM	NS	PS	PS
	NM	PS	PM	NS	NS	NM	PS	NS
	NS	ZO	NB	NM	ZO	NS	NS	NB
	PB	PM	NS	PS	ZO	PS	PS	NS
	NS	NB	NM	PS	NS	ZO	NM	PS
	NM	NB	ZO	NS	PS	NS	NB	ZO
	PS	PS	PS	PS	ZO	PS	PS	NM
	ZO	NS	NS	NS	ZO	NS	NS	PS
	NB	NM	NB	ZO	NB	NB	NB	PS
	PS	NS	ZO	NS	PS	NS	NS	NB
	PS	NS	PS	ZO	PS	NS	PS	PS
	NB	NS	NS	NS	NS	ZO	ZO	PS
	PM	NS	NS	NS	NS	NM	PM	NB
	PM	NS	ZO	PS	PM	PS	NM	PB
	ZO	NM	NS	NS	NS	ZO	ZO	PS
	NS	NS	NS	NS	NS	NB	PB	PB
	PB	ZO	PS	PS	PS	PS	NS	NB
	PS	NS	ZO	ZO	ZO	ZO	NS	PS

### 3.5.3 Modified Fuzzy Gain Scheduling (M.F.G.S)

Fuzzy Gain Scheduler proposed by Zhao, Tomizuka, and Isaka (1993) was tested and the results were unsatisfying as it takes very long time to achieve the desired speed as the values of Derivative Gain ( $K_d$ ), Integral Gain ( $K_i$ ) and Proportional Gain ( $K_p$ ) that fed to the PID controller increases slowly and determined by the error. To overcome this problem, a Modified Fuzzy Gain Scheduler (M.F.G.S) was proposed to achieve faster responds as shown in Figure 3.22.

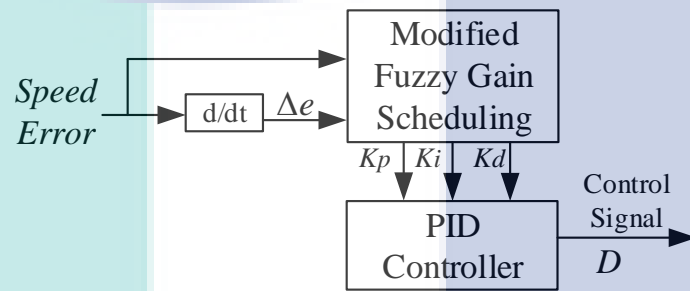


Figure 3.22 Modified Fuzzy Gain Scheduling Speed control system

This controller uses the PID controller's mathematical equivalent as depicted by Equation 3.10. This parameter could be modified further to obtain the best response based on the requirement. By including the fuzzy logic, the  $K_p$  and  $K_d$  become a ranged gain. The suitable values are determined by the fuzzy rules. For conveniences  $K_p$  and  $K_d$  are simplified using the following formulas:

$$K_p = (K_{pmax} - K_{pmin})K'p - K_{pmin} \quad 3.14$$

$$K_d = (K_{dmax} - K_{dmin})K'd - K_{dmin} \quad 3.15$$

where  $K_{pmax}$  and  $K_{dmax}$  are the highest previous coefficient gain while the  $K_{pmin}$  and  $K_{dmin}$  are the smallest previous coefficient gain.  $K'p$  and  $K'd$  are the fuzzy membership function. By using the current error  $e(k)$  and rate of error  $\Delta e(k)$ , the PID parameters were determined.



The equation 3.16 and 3.17 is used to determine the integral time constant and integral gain respectively.

$$T_i = \alpha T_d \quad 3.16$$

$$K_i = \frac{K_p}{\alpha T_d} = K_p^2 / (\alpha K_d) \quad 3.17$$

where the alpha ( $\alpha$ ) is the ratio of integral constant. Internal structure of the proposed fuzzy uses current error  $e(k)$  and rate of error  $\Delta e(k)$  as inputs and has three outputs. The three outputs are  $K'p$ ,  $K'd$  and alpha ( $\alpha$ ).

The degree of membership for both current error  $e(k)$  and rate of error  $\Delta e(k)$  as depicted by Figure 3.23, where Zero (ZO), Negative Big (NB), Positive Big (PB), Negative Medium (NM), Positive Medium (PM), Negative Small (NS), and Positive Small (PS). The degree of membership for  $K'p$  and  $K'd$  shown in Figure 3.24 while the degree of membership for alpha ( $\alpha$ ) is represented by Figure 3.25.

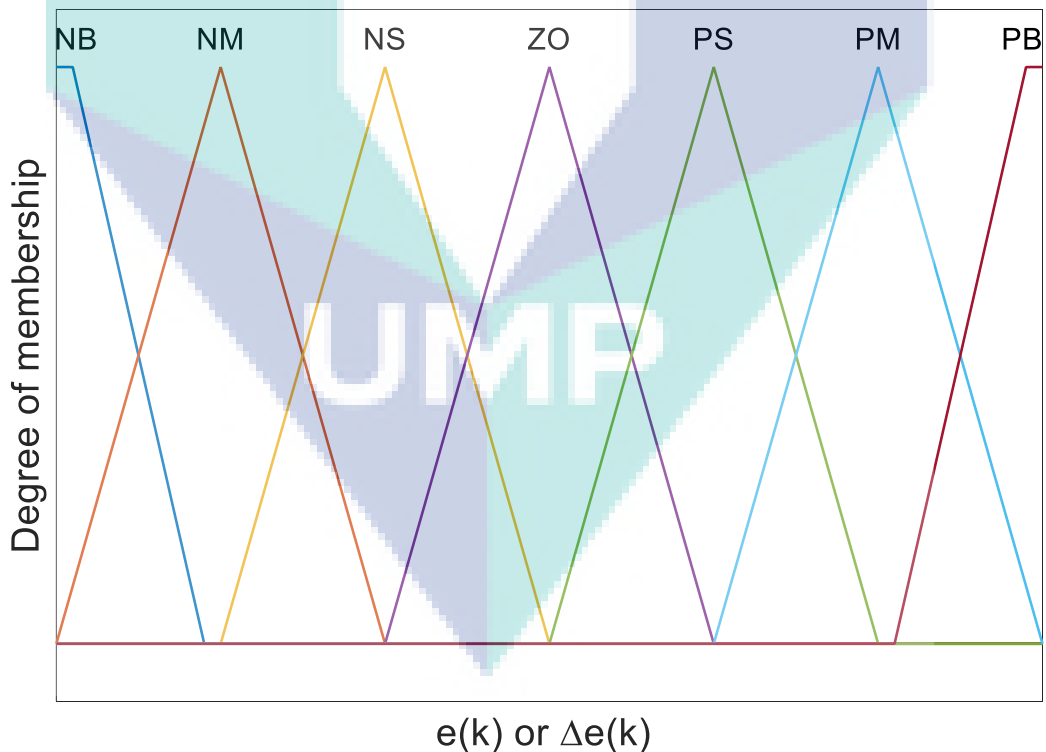


Figure 3.23 Degree of membership of  $e(k)$  and  $\Delta e(k)$

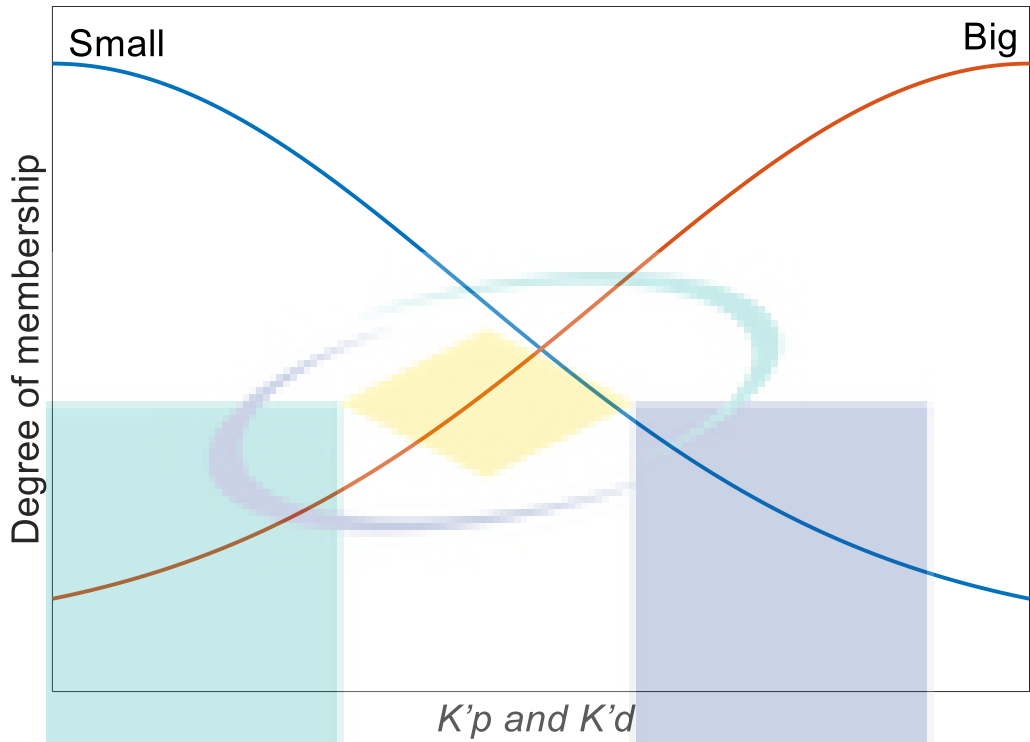


Figure 3.24 Degree of membership for  $K'p$  and  $K'd$

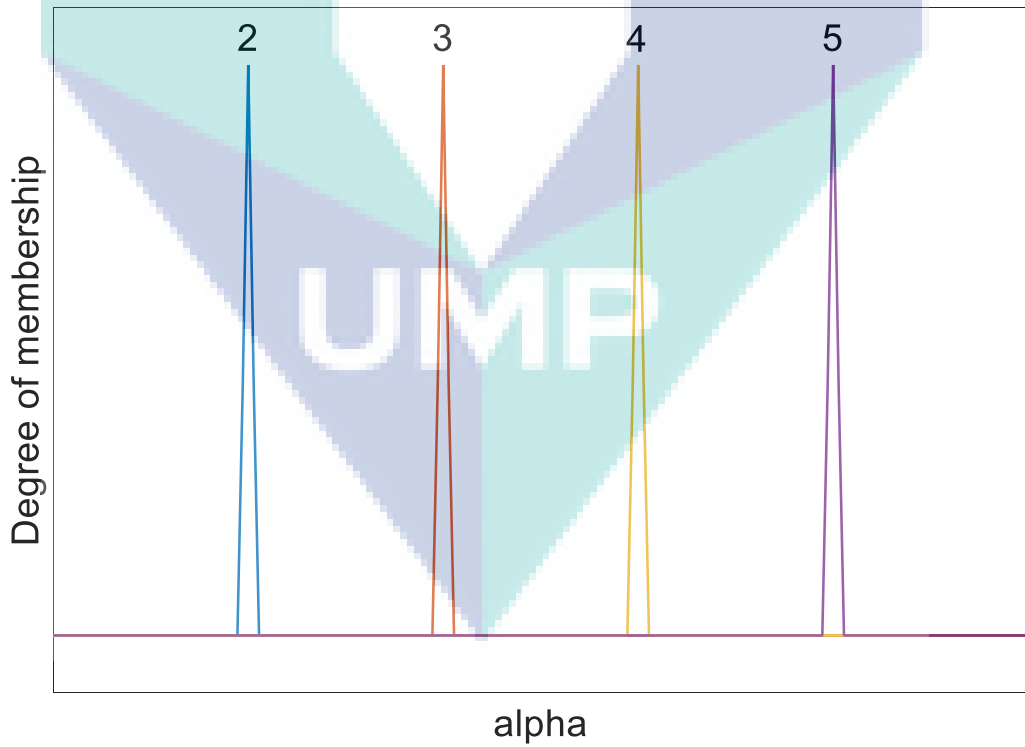


Figure 3.25 Degree of membership for  $\alpha$

Based on the membership functions rules table are used to obtain 49 set of rules. Tables 3.5, 3.6 and 3.7 are the rules table for  $K'p$ ,  $K'd$  and alpha respectively. The MATLAB simulation model for this controller is attached in Appendix A.

Table 3.5 Fuzzy Rules for  $K'p$

		$\Delta e(k)$							
		NB	NM	NS	ZO	PS	PM	PB	
$e(k)$	NB	B	B	B	B	B	B	B	
	NM	S	B	B	B	B	B	S	
	NS	S	S	B	B	B	S	S	
	ZO	S	S	S	B	S	S	S	
	PS	S	S	B	B	B	S	S	
	PM	S	B	B	B	B	B	S	
	PB	B	B	B	B	B	B	B	

Table 3.6 Fuzzy Rules for  $K'd$

		$\Delta e(k)$							
		NB	NM	NS	ZO	PS	PM	PB	
$e(k)$	NB	S	S	S	S	S	S	S	
	NM	B	S	S	S	S	S	B	
	NS	B	B	S	S	S	B	B	
	ZO	B	B	B	S	B	B	B	
	PS	B	B	S	S	S	B	B	
	PM	B	S	S	S	S	S	B	
	PB	S	S	S	S	S	S	S	

Table 3.7 Fuzzy Rules for Alpha

		$\Delta e(k)$							
		NB	NM	NS	ZO	PS	PM	PB	
$e(k)$	NB	2	2	2	2	2	2	2	
	NM	3	3	2	2	2	3	3	
	NS	4	3	3	2	3	3	4	
	ZO	5	4	3	3	3	4	5	
	PS	4	3	3	2	3	3	4	
	PM	3	3	2	2	2	3	3	
	PB	2	2	2	2	2	2	2	

### 3.6 Summary

This chapter explained the methodology that applied during this study. This study was started by modelling the BLDC motor in MATLAB. The BLDC motor was modelled based on specifications by Joice et al., (2013). Later the modelled BLDC motor is incorporated into a test platform that developed based on the study by Joice et al., (2013). The test platform was assessed and verified its capabilities to simulate real-time results by comparing with Joice et al., (2013) results.

Next was to overcome the limitations of S.Joice commutation method, a commutation scheme was developed to drive the BLDC motor bidirectionally. DCS scheme was developed to address this issue and the performance of the controller was assessed by comparing with Joice commutation method.

Final part is to develop a speed control technique that has better step respond time and transient capabilities compared to existing BLDC speed control techniques such as PID and S.T.Fuzzy. The M.F.G.S speed controller was developed to address this issue. The controller's performance was asses for several test-cases and compared with existing BLDC speed control techniques such as PID and S.T.Fuzzy.

The logo for UIMP (Universiti Malaysia Perlis) is a large, stylized 'V' shape. The left side of the 'V' is light blue, the right side is light purple, and the bottom point is a darker shade of purple. The letters 'UIMP' are written in white, bold, sans-serif font across the bottom of the 'V'.

## CHAPTER 4

### RESULTS AND DISCUSSION

#### 4.1 Introduction

In this chapter, the simulation results for the developed control schemes for bidirectional and BLDC speed control techniques were presented and discussed. For the test platform, the results will discuss on the ability of simulating real-time results. The test platform was tested using a PID speed controller for commutation method in Chapter 3.2 and DCS method. The performance of the commutation method was assessed in the term of ability to achieve bidirectional operations were discussed.

Transient capabilities as well as the capabilities to adapt for four quadrant operations with dynamic load was assessed with the with S.T.Fuzzy and PID speed controller. To further improve the step-respond time and transient capabilities of the BLDC controller, M.F.G.S speed controller was developed and its performance was assessed with S.T.Fuzzy and PID for six test cases. The outcome of each test case was observed and analysed. The results were discussed.

#### 4.2 Verification Development of Test Platform

The test platform was developed based design in chapter 3.2 including the motor's specification as well as power electronic side. The Matlab Simulink design for the test platform is as shown in Appendix A. The test platform was tested for the capabilities to simulate real-time. The simulated results obtained in the study is depicted by Figure 4.1 and the test platform results is depicted in Figure 4.2.

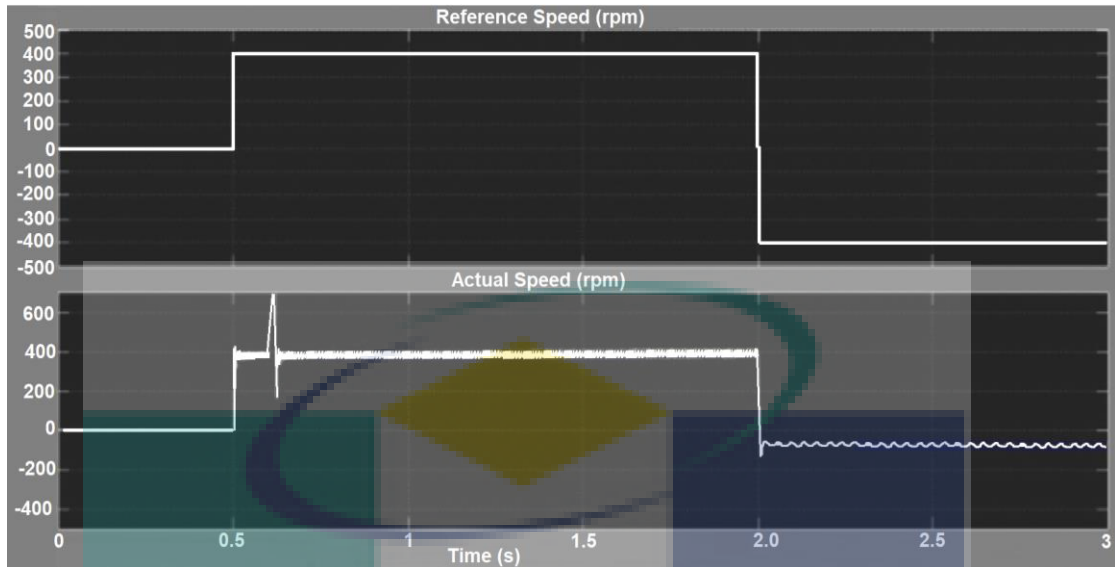


Figure 4.1 The Matlab results obtained by the original developer

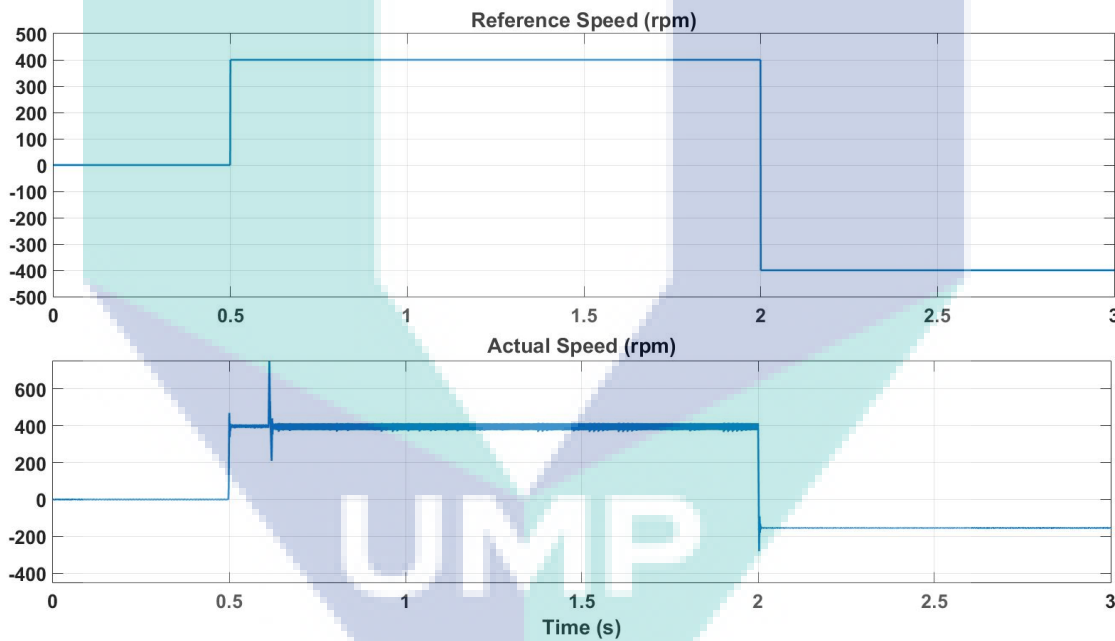


Figure 4.2 The Matlab results obtained using the test platform

By comparing the results in both Figure 4.1 and Figure 4.2, the test platform was able to simulate exactly similar results as the original developer in Chapter 3.2. The rise time of the simulations are the exact same at 0.5 s. The error during counter-clockwise direction at  $t = 2$  s is also similar however the controller in the test platform does not have large ripple as obtained by Joice. This may be caused by different type of IGBT value used as no exact values provided.

The hardware results obtained by the original developer is depicted by Figure 4.3 and the test platform results is depicted in Figure 4.4.

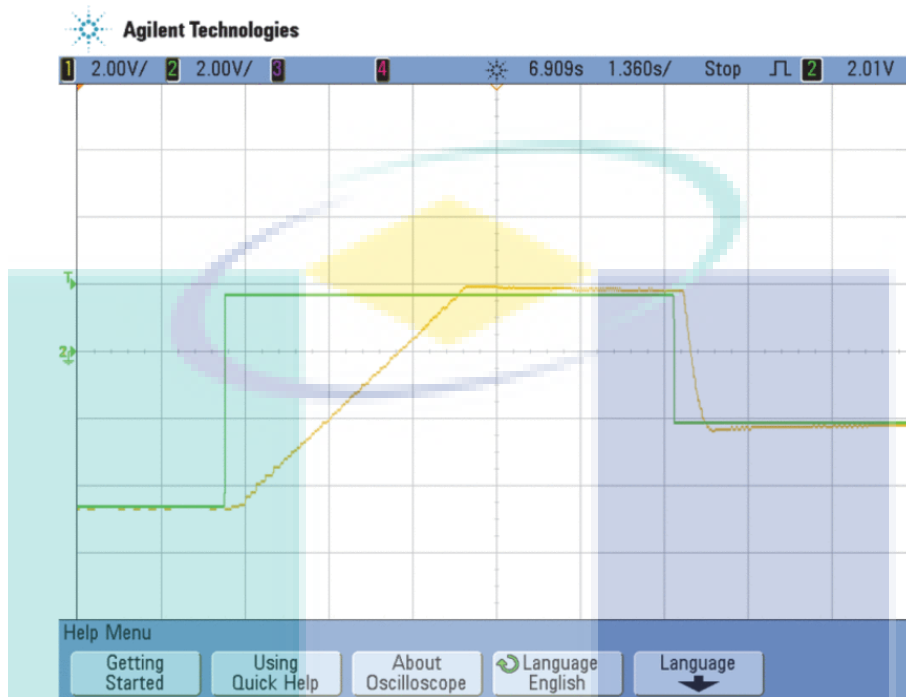


Figure 4.3 The hardware results obtained by the original developer

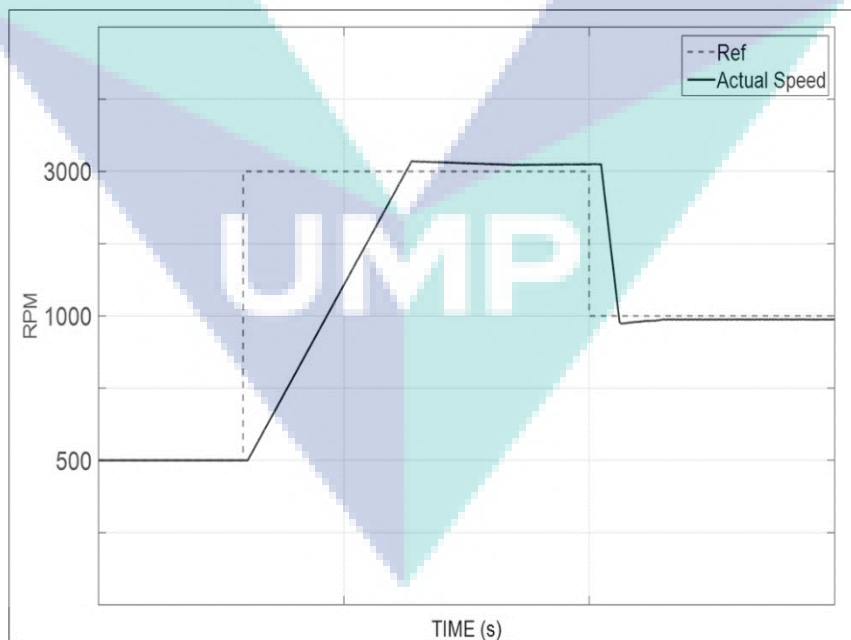


Figure 4.4 The hardware results obtained using the test platform

The test platform results obtained for simulating real-time conditions were the same as hardware results obtained in Chapter 3.2 with slight disparity due to computational delay. Hence, the test platform can be used to obtain real time results and the commutation technique developed in Chapter 3.2 was not able bidirectional capabilities as it focuses on forward motoring only and a much more robust commutation scheme was required to allow the BLDC motor to operate bidirectionally.

### 4.3 Simulation of PID controller using Direct Commutation Switching (DCS)

#### Scheme and conventional method

Based on the both simulation and hardware results in Chapter 4.2, it can be concluded that the system was not able to operate at counter-clockwise direction efficiently. To allow the system operate in counter-clockwise direction, a direct commutation scheme (DCS) was introduced and the system was tested with several speed control techniques. Two sets of test cases were conducted to assess the capabilities of the conventional controller and compared it with the controller with direct commutation scheme. The speed controller used was a PID speed controller.

#### 4.3.1 Step Response of the motor for clockwise direction for No Load conditions

The PID speed controller was used for both conditions. The motor's responds during clockwise directions for No-Load (NL) condition is depicted by Figure 4.5 while the time response data is tabulated in Table 4.1.

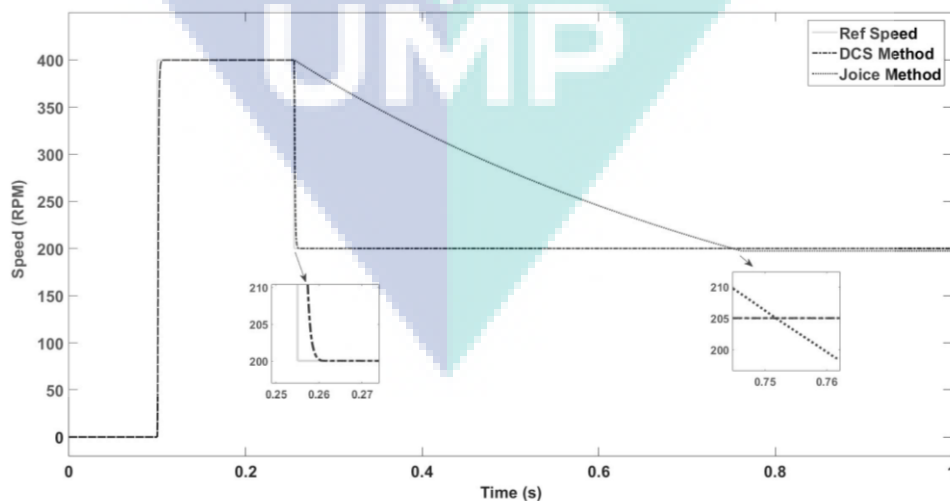


Figure 4.5 Motor respond during clockwise directions for NL conditions



Table 4.1 Motor response during clockwise for No Load

Techniques	400 RPM				200 RPM			
	Peak Over shoot	Rise Time	Settling Time	Steady State Error	Over shoot	Rise Time	Settling Time	Steady State Error
	$Mp$ (%)	$Tr$ (ms)	$Ts$ (ms)	$e_{ss}$ (%)	$Mp$ (%)	$Tr$ (ms)	$Ts$ (ms)	$e_{ss}$ (%)
DCS Method	-	9.60	9.65	0.0114	-	7.60	7.60	0.0010
Joice Method	-	9.60	9.65	0.0114	1.500	495.00	495.00	1.3375

It can be observed that during speed step-changing occurs from 0 rpm to 400 rpm at  $t = 0.005$  s both controllers using DCS and Joice method has similar rise time ( $T_r$ ) of 9.60 ms and steady state error ( $e_{ss}$ ) of 0.0114 % as the controller tries to maintain the required speed. The peak overshoot is determined as following. The same formula is used to determine the  $Mp$  throughout the study.

$$Mp = \left| \frac{(\text{Peak Overshoot} - \text{Reference})}{\text{Reference}} \right| \times 100\%$$

$$Mp = \left| \frac{(197 - 200)}{200} \right| \times 100\%$$

$$Mp = 1.5\%$$

When the speed is reduced from 400 rpm to 200 rpm at  $t = 0.255$  s, the Joice method takes a longer settling time ( $T_s$ ) to reach the required speed at 495.00 ms. The controller also has a higher steady state error ( $e_{ss}$ ) at 1.3375 % compared to with controller using DCS. Overall the controller with DCS performed better compared to Joice method controller under the same conditions.

#### 4.3.2 Step Response of the motor for counter-clockwise direction for No Load conditions

The motor's responds during counter-clockwise directions for NL condition is depicted by Figure 4.6 while the time response data is tabulated in Table 4.2. It can be observed that during speed step-changing occurs from 0 rpm to 400 rpm at  $t = 0.005$  s, the controller with DCS was able to achieve the required speed and direction and Joice method controller could not drive the BLDC motor during counter-clockwise direction.

Joice technique focus on forward motoring only and depend on motor's inertia to slow down. The time response characteristics for the controller with DCS was similar during clockwise directions. Overall the controller with DCS performed better compared to Joice method controller under the same conditions.

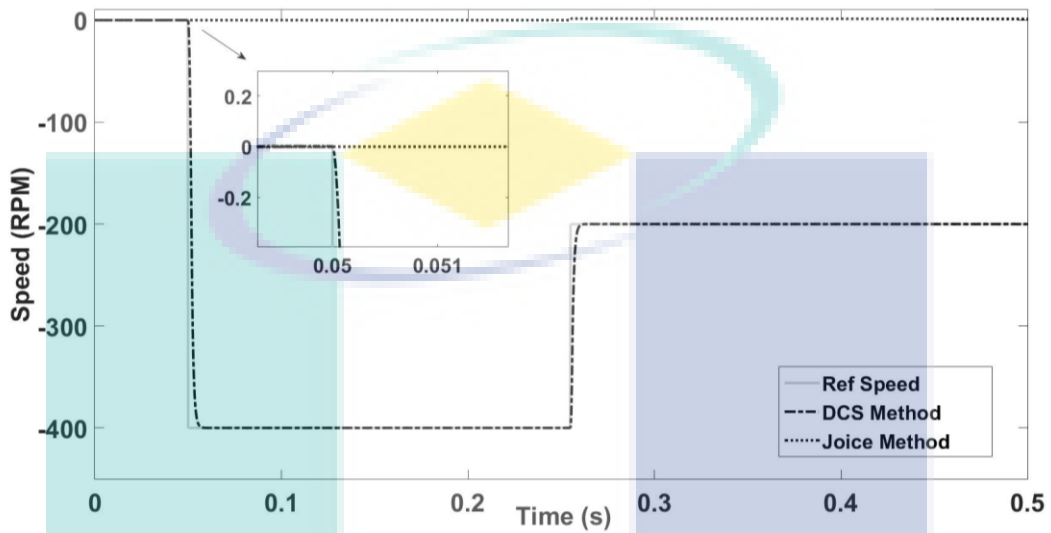


Figure 4.6 Motor respond during counter-clockwise directions for NL conditions

Table 4.2 Motor response during counter-clockwise for No Load

Techniques	400 RPM				200 RPM			
	Peak Over shoot	Rise Time	Settling Time	Steady State Error	Over shoot	Rise Time	Settling Time	Steady State Error
	$M_p$ (%)	$T_r$ (ms)	$T_s$ (ms)	$ess$ (%)	$M_p$ (%)	$T_r$ (ms)	$T_s$ (ms)	$ess$ (%)
DCS Method	-	9.65	9.65	0.0010	-	7.60	7.60	0.0010
Joice Method	-	-	-	-	-	-	-	-

### 4.3.3 DCS Scheme overall discussion

Based on BLDC motor response for both directions, Joice method was not able to drive the BLDC motor during counter-clockwise direction despite the claim as the motor focus only forward motoring and depends on the motor's inertia to slow down. To allow the BLDC motor to operate in both directions with better speed response characteristics DCS scheme controller could be implemented. Hence, the controller with DCS can be used to drive a BLDC motor bidirectionally.

#### 4.4 Simulation of transient capabilities using DCS

To further improve the ability of the developed controller to achieve a seamless speed reversal, a Modified Fuzzy Gain Scheduling (M.F.G.S) speed controller was proposed and developed. The controller's performance was compared to conventional speed control techniques such as PID and Self-Tuning Fuzzy (S.T.Fuzzy) for eight test cases.

##### 4.4.1 Step Response of the motor for clockwise and counter-clockwise direction for No Load conditions

For both clockwise and counter-clockwise direction, the speed was set at 1500 rpm with no load. The results are depicted by Figure 4.7 for CW direction and Figure 4.8 for counter-clockwise direction. The response was tabulated in Table 4.3 and Table 4.4. It could be observed that during both directions the S.T.Fuzzy and M.F.G.S controller has overshoot while the PID controller does not have overshoot.

The rise time during both directions for S.T.Fuzzy controller was obtained at 3.6 ms which was the fastest settling time among the tested controllers. However, the M.F.G.S controller compensates the deference by obtaining the fastest settling time during both directions. Furthermore, there was a delay of 0.2 ms during counter-clockwise direction for S.T.Fuzzy controller. Among all the controllers under test, the PID controller has the worse rise time, settling time and steady state error despite not having any overshoot.

During both directions, the M.F.G.S controller has the lowest steady state error at 0.00067 %. Hence, for no load conditions the M.F.G.S controller performed better compared to the PID and S.T.Fuzzy speed controllers.

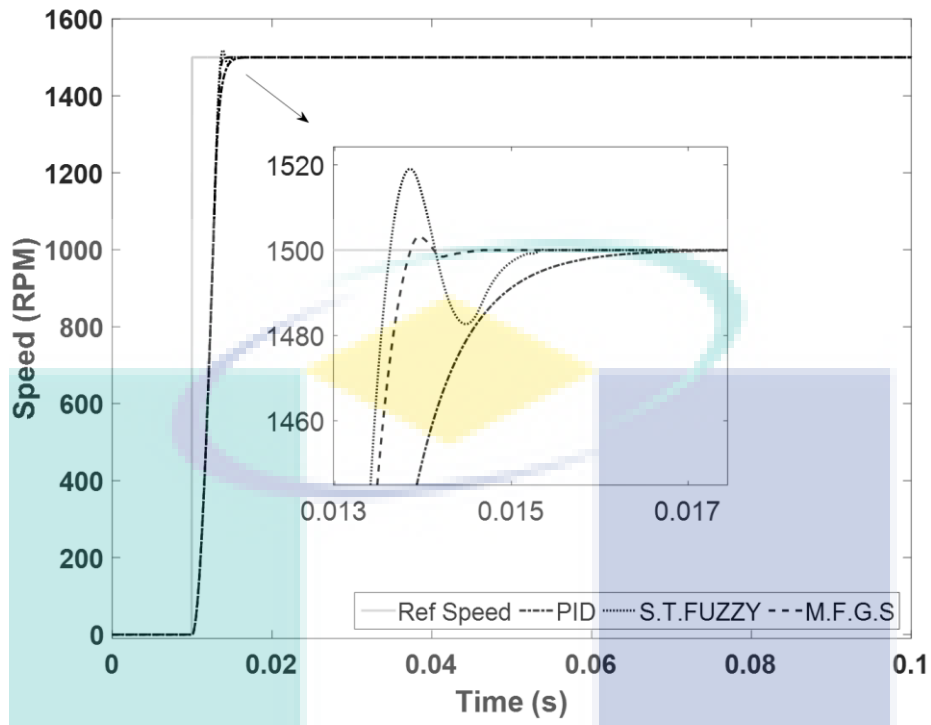


Figure 4.7 Motor speed response during No Load for clockwise direction

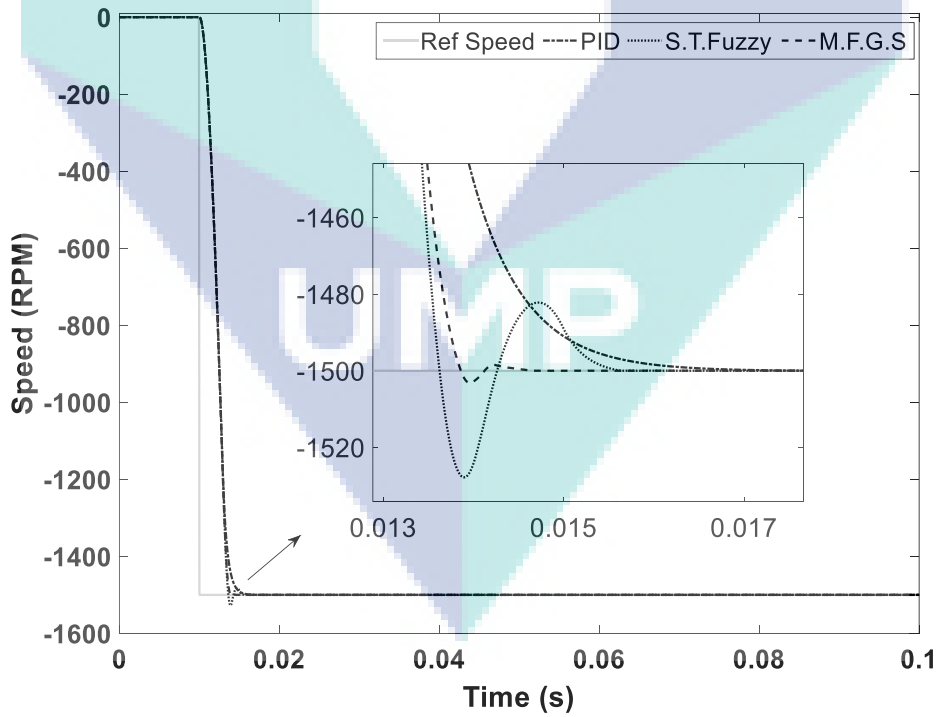


Figure 4.8 Motor speed response during no load for counter-clockwise direction

Table 4.3 Motor response during clockwise for No Load

Techniques	Overshoot	Rise Time	Settling Time	Steady State Error
	$M_p$ (%)	$T_r$ (ms)	$T_s$ (ms)	$e_{ss}$ (%)
PID	-	7.70	7.70	0.00151
S.T.Fuzzy	1.27	3.60	5.40	0.00075
M.F.G.S	0.26	3.90	4.50	0.00067

Table 4.4 Motor response during counter-clockwise for No Load

Techniques	Overshoot	Rise Time	Settling Time	Steady State Error
	$M_p$ (%)	$T_r$ (ms)	$T_s$ (ms)	$e_{ss}$ (%)
PID	-	7.70	7.70	0.00151
S.T.Fuzzy	1.86	3.60	5.40	0.00075
M.F.G.S	0.26	3.90	4.50	0.00067

#### 4.4.2 Step Response of the motor for step change for constant load condition of 10 Nm

The response for the step-changing speed during full load of 10 Nm at  $t = 0.05$  s represented by Figure 4.9 and the data is tabulated in both Table 4.5 and Table 4.6.

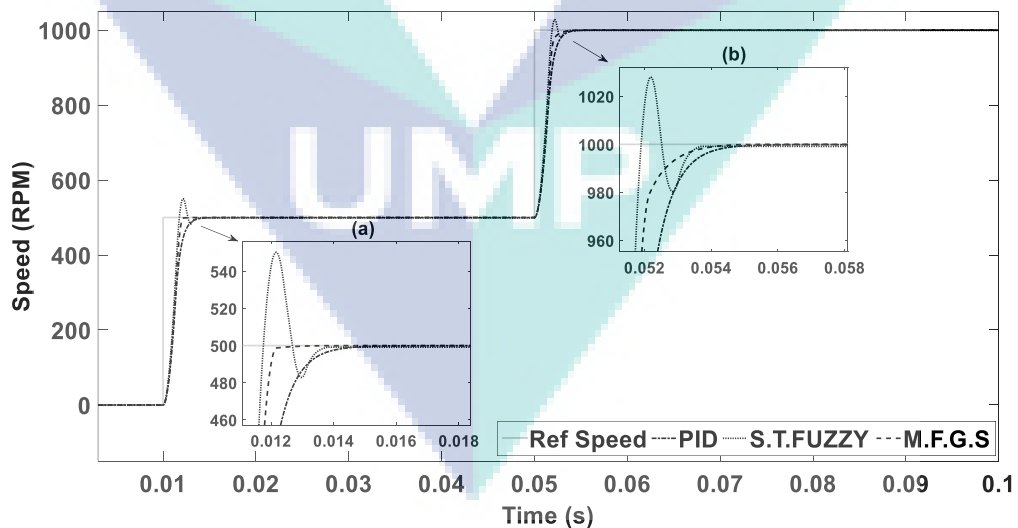


Figure 4.9 Motor speed response during clockwise direction for 10 Nm

Table 4.5 Motor response for the step-changing speed (a)

Techniques	Overshoot	Rise Time	Settling Time	Steady State Error
	$M_p$ (%)	$T_r$ (ms)	$T_s$ (ms)	$e_{ss}$ (%)
PID	-	-	8.80	0.02382
S.T.Fuzzy	10.06	2.91	5.90	0.00420
M.F.G.S	-	3.70	3.70	0.00120

Table 4.6 Motor response for the step-changing speed (b)

Techniques	Overshoot	Rise Time	Settling Time	Steady State Error
	$M_p$ (%)	$T_r$ (ms)	$T_s$ (ms)	$e_{ss}$ (%)
PID	-	-	7.00	0.02382
S.T.Fuzzy	5.90	3.05	4.60	0.00100
M.F.G.S	-	3.70	3.70	0.00097

During the speed change from zero rpm to 500 rpm, overshoot by the S.T.Fuzzy controller was observed. It had overshoot of 10.06 % despite having the fastest rise time of 2.91 ms. Both PID and M.F.G.S has no overshoot but the settling time and steady state error of PID is much higher than M.F.G.S. The PID controller was not able to achieve required speed under the 10 Nm load.

During the speed change from 500 rpm to 1000 rpm, the S.T.Fuzzy controller has the best rise time of 3.05 ms along with 5.9 % of overshoot. Both S.T.Fuzzy and M.F.G.S controller's steady state error has decreased. However, the PID controller's steady state error remained the same during the speed change. Overall, the M.F.G.S speed controller performed better as it does not have overshoot and has the fastest settling time thought the step-changing speed and the smallest steady state error for both step changes.

The response for the step-changing speed during full load of 10 Nm at  $t = 0.05$  s represented by Figure 4.10 and the data is tabulated in both Table 4.7 and Table 4.8. During the speed change from zero rpm to 500 rpm, overshoot by the S.T.Fuzzy controller was observed. It had overshoot of 11.58 % despite having the fastest rise time of 2.85 ms. Both PID and M.F.G.S controllers does not have any overshoot but the settling time and steady state error of PID controller is much higher than M.F.G.S controller. The PID controller was not able to achieve required speed under the 10 Nm load.

During the speed change from 500 rpm to 1000 rpm, the S.T.Fuzzy controller has the best rise time of 2.3 ms along with 5.9 % of overshoot. Both S.T.Fuzzy and M.F.G.S controller's steady state error has decreased. However, the PID controller's steady state error remained the same during the speed change.

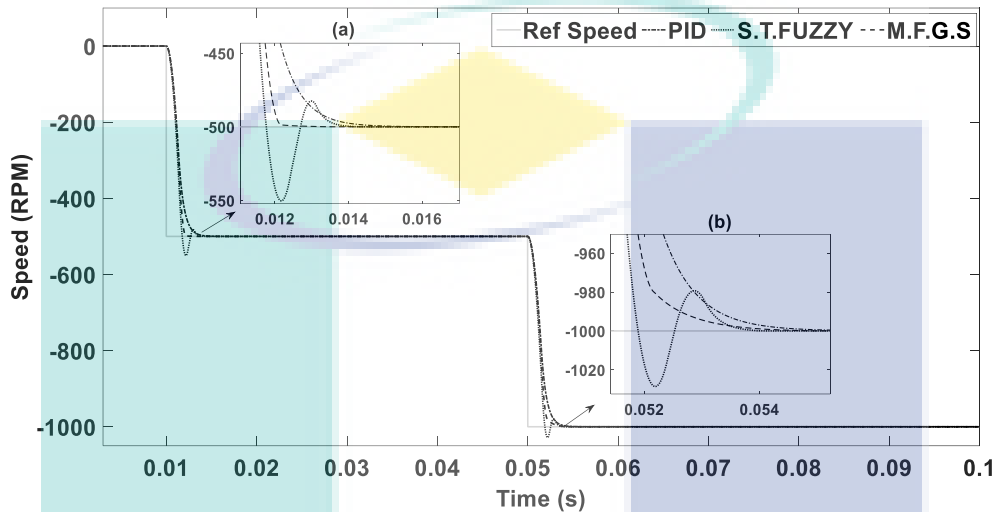


Figure 4.10 Motor speed response during counter-clockwise direction for 10 Nm

Table 4.7 Motor response for the step-changing speed (a)

Techniques	Overshoot $M_p$ (%)	Rise Time $T_r$ (ms)	Settling Time $T_s$ (ms)	Steady State Error $e_{ss}$ (%)
PID	-	-	8.80	0.02382
S.T.Fuzzy	11.58	2.85	5.72	0.00158
M.F.G.S	-	3.70	3.70	0.00120

Table 4.8 Motor response for the step-changing speed (b)

Techniques	Overshoot $M_p$ (%)	Rise Time $T_r$ (ms)	Settling Time $T_s$ (ms)	Steady State Error $e_{ss}$ (%)
PID	-	-	8.80	0.02382
S.T.Fuzzy	5.90	2.30	4.30	0.00100
M.F.G.S	-	3.70	3.70	0.00097

Overall, the M.F.G.S speed controller performed better as it does not have overshoot and has the fastest settling time thought the step-changing speed and the smallest steady state error for both step changes.

#### 4.4.3 Step Response of the motor for constant speed dynamic load conditions

Under this test case, four dynamic load conditions were tested. The first case is load change from 0 Nm to 5 Nm. The second case is load was changed from 10 Nm to 15 Nm. The third case is during load changes form 10 Nm to 5 Nm the final case is during load changes form 10 Nm to 0 Nm.

For the first test case at  $t = 0.05$  s, the load was changed from 0 Nm to 5 Nm. The motor speed response is shown in Figure 4.11 and the data is tabulated in Table 4.9. The recovery time of the PID controller is the worse at 3.5 ms. The M.F.G.S controller has the fastest recovery time of 1.10 ms and the smallest steady state error for both before and after load change compared to controllers under test.

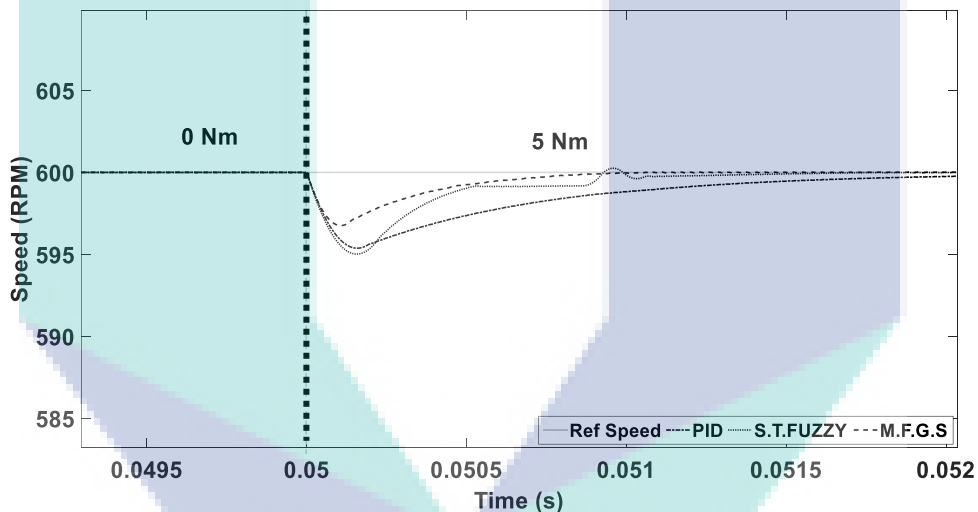


Figure 4.11 Motor speed response during 0 Nm to 5 Nm Load for clockwise direction

Table 4.9 Motor response during 0 Nm to 5 Nm Load

Techniques	Recovery Time (ms)	Before Load Change ess (%)	After Load Change ess (%)
PID	3.50	0.00123	0.01358
S.T.Fuzzy	1.86	0.00023	0.01088
M.F.G.S	1.10	0.00018	0.00302



For second case study for dynamic load, the load was changed from 10 Nm to 15 Nm at  $t = 0.05$  s. The motor speed response is shown in Figure 4.12 and the data is tabulated in Table 4.10. During this load change, the PID controller unable to reach reference speed of 600 rpm.

The M.F.G.S controller has the fastest recovery time of 1.10 ms and the smallest steady state error for both before and after load change compared with other controllers under test. The S.T.Fuzzy speed controller's steady state error increased greatly as the load change increased.

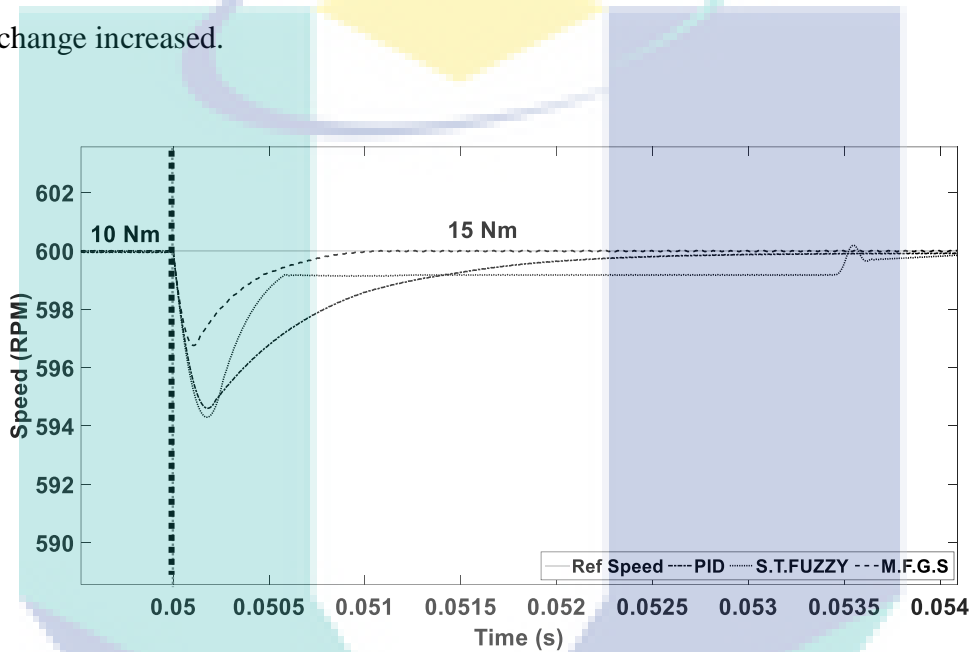


Figure 4.12 Motor speed response during 10 Nm to 15 Nm Load for clockwise direction

Table 4.10 Motor response during 10 Nm to 15 Nm Load

Techniques	Recovery Time (ms)	Before Load Change ess (%)	After Load Change ess (%)
PID	-	0.02382	0.01358
S.T.Fuzzy	4.71	0.00159	0.01218
M.F.G.S	1.16	0.00097	0.00302

For third case study for dynamic load, the motor response of the motor during load changes form 10 Nm to 5 Nm at  $t = 0.05$  s, is depicted by Figure 4.13 and the data is tabulated in Table 4.11. The M.F.G.S controller recorded the best recover time at 1.2 ms during the load changes followed by S.T.Fuzzy controller at 1.7 ms and PID controller at 4.0 ms.

The controller with highest steady-state error after load changes occurs is the PID controller at 0.02000 %. All the controller experiences drop in steady state error expect for the M.F.G.S controller which has increased of 2.3 % more during the load reduction conditions. This is to be expected as the controller sacrifices its stability for better dynamic performance.

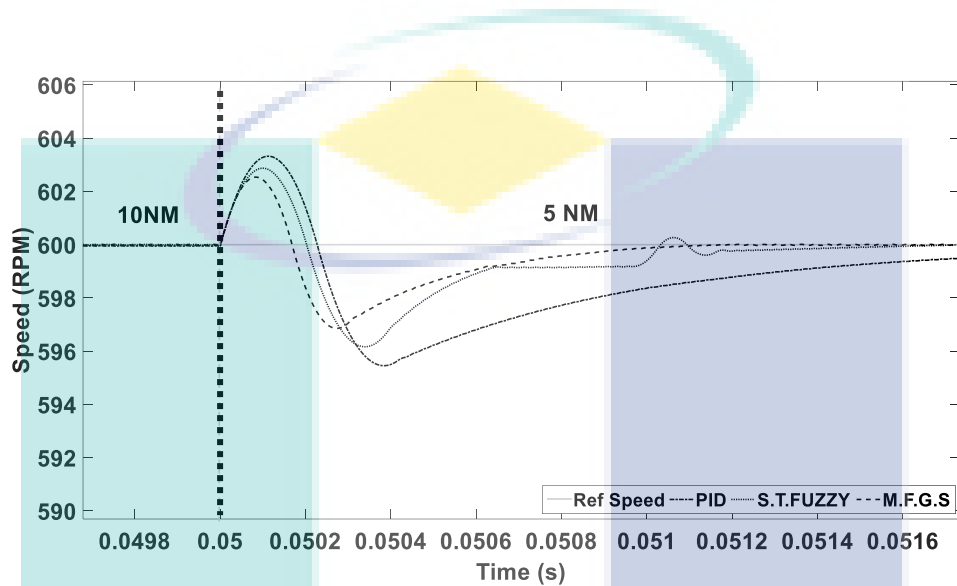


Figure 4.13 Motor speed response during 10 Nm to 5 Nm Load for clockwise direction

Table 4.11 Motor response during 10 Nm to 5 Nm Load

Techniques	Recovery Time	Before Load Change	After Load Change
	(ms)	ess (%)	ess (%)
PID	4.00	0.02382	0.02000
S.T.Fuzzy	1.70	0.00420	0.00393
M.F.G.S	1.20	0.00097	0.00223

The motor response of the motor during load changes form 10 Nm to 5 Nm at  $t = 0.05$  s, is depicted by Figure 4.14 and the data is tabulated in Table 4.12. The M.F.G.S controller recorded the best recover time at 1.3 ms during the load changes followed by S.T.Fuzzy controller with 0.1 ms delay and PID controller at 2.8 ms.

The controller with highest steady-state error after load removal is the PID controller at 0.00123 %. All the controllers experienced a drop in steady state error and the steady state error after load removal is the same for M.F.G.S and S.T.Fuzzy controllers at 0.00073 %. This shows the M.F.G.S controller is much more robust to load changes compared to the PID controller

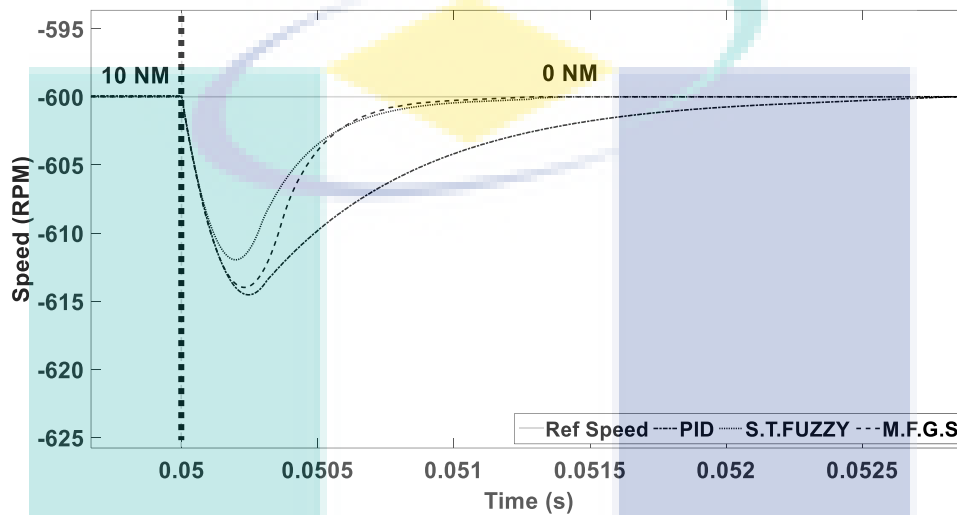


Figure 4.14 Motor speed response during 10 Nm to 0 Nm Load for counter-clockwise direction

Table 4.12 Motor response during 10 Nm to 0 Nm Load

Techniques	Recovery Time (ms)	Before Load Change ess (%)	After Load Change ess (%)
PID	2.80	0.02382	0.00123
S.T.Fuzzy	1.40	0.00420	0.00073
M.F.G.S	1.30	0.00099	0.00073

Overall, the M.F.G.S speed controller performed better than other controllers under test as it has the shortest recovery time throughout dynamic load case study and overall smallest steady state error. This controller experiences slight increase in steady state error during loaded conditions however this increase is to be expected as the controller sacrifices its stability for better dynamic performance. Despite increase in the steady state error, it is still within controllers accepted range which is less than 2 %.

#### 4.4.4 Step Response of the motor during quadrant change for No Load conditions

During the first test case, the transient capabilities of the controller to transient from clockwise to counter-clockwise directions was tested with no load present. The motor response of the BLDC motor for direction change from clockwise to counter-clockwise is depicted by Figure 4.15 and the data is tabulated in Table 4.13 and Table 4.14. For the clockwise direction the reference speed was set 1500 rpm and 500 rpm for counter-clockwise direction.

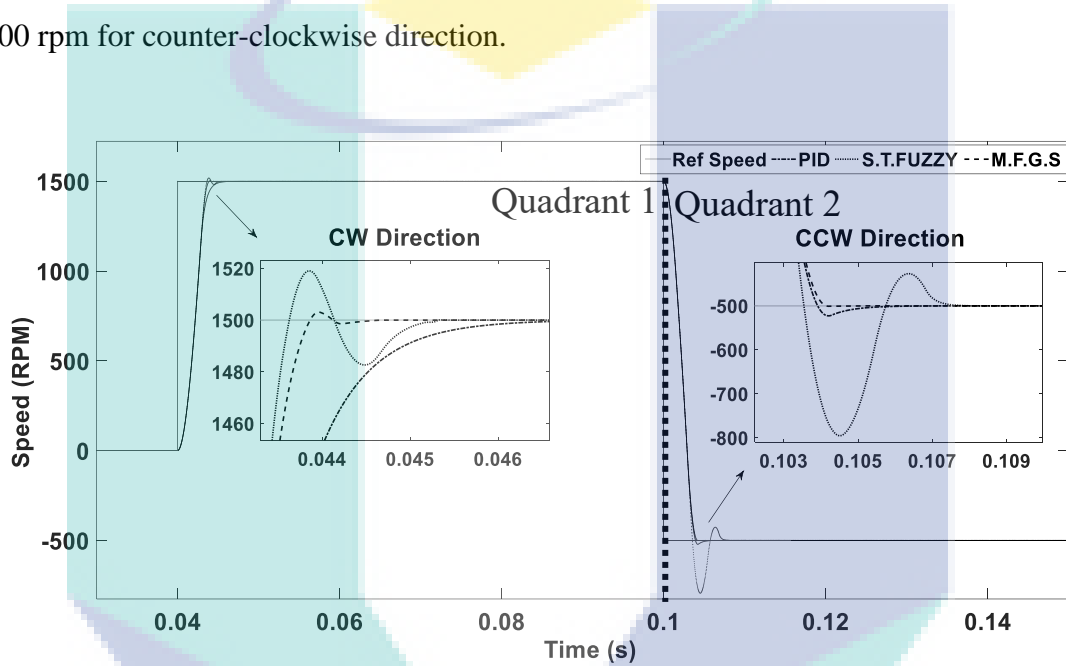


Figure 4.15 Motor speed response during No Load for direction change from clockwise to counter-clockwise direction

Table 4.13 Motor response for the clockwise direction

Techniques	Overshoot $M_p$ (%)	Rise Time $T_r$ (ms)	Settling Time $T_s$ (ms)	Steady State Error $e_{ss}$ (%)
PID	-	7.70	7.70	0.00151
S.T.Fuzzy	1.26833	3.60	5.40	0.00075
M.F.G.S	0.26333	3.90	4.50	0.00067

Table 4.14 Motor response for the counter-clockwise direction

Techniques	Overshoot $M_p$ (%)	Rise Time $T_r$ (ms)	Settling Time $T_s$ (ms)	Steady State Error $e_{ss}$ (%)
PID	-	7.70	7.70	0.00151
S.T.Fuzzy	1.85734	3.60	5.40	0.00075
M.F.G.S	0.26353	3.90	4.49	0.00068

During clockwise direction, no overshoot was observed for PID controller however it's rise time is the highest at 7.70 ms compared to the other controllers. The rise time for M.F.G.S controller and S.T.Fuzzy controller is 3.90 ms and 3.60 ms respectively. The M.F.G.S controller obtained the fastest settling time at 4.49 ms and the smallest steady state error.

For the direction change to counter-clockwise, it can be observed that both the S.T.Fuzzy and M.F.G.S controllers' overshoot increased from 1.2683 % to 1.8573 % and from 0.2633 % to 0.2353 % respectively despite not having any load. Overall during this test case, the M.F.G.S controller displayed better control compared to other controllers under test.

In this case study, the transient capabilities of the controller to transient from counter-clockwise to clockwise directions was tested with no load present. The motor response of the BLDC motor for direction change from counter-clockwise to clockwise directions was depicted by Figure 4.16 and the data is tabulated in Table 4.15 and Table 4.16. For the counter-clockwise direction the reference speed was set 1500 rpm and 500 rpm for clockwise direction.

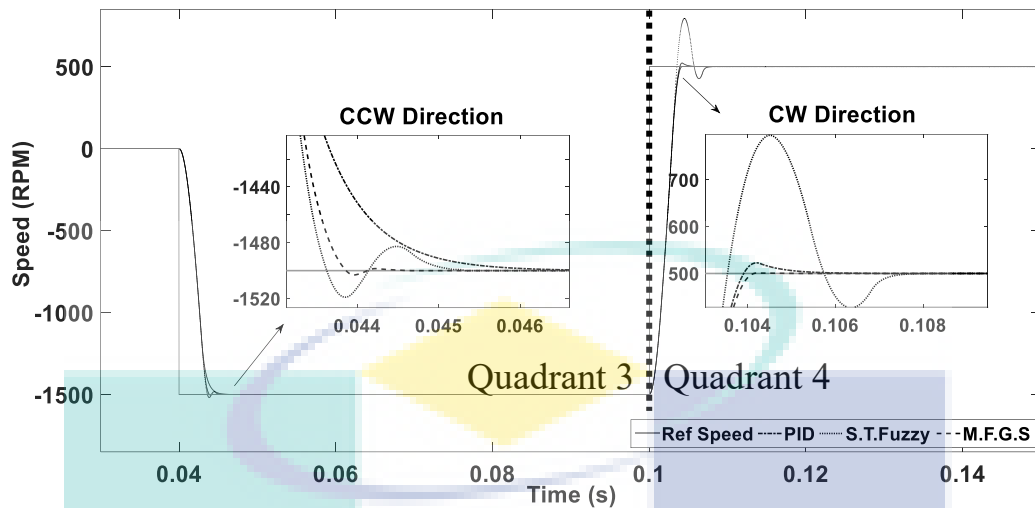


Figure 4.16 Motor speed response during No Load for direction change from counter-clockwise to clockwise direction

Table 4.15 Motor response for the counter-clockwise direction

Techniques	Overshoot	Rise Time	Settling Time	Steady State Error
	$M_p$ (%)	$T_r$ (ms)	$T_s$ (ms)	$e_{ss}$ (%)
PID	-	7.70	7.70	0.00151
S.T.Fuzzy	1.85690	3.59	5.39	0.00075
M.F.G.S	0.26353	3.90	4.49	0.00068

Table 4.16 Motor response for the clockwise direction

Techniques	Overshoot	Rise Time	Settling Time	Steady State Error
	$M_p$ (%)	$T_r$ (ms)	$T_s$ (ms)	$e_{ss}$ (%)
PID	-	7.70	7.70	0.00151
S.T.Fuzzy	1.27843	3.60	5.40	0.00075
M.F.G.S	0.26332	3.90	4.49	0.00067

During counter-clockwise direction, no overshoot was observed for PID controller however it's rise time is the highest at 7.70 ms compared to the other controllers. The rise time for M.F.G.S controller and S.T.Fuzzy controller is 3.90 ms and 3.59 ms respectively. The M.F.G.S controller obtained the fastest settling time at 4.49 ms and the smallest steady state error. During the direction change to counter-clockwise, it can be observed that both the S.T.Fuzzy and M.F.G.S controllers' overshoot decreased from 1.85690 % to 1.27843 % and from 0.2653 % to 0.2332 % respectively despite not having any load.

Overall during this test case study, the M.F.G.S controller displayed better control compared to other controllers under test for both test cases. It must be noted that there is slight difference between during overshoot as the directions of the controller varies despite under the same test case. This is caused by the delay of the controller's decision making based on direction.

#### 4.4.5 Step Response of the motor during quadrant change for load condition of 10 Nm

During the first test case, the transient capabilities of the controller to transient from clockwise to counter-clockwise directions was tested with load of 10 Nm present. The motor response of the BLDC motor for direction change from clockwise to counter-clockwise is depicted by Figure 4.17 and the data is tabulated in Table 4.17 and Table 4.18. For the clockwise direction the reference speed was set 700 rpm and 900 rpm for counter-clockwise direction.

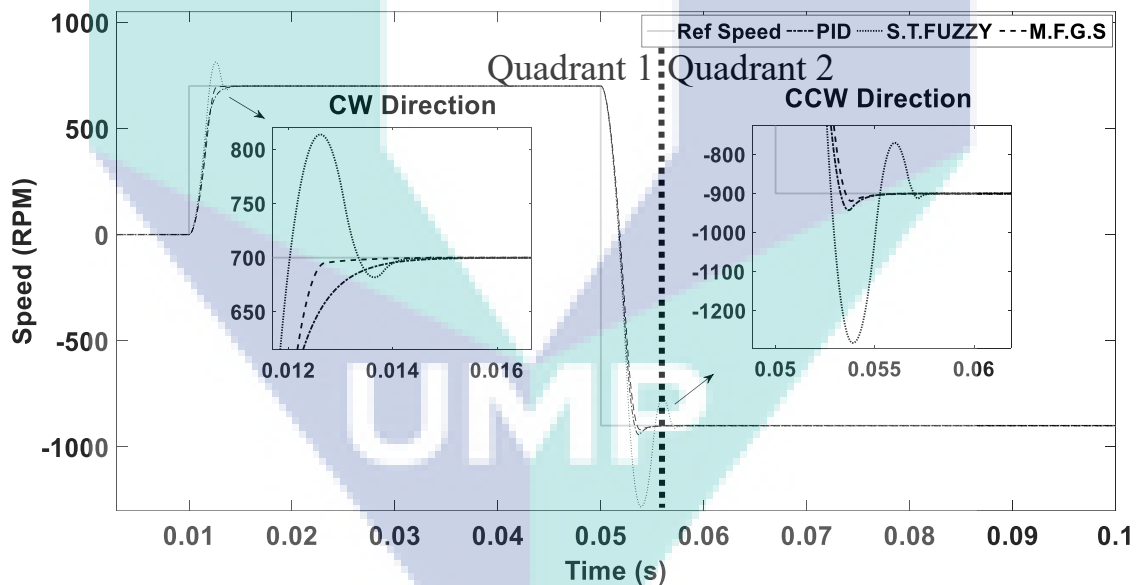


Figure 4.17 Motor speed response during 10 Nm Load for direction change from clockwise to counter-clockwise direction

Table 4.17 Motor response for the clockwise direction

Techniques	Overshoot $M_p$ (%)	Rise Time $T_r$ (ms)	Settling Time $T_s$ (ms)	Steady State Error $e_{ss}$ (%)
PID	-	-	9.00	0.02373
S.T.Fuzzy	11.29	2.50	5.30	0.00420
M.F.G.S	-	3.70	3.70	0.00110

Table 4.18 Motor response for the counter-clockwise direction

Techniques	Overshoot $M_p$ (%)	Rise Time $T_r$ (ms)	Settling Time $T_s$ (ms)	Steady State Error $e_{ss}$ (%)
PID	0.48	3.30	7.80	0.078
S.T.Fuzzy	41.00	1.80	8.00	0.181
M.F.G.S	0.21	3.60	6.50	0.015

During clockwise direction, no overshoot was observed for PID controller and M.F.G.S controllers. The PID controller was not achieve desired speed dur to the load and it's settling time was the highest at 9.0 ms compared to the other controllers. It can be observed the S.T.Fuzzy controller had 11.29 % of overshoot with shortest rise time at 2.5 ms. The M.F.G.S controller obtained the fastest settling time at 3.70 ms and the smallest steady state error.

During the direction change to counter- clockwise, it can be observed that both the PID controller and M.F.G.S controller's overshoot increased from none to 0.47 % and from none to 0.21 % while the S.T.Fuzzy controller had 41 % of overshoot. This overshoot is due to quadrant change from first quadrant to second quadrant as the load remained positive while the motor's direction changes. This causes the motor to accelerate towards counter-clockwise direction faster. However, the M.F.G.S controller was able to keep the overshoot at minimal despite no changes to the load.

For the second test case, the transient capabilities of the controller to transient from counter-clockwise to clockwise directions was tested with load of 10 Nm present. The motor response of the BLDC motor for direction change from counter-clockwise to counter-clockwise is depicted by Figure 4.18 and the data is tabulated in Table 4.19 and Table 4.20. For the counter-clockwise direction the reference speed was set 700 rpm and 900 rpm for clockwise direction.



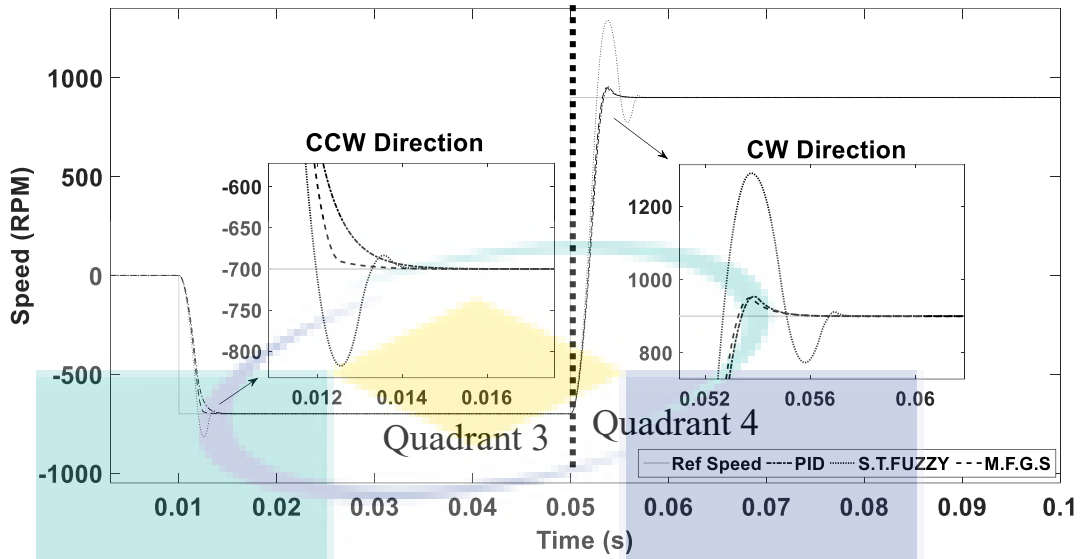


Figure 4.18 Motor speed response during 10 Nm Load for direction change from counter-clockwise to clockwise direction

Table 4.19 Motor response for the counter-clockwise direction

Techniques	Overshoot $M_p$ (%)	Rise Time $T_r$ (ms)	Settling Time $T_s$ (ms)	Steady State Error $e_{ss}$ (%)
PID	-	-	9.00	0.02382
S.T.Fuzzy	11.58	1.80	4.90	0.00158
M.F.G.S	-	3.70	3.70	0.00120

Table 4.20 Motor response for the clockwise direction

Techniques	Overshoot $M_p$ (%)	Rise Time $T_r$ (ms)	Settling Time $T_s$ (ms)	Steady State Error $e_{ss}$ (%)
PID	0.60	3.40	9.20	0.01778
S.T.Fuzzy	40.33	2.60	8.20	0.18111
M.F.G.S	0.51	3.20	6.51	0.00222

During counter-clockwise direction, no overshoot was observed for PID and M.F.G.S controllers. The PID controller was not achieve desired speed due to the load and it's settling time was the highest at 9.00 ms compared to the other controllers. It can be observed the S.T.Fuzzy controller had 11.58 % of overshoot with shortest rise time at 1.8 ms. The M.F.G.S controller obtained the fastest settling time at 3.7 ms and has the smallest steady state error. The overshoot for the S.T.Fuzzy controller has increased for the from 11.58 % to 40.33 %.

Furthermore, it can be observed that both the PID and M.F.G.S controllers' overshoot increased from none to 0.60 % and from none to 0.51 %. This overshoot increase is due to quadrant change from third quadrant to fourth quadrant as the load remained negative while the motor's direction changes. This causes the motor to accelerate towards counter-clockwise direction faster as the load acts as speed buffer. However, the M.F.G.S controller was able to keep the overshoot at minimal.

Overall for this test case, the and M.F.G.S controller displayed better control compared to other controllers under test despite having overshoot during quadrant change. The controller's time response was satisfactory as it has the fastest recovery time and small steady state error.

#### **4.5 Summary**

In this chapter, the main discussion involved the assessment of the test platform's ability to simulate real-time results, results obtain from the development of the DCS scheme and the comparison M.F.G.S speed controller's performance of the with conventional speed control techniques such as PID and S.T.Fuzzy. The first objective to assess the step response of developed bidirectional controller for BLDC motor as in Chapter 3.2 was achieved by developing the test platform that able to simulate the results as in Chapter 3.2. The second objective to develop a controller that allows BLDC motor to operate bidirectionally using PID speed controller. This objective was achieved by developing DCS scheme. The DCS scheme's performance was compared with the technique used in Chapter 3.2 and clearly the DCS scheme was able achieve bidirectional capabilities. The third objective was to further improve step-response and achieve transient capabilities for seamless speed reversal. The objective was achieved by developing the M.F.G.S speed controller. Its capabilities were assessed and compared with PID and S.T.Fuzzy speed controllers.

## CHAPTER 5

### CONCLUSION

#### 5.1 Introduction

This study presented the application of M.F.G.S for BLDC motor speed control with seamless speed reversal capability. To conclude this study, the objectives of the study need to be identified if achieved or otherwise. The first objective of the study was to assess the step response of developed bidirectional controller for BLDC motor by (Joice et al., 2013). This objective was achieved through the developing a test platform that able to simulate the results as in Chapter 3.2 and produce real-time results. The test platform was able to obtain similar results as obtained in the Chapter 3.2 study for both simulation and hardware results.

The second objective was to develop a controller that allows BLDC motor to operate bidirectionally using PID speed controller as it was realized by using the commutation method in Chapter 3.2, the BLDC motor was unable to achieve speed reversal. This objective was successfully achieved by developing DCS method to drive the BLDC motor bidirectionally. The DCS method performances were compared to Joice's method, the DCS method was able to drive the BLDC motor bidirectionally while Joice method was not able to do so.

The final objective was to further improve step-response and achieve transient capabilities for seamless speed reversal. The objective was achieved by developing the M.F.G.S speed controller. The developed controller's performance was compared to S.T.Fuzzy controller and PID speed controller for several test cases. The M.F.G.S speed controller performed better compared to the other controllers for all the test cases.

## **5.2 Statement of Contribution**

The first contribution of the study is the development of DCS commutation method that allow the BLDC motor to be driven bidirectionally and achieve the capabilities to transient between quadrants. This method was developed by developing a lookup table based on BLDC motor operations. This method was tested for several test cases and compared with commutation method developed by S.Joice. The DCS method was able to drive the BLDC motor bidirectionally while S.Joice was not able because it focuses on forward motoring only. However, the DCS method has delay of 0.1ms during counter-clockwise direction operations due computation delay.

The second contribution is the development of M.F.G.S speed controller to further improve the step-respond time and transient capabilities to achieve seamless speed reversal. The developed controller's performance was tested using the test platform for several test cases and was able to outperform other controllers under same test cases. The newly developed controller was well adapted during dynamic load change occurs and able to handle with minimal overshoot during transiting between quadrants. Despite able to reduce overshoot during transiting between quadrants, there is an increase of steady state error was observed. However, the increase of steady state error is to be expected as the controller sacrifices its stability for better dynamic performance.

## **5.3 Recommendation for future research**

BLDC motor's characteristic has increased the demand for this motor in various sectors. This also demands for a better BLDC controller. To further improve the controller the delay during counter-clockwise direction need to be addressed.

During the study it was found during quadrant transient overshoot occurs. This problem should be addressed using much more robust intelligent controller.

## REFERENCES

- Ahmed, S., Topalov, A., Dimitrov, N., & Bonev, E. (2016). Industrial implementation of a fuzzy logic controller for brushless DC motor drives using the PicoMotion control framework. In *IEEE 8th International Conference on Intelligent Systems (IS), 2016* (pp. 629–634).
- Ansari, U., & Alam, S. (2011). Modeling and control of three phase BLDC motor using PID with genetic algorithm. In *UkSim 13th IEEE International Conference on Computer Modelling and Simulation (UKSim), 2011* (pp. 189–194).
- Araki, M. (2009). PID control. *Control Systems, Robotics and Automation: System Analysis and Control: Classical Approaches II*, Unbehauen, H.(Ed.). EOLSS Publishers Co. Ltd., Oxford, UK., ISBN-13: 9781848265912, 58–79.
- Aris, R., & Adiimah, R. S. N. (2011). Simulation of a variable speed brushless DC motor using neural network controller. Universiti Tun Hussein Onn Malaysia.
- Bennett, S. (1996). A brief history of automatic control. *IEEE Control Systems*, 16(3), 17–25.
- Bennett, S. (2001). The past of PID controllers. *Annual Reviews in Control*, 25, 43–53. [https://doi.org/10.1016/S1367-5788\(01\)00005-0](https://doi.org/10.1016/S1367-5788(01)00005-0)
- Blessy, M. S. E., & Murugan, M. (2014). Modeling and controlling of BLDC motor based fuzzy logic. In *International Conference on Information Communication and Embedded Systems (ICICES2014)* (pp. 1–6).
- Brailsford Harrison D. (1955). U.S Patent No. US2719944 A. The United States Of America: U.S. Patent and Trademark Office.
- Ch, L., & Palakeerthi, R. (2015). BLDC Drive Control using Artificial Intelligence Technique. *International Journal of Computer Applications*, 118(4).
- Concari, C., & Troni, F. (2010). Sensorless control of BLDC motors at low speed based on differential BEMF measurement. In *Energy Conversion Congress and Exposition (ECCE), 2010* (pp. 1772–1777).
- Davoudkhani, I. F., & Akbari, M. (2016). Adaptive speed control of brushless DC (BLDC) motor based on interval type-2 fuzzy logic. *2016 24th Iranian Conference on Electrical Engineering (ICEE)*. <https://doi.org/10.1109/IranianCEE.2016.7585689>
- Feng, Y., Yu, X., & Han, F. (2013). High-order terminal sliding-mode observer for parameter estimation of a permanent-magnet synchronous motor. *IEEE Transactions on Industrial Electronics*, 60(10), 4272–4280.

- Hagglund, T. (1992). A predictive PI controller for processes with long dead times. *IEEE Control Systems*, 12(1), 57–60.
- Hanselman, D. C. (2003). *Brushless permanent magnet motor design*. The Writers' Collective.
- Hazen, H. L. (1934). Theory of servo-mechanisms. *Journal of the Franklin Institute*, 218(3), 279–331.
- Hentunen, A., Suomela, J., Leivo, A., Liukkonen, M., & Sainio, P. (2011). Full-scale hardware-in-the-loop verification environment for heavy-duty hybrid electric vehicles. *World Electric Vehicle Journal*, 4(1), 119–127.  
<https://doi.org/10.1109/VPPC.2010.5729144>
- Ho, W. K., Hang, C. C., & Cao, L. S. (1992). Tuning of PI controllers based on gain and phase margin specifications. In *Proceedings of the IEEE International Symposium on Industrial Electronics, 1992*. (pp. 879–882).
- Hughes, T. P. (1971). *Elmer Sperry: Inventor and Engineer*. Johns Hopkins University Press.
- Ibrahim, H. E. A., Hassan, F. N., & Shomer, A. O. (2014). Optimal PID control of a brushless DC motor using PSO and BF techniques. *Ain Shams Engineering Journal*, 5(2), 391–398.
- Jang, G. H., Park, J. H., & Chang, J. H. (2002). Position detection and start-up algorithm of a rotor in a sensorless BLDC motor utilising inductance variation. *IEE Proceedings-Electric Power Applications*, 149(2), 137–142.
- Joice, C. S., Paranjothi, S. R., & Kumar, J. S. (2011). Practical implementation of four quadrant operation of three phase Brushless DC motor using dsPIC. In *2011 International Conference on Recent Advancements in Electrical, Electronics and Control Engineering, IConRAEeCE'11 - Proceedings* (pp. 91–94).  
<https://doi.org/10.1109/ICONRAEeCE.2011.6129762>
- Joice, C. S., Paranjothi, S. R., & Kumar, V. J. S. (2013). Digital control strategy for four quadrant operation of three phase BLDC motor with load variations. *IEEE Transactions on Industrial Informatics*, 9(2), 974–982.  
<https://doi.org/10.1109/TII.2012.2221721>
- Kamal, C., Thyagarajan, T., Selvakumari, M., & Kalpana, D. (2017). Cogging torque minimization in brushless DC motor using PSO and GA based optimization. In *Trends in Industrial Measurement and Automation (TIMA), 2017* (pp. 1–5).
- Krause, P. C., Wasynczuk, O., & Sudhoff, S. D. (2002). Analysis of Electric Machinery and Drive Systems. *Power Engineering*, 1–65.  
<https://doi.org/10.1109/9780470544167>

- Krishnan, R., Park, S.-Y., & Ha, K. (2005). Theory and operation of a four-quadrant switched reluctance motor drive with a single controllable switch-the lowest cost four-quadrant brushless motor drive. *IEEE Transactions on Industry Applications*, 41(4), 1047–1055.
- Krohling, R. A., & Rey, J. P. (2001). Design of optimal disturbance rejection PID controllers using genetic algorithms. *IEEE Transactions on Evolutionary Computation*, 5(1), 78–82.
- Larminie, J., & Lowry, J. (2003). *Electric Vehicle Technology Explained* (5th ed.). John Wiley & Sons. <https://doi.org/10.1002/9781118361146>
- Leena, N., & Shanmugasundaram, R. (2014). Artificial neural network controller for improved performance of brushless DC motor. In *2014 International Conference on Power Signals Control and Computations (EPSCICON)*, (pp. 1–6).
- Manikandan, R., & Arulmozhiyal, R. (2016). Intelligent position control of a vertical rotating single arm robot using BLDC servo drive. *Journal of Power Electronics*, 16(1), 205–216. <https://doi.org/10.6113/JPE.2016.16.1.205>
- Matsui, N., & Shigyo, M. (1992). Brushless DC motor control without position and speed sensors. *IEEE Transactions on Industry Applications*, 28(1), 120–127.
- Minorsky., N. (1922). Directional Stability Of Automatically Steered Bodies. *Journal of the American Society for Naval Engineers*, 34(2), 280–309. <https://doi.org/10.1111/j.1559-3584.1922.tb04958.x>
- Morris E. Leeds. (1920). System of automatic control. The United States Of America: U.S. Patent and Trademark Office.
- Nag, T., Chatterjee, D., Ganguli, A. K., Santra, S. B., & Chatterjee, A. (2016). Fuzzy logic-based loss minimisation scheme for brushless DC motor drive system. *IET Power Electronics*, 9(8), 1581–1589. <https://doi.org/10.1049/iet-pel.2015.0714>
- Navaneethakkannan, C., & Sudha, M. (2012). An Adaptive Sliding Surface Slope Adjustment in Sliding Mode Fuzzy Control Techniques for Brushless DC Motor Drives. *International Journal of Computer Applications*, 54(2).
- Nola, F. J. (1987). US4644234 A. The United States Of America: U.S. Patent and Trademark Office.
- Park, S.-I., Kim, T.-S., Ahn, S.-C., & Hyun, D.-S. (2003). An improved current control method for torque improvement of high-speed BLDC motor. In *Eighteenth Annual IEEE Applied Power Electronics Conference and Exposition, 2003. APEC'03*. (Vol. 1, pp. 294–299).

- Pillay, P., & Krishnan, R. (1988). An investigation into the torque behavior of a brushless DC motor drive. In *IEEE Industry Applications Society Annual Meeting, 1988., Conference Record of the 1988* (pp. 201–208).
- Pillay, P., & Krishnan, R. (1989a). Modeling, simulation, and analysis of permanent-magnet motor drives. I. The permanent-magnet synchronous motor drive. *IEEE Transactions on Industry Applications*, 25(2), 265–273. <https://doi.org/10.1109/28.25541>
- Pillay, P., & Krishnan, R. (1989b). Modeling, simulation, and analysis of permanent-magnet motor drives. II. The brushless DC motor drive. *IEEE Transactions on Industry Applications*, 25(2), 274–279. <https://doi.org/10.1109/28.25542>
- Prabu, M. J., Poongodi, P., & Premkumar, K. (2016). Fuzzy supervised online coactive neuro-fuzzy inference system-based rotor position control of brushless DC motor. *IET Power Electronics*. <https://doi.org/10.1049/iet-pel.2015.0919>
- Premkumar, K., & Manikandan, B. V. (2015a). Bat algorithm optimized fuzzy PD based speed controller for brushless direct current motor. *Engineering Science and Technology, an International Journal*. <https://doi.org/10.1016/j.jestch.2015.11.004>
- Premkumar, K., & Manikandan, B. V. (2015b). Fuzzy PID supervised online ANFIS based speed controller for brushless dc motor. *Neurocomputing*, 157, 76–90. <https://doi.org/10.1016/j.neucom.2015.01.032>
- Premkumar, K., & Manikandan, B. V. (2013). Adaptive fuzzy logic speed controller for brushless DC motor. *2013 International Conference on Power, Energy and Control (ICPEC)*. <https://doi.org/10.1109/ICPEC.2013.6527668>
- Premkumar, K., & Manikandan, B. V. (2014). Adaptive Neuro-Fuzzy Inference System based speed controller for brushless DC motor. *Neurocomputing*, 138, 260–270.
- Ramya, A., Imthiaz, A., & Balaji, M. (2016). Hybrid Self Tuned Fuzzy PID controller for speed control of Brushless DC Motor. *Automatika*, 57(3), 672–679.
- Rigatos, G. G. (2009). Adaptive fuzzy control of DC motors using state and output feedback. *Electric Power Systems Research*, 79(11), 1579–1592. <https://doi.org/10.1016/j.epsr.2009.06.007>
- Sanita, C. S., & Kuncheria, J. T. (2013). Modelling and Simulation of Four Quadrant Operation of Three Phase Brushless DC Motor With Hysteresis Current Controller. *International Journal of Advanced Research in Electrical, Electronics and Instrumentation Engineering*, 2(6).
- Schauder, C. D., & Caddy, R. (1982). Current control of voltage-source inverters for fast four-quadrant drive performance. *IEEE Transactions on Industry Applications*, (2), 163–171.

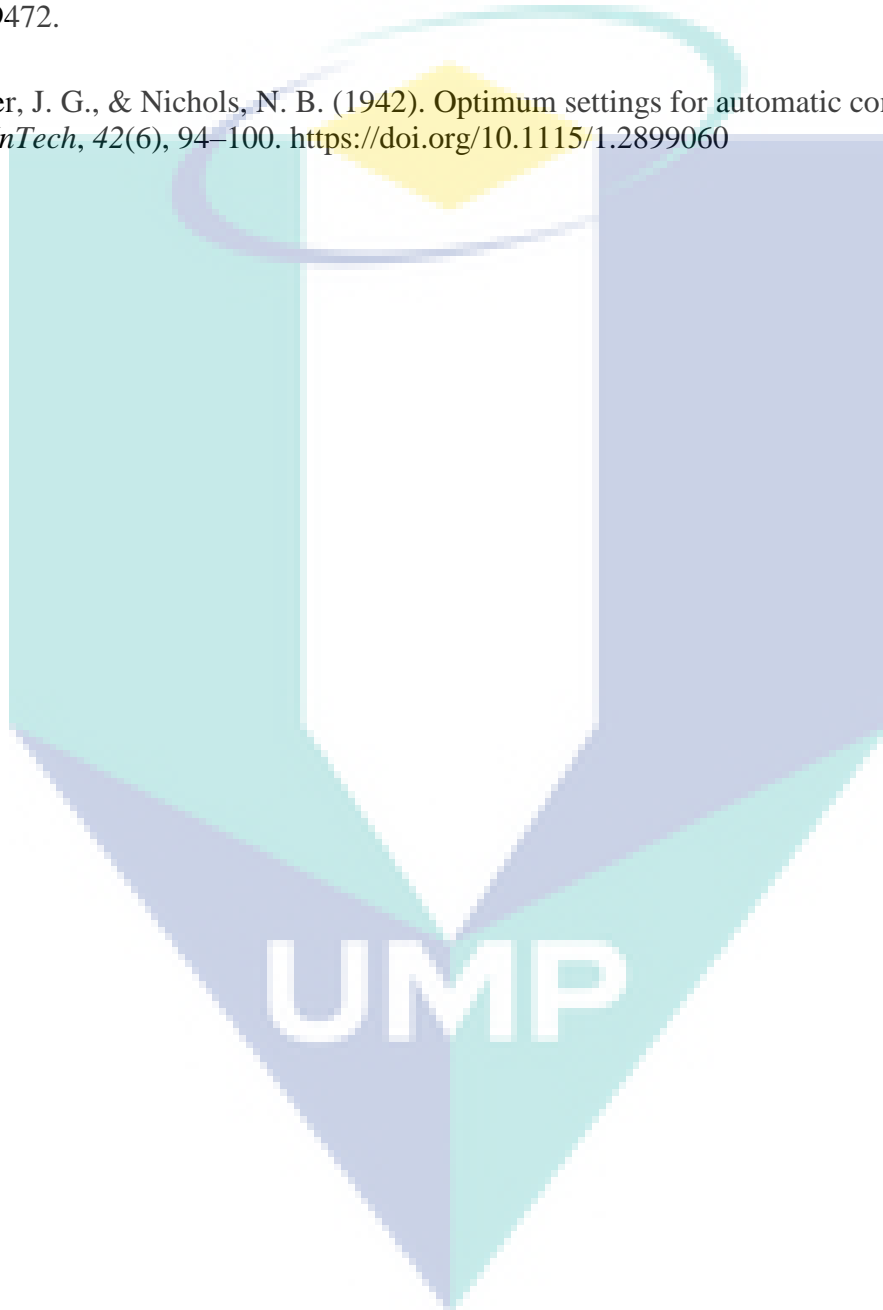


- Senjyu, T., Urasaki, N., & Uezato, K. (1997). Vector control of brushless DC motors using neural network. In *International Conference on Power Electronics and Drive Systems, 1997. Proceedings., 1997* (Vol. 1, pp. 291–296).
- Shamseldin, M. (2016). *Speed Control of High Performance Brushless DC Motor*. <https://doi.org/10.13140/RG.2.1.1472.9202>
- Shin, H.-B. (1998). New antiwindup PI controller for variable-speed motor drives. *IEEE Transactions on Industrial Electronics*, 45(3), 445–450.
- Sivarani, T. S., Jawhar, S. J., & Kumar, C. A. (2016). Novel bacterial foraging-based ANFIS for speed control of matrix converter-fed industrial BLDC motors operated under low speed and high torque. *Neural Computing and Applications*, 1–24.
- Suganya, K., & Rameshkumar, S. (2014). Simulation of Four Quadrant Operation of Three Phase BLDC Motor Using Fuzzy. *International Journal of Innovative Research in Science, Engineering and Technology*, 3.
- TechNavio. (2016). *Global Brushless DC Market 2016-2020*.
- Usman, A., & Rajpurohit, B. S. (2016). Speed control of a BLDC Motor using Fuzzy Logic Controller. In *International Conference on Power Electronics, Intelligent Control and Energy Systems (ICPEICES), IEEE* (pp. 1–6).
- Vikkaraga, J. V. (2014). Fuzzy based digital Control Strategy for Four Quadrant , 3 Phase BLDC Motor with speed stability. *International Journal of Engineering Development and Research (Www.ijedr.org)*, 2(2), 1437–1440.
- Wilson, T. G., & Trickey, P. H. (1962). D-C machine with solid-state commutation. *Electrical Engineering*. <https://doi.org/10.1109/EE.1962.6446586>
- Woo, Z.-W., Chung, H.-Y., & Lin, J.-J. (2000). A PID type fuzzy controller with self-tuning scaling factors. *Fuzzy Sets and Systems*, 115(2), 321–326. [https://doi.org/10.1016/S0165-0114\(98\)00159-6](https://doi.org/10.1016/S0165-0114(98)00159-6)
- Xia, C., Guo, P., Shi, T., & Wang, M. (2004). Speed control of brushless DC motor using genetic algorithm based fuzzy controller. In *Proceeding of the 2004 International Conference on Intelligent Mechatronics and Automation, Chengdu, China, 3rd edn. A Treatise on Electricity and Magnetism* (Vol. 2, pp. 68–73).
- Zhang, S., & Wang, Y. (2016). The simulation of BLDC motor speed control based-optimized fuzzy PID algorithm. In *IEEE International Conference on Mechatronics and Automation (ICMA), 2016* (pp. 287–292). IEEE.

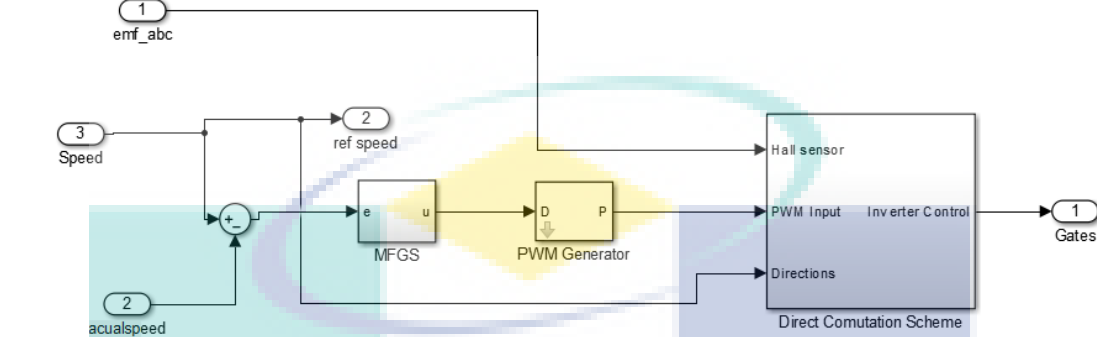
Zhao, Z. Y., Tomizuka, M., & Isaka, S. (1993). Fuzzy Gain Scheduling of PID Controllers. *IEEE Transactions on Systems, Man and Cybernetics*, 23(5), 1392–1398. <https://doi.org/10.1109/21.260670>

Zhou, X., Chen, X., Zeng, F., & Tang, J. (2017). Fast Commutation Instant Shift Correction Method for Sensorless Coreless BLDC Motor Based on Terminal Voltage Information. *IEEE Transactions on Power Electronics*, 32(12), 9460–9472.

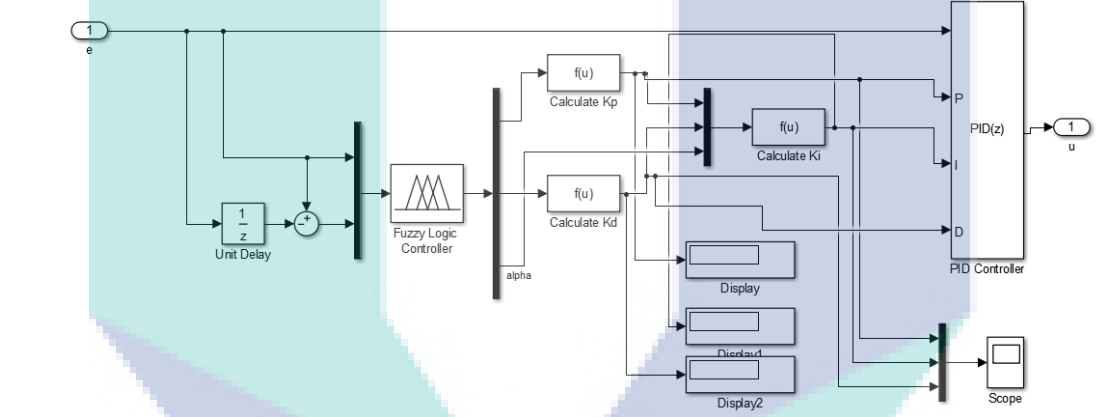
Ziegler, J. G., & Nichols, N. B. (1942). Optimum settings for automatic controllers. *InTech*, 42(6), 94–100. <https://doi.org/10.1115/1.2899060>



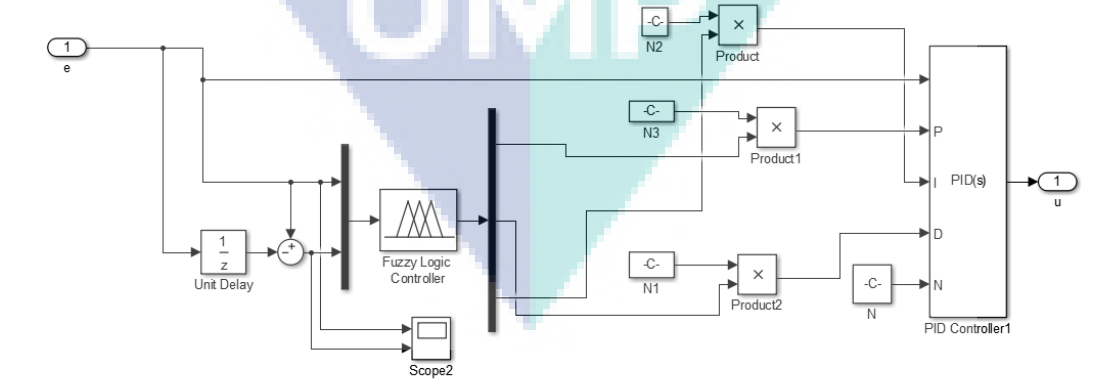
# APPENDIX A BLDC SPEED CONTROLLER



Internal part of controller block



MFSG controller



Self-Tuned Fuzzy controller

## **APPENDIX B**

### **LIST OF PUBLICATION**

**Satishrao Pothorajoo** and Hamdan Daniyal, "PID bidirectional speed controller for BLDC with seamless speed reversal using Direct Commutation Switching Scheme", IEEE 8th Control and System Graduate Research Colloquium (ICSGRC). 4-5 Aug. 2017, Shah Alam, Malaysia

**Satishrao Pothorajoo** and Hamdan Daniyal, "Hybrid Fuzzy-PID Bidirectional Speed Controller for BLDC with Seamless Speed Reversal using Direct Commutation Switching Scheme", Scopus Indexed Journal - Journal of Telecommunication, Electronic and Computer Engineering (JTEC). 16-17 Oct. 2017, Langkawi, Malaysia

**Satishrao Pothorajoo** and Hamdan Daniyal, "Modified Fuzzy Gain Scheduling Speed Controller for BLDC with Seamless Speed Reversal using Direct Commutation Switching Scheme", article has been queued for future publication of Jurnal Teknologi (Sciences and Engineering): Vol. 80 :2 March 2018



**UMP**